NUREG/CR-6870

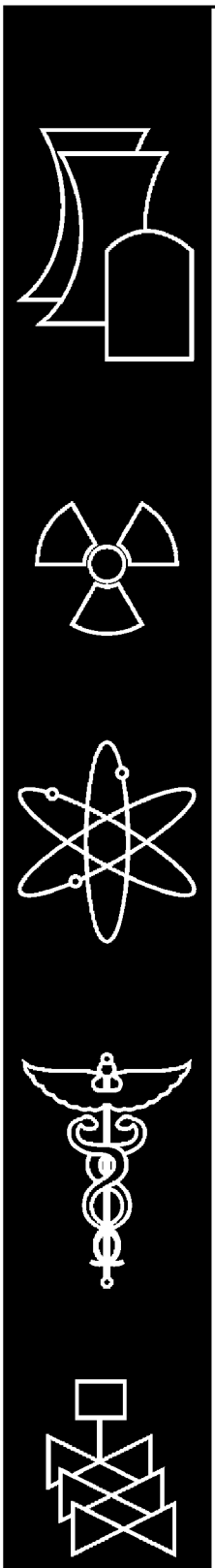

Consideration of Geochemical Issues in Groundwater Restoration at Uranium In-Situ Leach Mining Facilities

Draft Report for Comment

U.S. Geological Survey

U.S. Nuclear Regulatory Commission
Office of Nuclear Regulatory Research
Washington, DC 20555-0001

NUREG/CR-6870

Consideration of Geochemical Issues in Groundwater Restoration at Uranium In-Situ Leach Mining Facilities

Draft Report for Comment

Manuscript Completed: December 2004
Date Published: June 2005

Prepared by
J.A. Davis, G.P. Curtis

U.S. Geological Survey
Menlo Park, CA 94025

J.D. Randall, NRC Project Manager

Prepared for
Division of Systems Analysis and Regulatory Effectiveness
Office of Nuclear Regulatory Research
U.S. Nuclear Regulatory Commission
Washington, DC 20555-0001
NRC Job Code Y6462

Consideration of Geochemical Issues in Groundwater Restoration at Uranium In-Situ Leach Mining Facilities

Prepared by James A. Davis and Gary P. Curtis
U. S. Geological Survey
Menlo Park, CA 94025
December 15, 2004

Prepared for the U. S. Nuclear Regulatory Commission
To be published in the NUREG Report series

ABSTRACT

The geochemistry of relevance to groundwater quality restoration at in-situ uranium leach mining facilities is reviewed and discussed, with a particular focus on the elements uranium, selenium, arsenic, and vanadium. The computer code PHREEQC Interactive (Parkhurst and Appelo, 1999) is used to model the chemical evolution of groundwater in a typical groundwater restoration and stabilization effort, with one pore volume of groundwater sweep, followed by several pore volumes of reverse osmosis treatment with re-injection of the permeate water, and stabilization simulations out to 100 pore volumes with either oxic or reducing influent groundwater. The database for the pilot plant groundwater restoration project at the Ruth In-Situ Leach Uranium Mine facility (Wyoming) (Schmidt, 1989) was used to set initial post-mining conditions and to compare the model results for various geochemical/hydrologic scenarios with actual field observations of water quality evolution. The modeling and field data suggest that there was little pyrite or uraninite left in the mined ore zone that was in good hydrologic contact with flowing groundwater. These reduced minerals may be present in regions of low permeability that transfer solutes slowly to the high permeability regions, however, this is not likely to lead to chemically reducing conditions in the permeable regions during the active phases of groundwater restoration. The addition of a reductant (such as hydrogen sulfide gas) to the re-injected reverse osmosis permeate water is very effective at creating reducing conditions in the mined ore zone for a period of time. The ability of the model to simulate the conditions in the subsurface requires a knowledge of the mineral phases formed in the mined zone after hydrogen sulfide addition. The formation of metastable phases, such as elemental sulfur, rather than thermodynamically stable phases, such as pyrite, has a very significant effect on the modeling results if oxic water flows into the mined region during the stabilization phase of restoration. The stability of chemically reducing conditions in the subsurface after hydrogen sulfide addition is difficult to predict and likely depends on the actual reduced minerals formed, the rate of groundwater flow into the mined ore zone region, and the dissolved oxygen concentration of the groundwater under natural gradient conditions. Long-term stabilization of the mined zone is likely if sufficient hydrogen sulfide is added during a few pore volumes of RO treatment to achieve highly reducing conditions, ***and*** the influent groundwater under natural gradient conditions is anoxic. If the influent groundwater during stabilization is oxic, however, the reducing conditions caused by hydrogen sulfide addition will eventually be overcome, and increases in the concentrations of U, As, and Se will likely rebound significantly above the baseline for a long period of time (many tens of pore volumes under natural gradient conditions) before decreasing back to baseline conditions. Meaningful predictions for vanadium are difficult to make because of the lack of sorption constants for V(IV) and V(III).

Foreword

Some mining processes use fluids to dissolve (or leach) a mineral without the need physically to remove the ore containing the mineral from an ore deposit in the ground. In general, these "in-situ" leach mining operations at uranium mines are considerably more environmentally benign than traditional mining and milling of uranium ore. Nonetheless, the use of leaching fluids to mine uranium contaminates the groundwater aquifer in and around the region from which the uranium is extracted. Consequently, the U.S. Nuclear Regulatory Commission (NRC) requires licensees to restore the aquifer to established water-quality standards following the cessation of in-situ leach mining operations.

The NRC also requires licensees to ensure that sufficient funds will be available to cover the cost of decommissioning their facilities. For these uranium mines, restoration generally consists of pumping specially treated water into the affected aquifer and removing the displaced water — and thereby the undesirable contaminants — from the system. Because groundwater restoration represents approximately 40 percent of the cost of decommissioning a uranium leach mining facility, a good estimate of the necessary volume of treatment water is important to allow a good estimate of the cost of decommissioning.

This report summarizes the application of a geochemical model to the restoration process to estimate the degree to which a licensee has decontaminated a site where a leach mining process has been used. Toward that end, this report analyzes the respective amounts of water and chemical additives pumped into the mined regions to remove and neutralize the residual contamination using 10 different restoration strategies. The analyses show that strategies that used hydrogen sulfide in systems with low natural oxygen content provided the best results. On the basis of those findings, this report also summarizes the conditions under which various restoration strategies will prove successful. This, in turn, will allow more accurate estimates of restoration and decommissioning costs.

This report will be useful for licensees and State regulators overseeing uranium leach mining facilities, who need to estimate the volume of treatment water needed to decontaminate those facilities.

Carl J. Paperiello, Director
Office of Nuclear Regulatory Research

CONTENTS

FIGURES

TABLES

1 BACKGROUND

In-situ leaching (ISL) is a term that describes the process of contacting a mineral deposit with leaching fluids to dissolve the mineral without having to physically remove the ore from the subsurface. ISL uranium mining has the potential to produce uranium at lower costs than other mining methods. The ISL mining technology is primarily limited to roll-front uranium deposits that are located in sandstone aquifers. The water-bearing unit of the aquifer containing the ore body must be confined by less permeable materials; uranium deposits found in water-table aquifers are not mined by ISL technology (Rojas, 1989).

The leaching fluid in the ISL mining process is referred to as the lixiviant solution. Lixiviant solutions are injected into the ore zone and the mixed leaching fluid and groundwater are then pumped out of the ground at a production well (Figure 1). The ideal lixiviant is one that will oxidize the uranium in the ore and contains a complexing agent that will dissolve and form strong aqueous complexes that remain dissolved and interact little with the host rock. Typical lixiviants for in-situ leach mining are salt solutions of ions such as bicarbonate, carbonate, and sulfate that form stable complexes with the oxidized uranium, denoted as U(VI). Oxidants added to the lixiviant to cause the oxidation of uranium ore include oxygen, hydrogen peroxide, sodium chlorate, sodium hypochlorite, and potassium permanganate.

The principal regions of ISL mining facilities are located in the Wyoming Basins (Wind River, Shirley, Powder River, Great Divide), on the Colorado Plateau, or in the Gulf Coastal Plain of Texas. Leachable uranium deposits are found in sandstones that have been deposited in intermontane basins, along mountain fronts, or in near-shore marine or deltaic environments. The geologic environment favoring the formation of the roll front deposits is deficient in oxygen, has zones with less permeable siltstones and shales, and contains reducing agents such as carbonaceous material, hydrogen sulfide, or pyrite. Individual ore bodies in sandstone lenses rarely exceed a few hundred meters in length, commonly being a few tens of meters wide and 10 meters or less thick.

The spacing and arrangement of injection and production wells are unique for each ISL facility and depend on the hydraulic response of the aquifer to fluid injection or production. The arrangement of wells is similar to that in networks used for secondary recovery operations in oil fields. The net rates of injection and production are ideally balanced across all wells, such that fluid flow away from the well field is minimized.

Water-quality effects that can result from ISL mining may be caused by the excursion of lixiviant during injection or from natural migration of residual lixiviant and other ISL-affected ground water after mining has ceased. Numerous chemical interactions are possible between the lixiviant and the uranium ore, associated secondary minerals, and the host rock formation. The interactions can be divided into four broad chemical categories: 1) oxidation-reduction (redox) reactions, 2) dissolution reactions, 3) precipitation reactions, and 4) sorption and ion exchange reactions. The rates and degree to which these reactions occur are interdependent, that is to say, for example, precipitation reactions may be affected by sorption and ion exchange reactions. For this reason, it is useful to consider the possible reactions, or at least the most significant reactions, within an aqueous geochemical model. Common radioactive constituents that may be mobilized by uranium ISL mining activities include uranium, thorium, radium, radon, and their respective daughter products. Trace elements of concern with respect to water

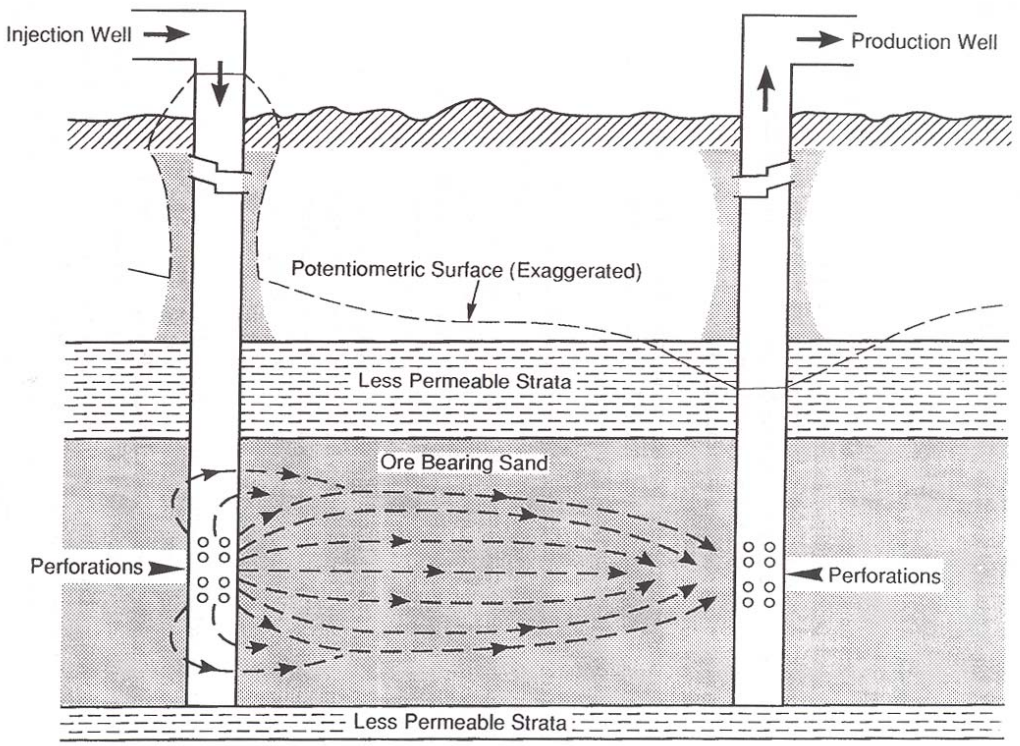

Figure 1. Schematic of the in-situ leach mining process, showing an injection well into which lixiviant solution is pumped and a production well for withdrawing dissolved elements from an ore (U. S. Nuclear Regulatory Commission, 1997).

quality include arsenic, vanadium, zinc, selenium, and molybdenum (Kasper et al., 1979).

At the conclusion of the mining phase, it is necessary to restore the groundwater quality according to the appropriate regulatory authority (USNRC, 2001; 2003). In the initial phase of groundwater restoration, water is pumped from the well field to the processing plant through all of the production and injection wells without re-injection, drawing native groundwater inward to flush contaminants from areas that have been affected by the lixiviant during the ISL mining. In some cases, some contaminants may be removed by above-ground treatment and the treated water is recirculated in the aquifer using the injection and production wells. Oxygen scavengers or a reducing agent such as hydrogen sulfide gas may be added to the recirculating water to re-establish reducing conditions in the ore-bearing unit of the aquifer (Deutsch et al., 1985; Schmidt, 1989; Rio Algom; 2001). In other cases, make-up groundwater may be pumped from a supply well known to contain hydrogen sulfide. At the end of the groundwater recirculation phase, aquifer water is monitored according to a schedule accepted by the regulatory authority to ensure that baseline or class-of-use conditions have been restored and that no impact on adjacent aquifers has occurred.

ISL uranium mining facilities are licensed by the U. S. Nuclear Regulatory Commission (NRC). The NRC requires licensees to bond for the cost of decommissioning and restoration at ISL facilities. Groundwater restoration represents a significant portion (approximately 40%) of the costs of decommissioning (Table 1). The major cost

Table 1. Estimated Decommissioning Costs for United States Nonconventional Uranium Production Facilities (1994 dollars). Source: (DOE, 1995)

Name	Well field Restoration Costs ($, thousands)	Groundwater Restoration Costs ($, thousands)	Other Costs ($, thousands)	Total Costs ($, thousands)	Groundwater Restoration Costs (% of Total)
Benavides	343	1,986	1,299	3,628	55
Bruni	246	3,311	5,051	8,608	38
Burns Ranch/Clay West	3,808	15,994	15,211	35,013	46
Chris. Ranch/Irigaray	1,130	2,868	4,360	8,358	34
Crow Butte	742	1,766	1,657	4,165	42
Highland	727	2,243	2,648	5,618	40
Holiday/El Mesquite	3,002	5,754	5,095	13,851	42
Kingsville Dome	270	540	686	1,496	36
Las Palmas	173	353	435	961	37
Mt. Lucas	633	908	7,362	8,903	10
North Butte/Ruth	445	1,668	1,556	3,669	45
Rosita	74	353	326	753	47
Tex-1	201	176	199	576	31
West Cole	233	1,540	1,076	2,849	54
Totals	13,027	39,460	46,961	98,448	40

of groundwater restoration activities is directly related to the volume of water pumped from or recirculated through the ore zone aquifer.

In this report we discuss geochemical considerations involved in determining the volume of water that must be pumped to achieve groundwater restoration standards and the possible role of aqueous geochemical modeling.

Very few examples of geochemical modeling of the groundwater restoration process exist in the open literature (e.g., Potter et al., 1979). Rio Algom (2001) submitted a geochemical model description of groundwater quality at the Smith Ranch ISL facility (Wyoming) to the NRC (Rio Algom, 2001). The model calculations considered the effects of chemical conditions and the redox environment after groundwater restoration on the concentrations of various solutes, using the aqueous geochemical modeling computer code, PHREEQC (Parkhurst, 1995).

2 GEOCHEMICAL CHARACTERISTICS OF URANIUM ROLL FRONT DEPOSITS AND ASSOCIATED GROUNDWATER SYSTEMS

Figure 2 shows a cross-section of an idealized sedimentary uranium deposit described as a roll front. A roll front is a dynamic feature migrating down a hydrologic gradient. As oxygenated ground water enters the sandstone aquifer by recharge, the oxygen oxidizes the uranium associated with the sandstone to U(VI), thereby mobilizing the uranium for transport within the aquifer. At a point deeper in the aquifer, the oxygen becomes depleted, and typically a curved (convex) redox interface is formed with reducing conditions on the downgradient side and oxidizing conditions on the upgradient side. The U(VI) transported by the oxic groundwater is reduced and precipitated as a U(IV) mineral, when it arrives at the redox interface. The term "roll front" is used because over time the redox interface (and the associated uranium mineralization) rolls downgradient as more oxygen is transported into the aquifer (Langmuir, 1997). The inner contacts of ore and altered sandstone are generally sharp, whereas the uranium concentration on the reduced side of the interface is gradational. The shape of the ore bodies is generally complex, consisting of several interconnected rolls (Dahlkamp, 1993).

Although Figure 2 suggests that the uranium roll front deposits are found at a redox interface, the normally oxidized upgradient sandstone can also be in a reduced state if new reductants are introduced to the sandstone, such as the influx of hydrogen sulfide in the south Texas deposits. Some of the Wyoming deposits, e.g., in the Powder River Basin, may have undergone recent remobilization, migration, and redeposition of the elements in older deposits. In the Shirley Basin, tilting of the sandstones may have caused a reversal of the direction of groundwater flow (Dahlkamp, 1993).

2.1 Wyoming Basins

The host rocks are poorly consolidated medium- to coarse-grained arkoses to feldspathic sandstones of Upper Cretaceous and Tertiary origin. The sandstones typically contain thin discontinuous beds of mudstone, and pyrite and carbonaceous matter in the form of woody remains and masses of humic components are abundant.

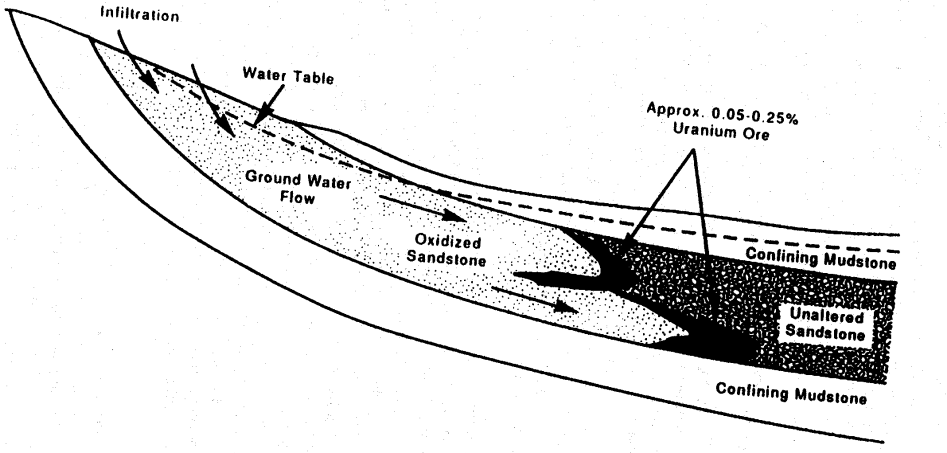

Figure 2. Schematic of an idealized uranium roll front deposit (U. S. Nuclear Regulatory Commission, 1997).

Organic carbon content averages 0.5% by weight (Dahlkamp, 1993). The principal ore minerals are pitchblende and coffinite ($USiO_4$), with associated pyrite, marcasite (FeS_2), hematite (Fe_2O_3), ferroselite ($FeSe_2$), native selenium, and calcite ($CaCO_3$).

Host rock alteration by oxidation processes leads to the formation of the uranium ore deposits at the edge of oxidized sandstone tongues. The ore minerals occur as coatings on sand grains and as void fillings in the sandstone. Partial or complete destruction of the pyrite may occur during the host rock alteration; pyrite is the principal reductant in the unaltered sandstone. Selenium occurs as native Se and ferroselite ($FeSe_2$) in the altered sandstone and as native Se in the unaltered sandstone near the ore. Jordisite (molybdenum sulfide, MoS_2), reduced vanadium oxide (V_2O_4), and calcite occur on the convex side of the roll front in the unaltered sandstone (Dahlkamp, 1993). Figure 3 shows alteration and mineralization zones, related authigenic minerals, and some of the chemical reactions involved in the different zones of the roll front.

Harshman (1974) investigated the distribution of the ore and associated trace elements and minerals around the redox fronts of the Wyoming ore deposits and found some major similarities in element distributions among the deposits (Figures 4-8). The redox interface for uranium in the deposits coincides with that for iron in some of the deposits; in others the uranium interface is separated from the iron interface by as much as 5 meters of reduced sandstone bearing pyrite. Se was found deposited in zones at the edges of the altered sandstone or in reduced mineralized sandstone close to the redox interface. Mo was observed in highly variable concentrations, usually concentrated in the altered sandstone near the redox boundary. Vanadium was found at concentrations of several hundred ppm (parts per million), deposited on the convex (reducing) side of the interface.

2.2 Gulf Coastal Plains of Texas

The host rocks consist of a variety of fluvial to marginal marine, poorly consolidated sandstones, interbedded with or overlain by volcanic ash or tuffaceous beds of several formations. The sandbeds are locally along faults, invaded by hydrocarbons, methane, and hydrogen sulfide. The principal ore minerals are pitchblende and coffinite. Associated elements include molybdenum, selenium, vanadium, and phosphorus. Some of the uranium ore is associated with a geochemical redox interface (as in the Wyoming roll front deposits), while other mineralized areas are found in sands that are currently entirely reduced. In oxidized zones of the deposits, a variety of U(VI) minerals have been found, including uranyl phosphates, vanadates, and silicates (Dahlkamp, 1993).

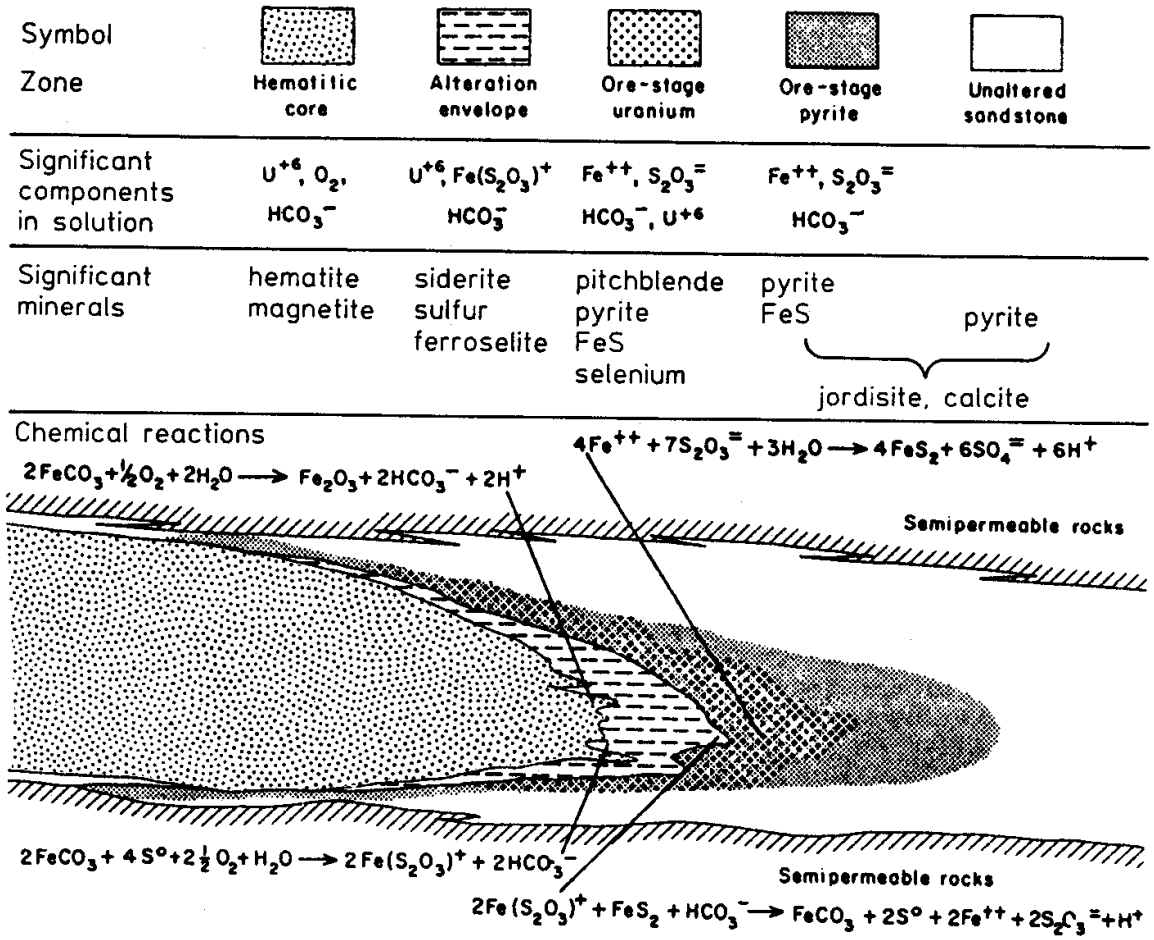

Figure 3. Schematic of idealized Wyoming Basin uranium roll front deposit showing alteration zones, related mineral components, solution components, and important aqueous chemical reactions for Fe, S, O, and CO_2 (after Granger and Warren, 1974).

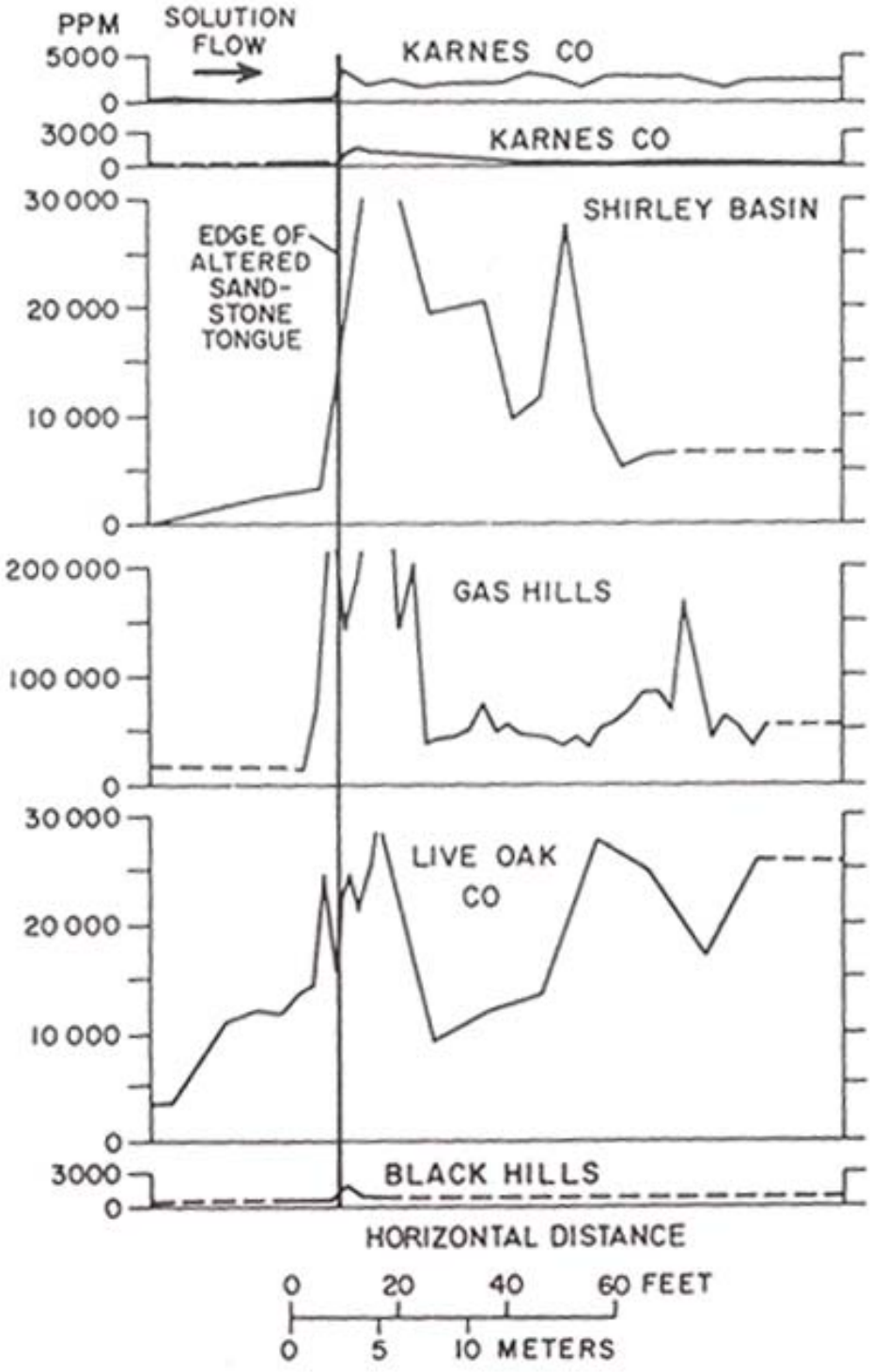

Figure 4. Concentration and distribution of pyrite in various uranium roll front deposits (after Harshman, 1974).

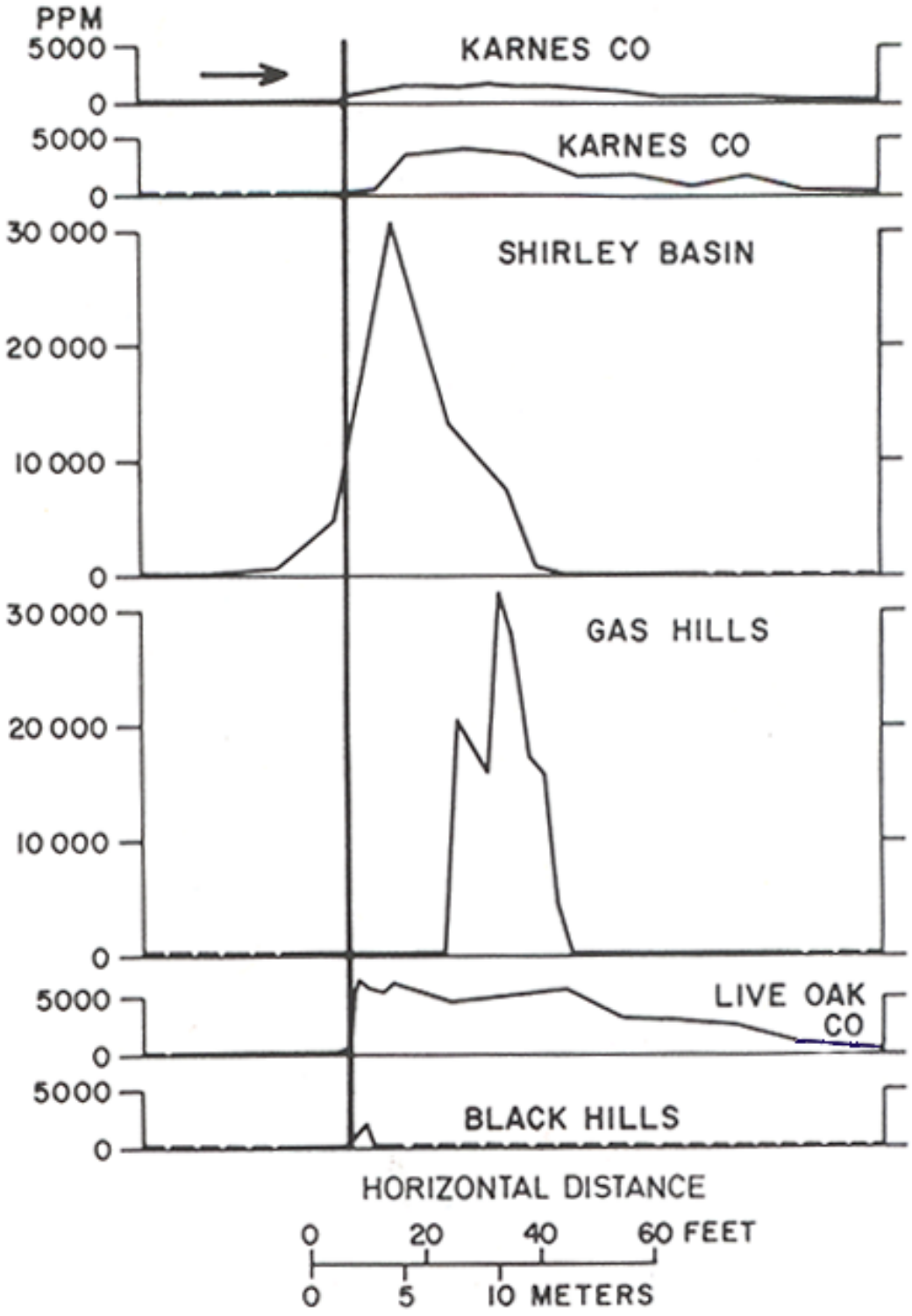

Figure 5. Concentration and distribution of uranium in various roll front deposits (after Harshman, 1974).

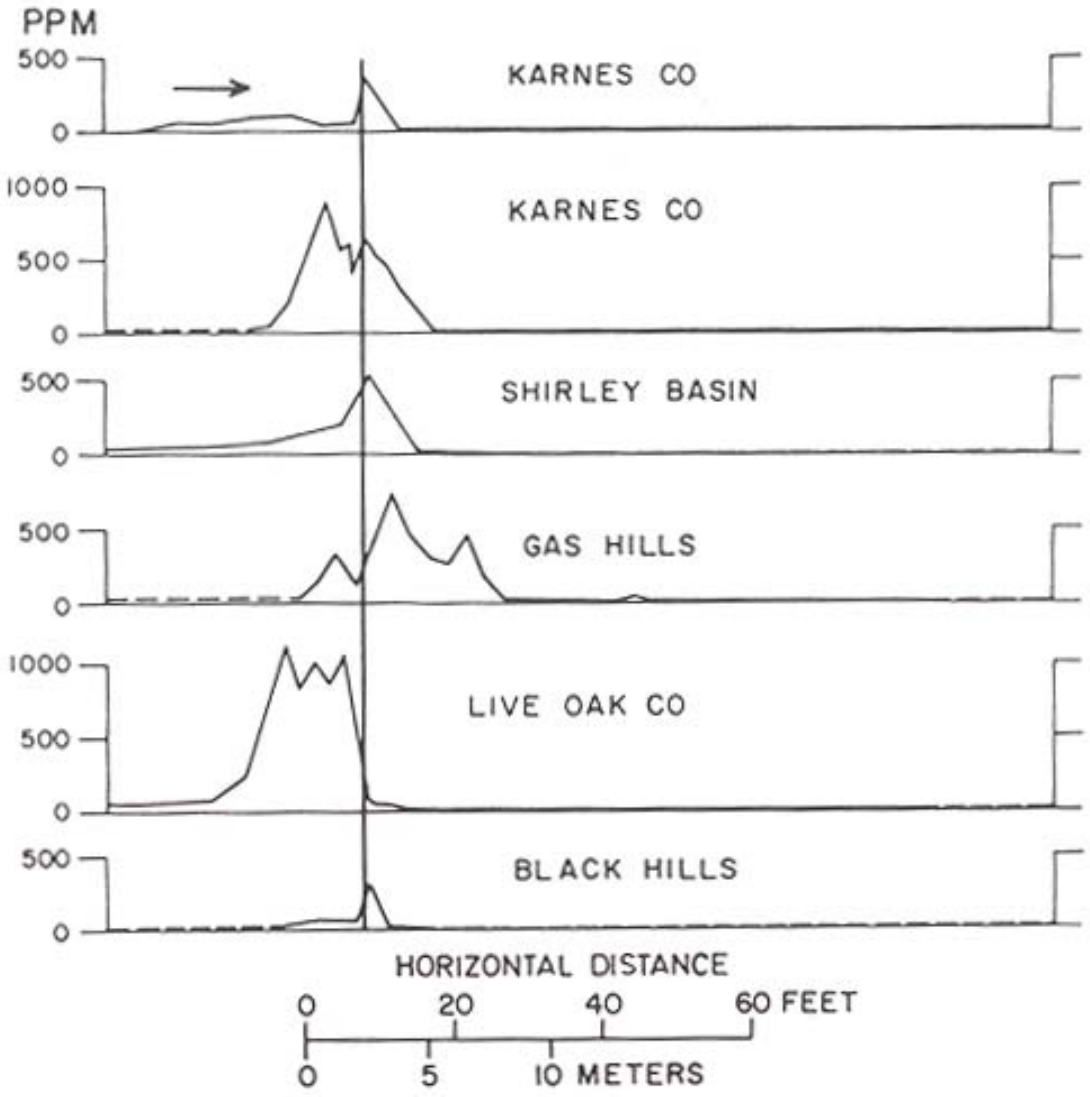

Figure 6. Concentration and distribution of selenium in various uranium roll front deposits (after Harshman, 1974).

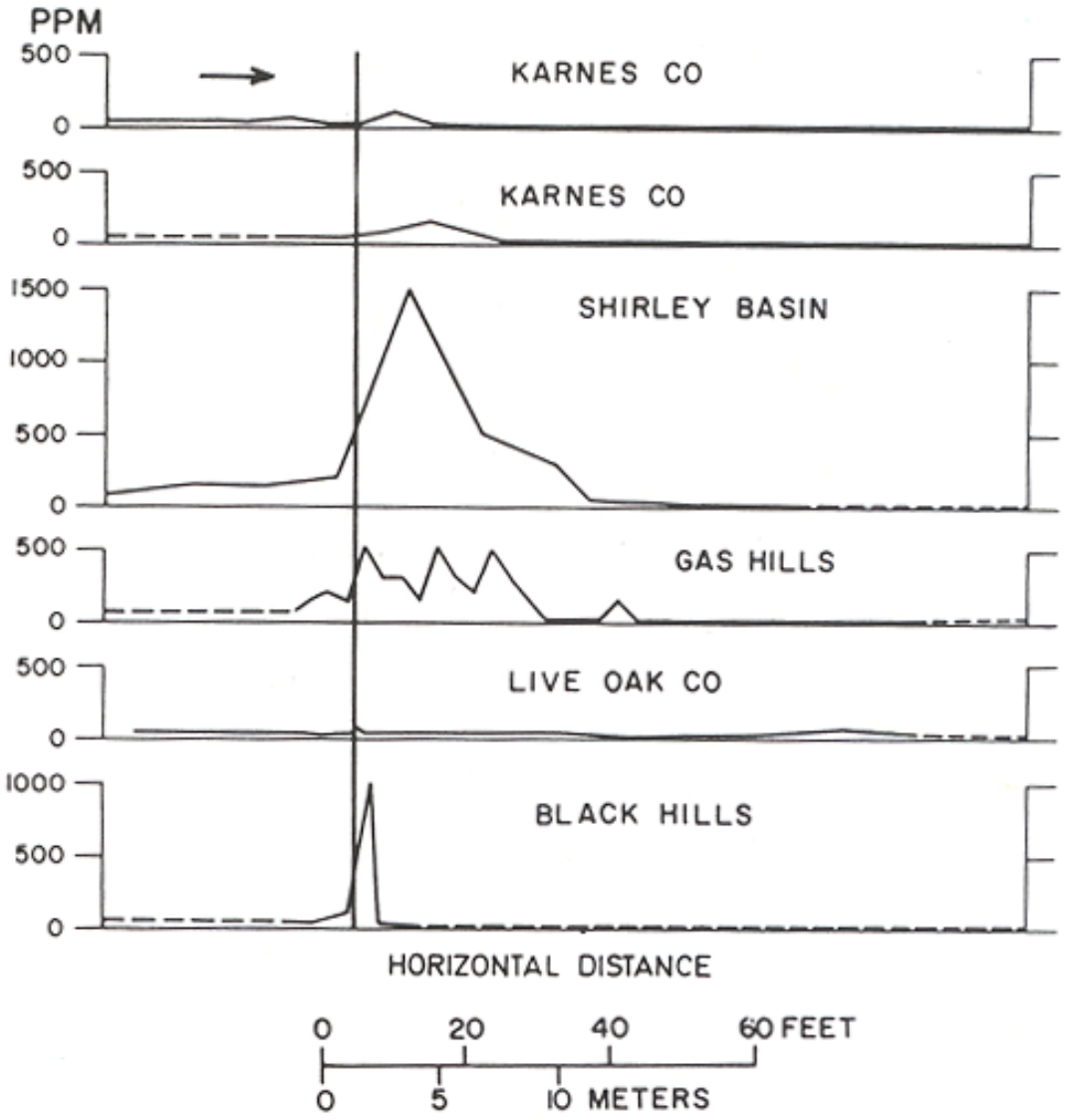

Figure 7. Concentration and distribution of vanadium in various uranium roll front deposits (after Harshman, 1974).

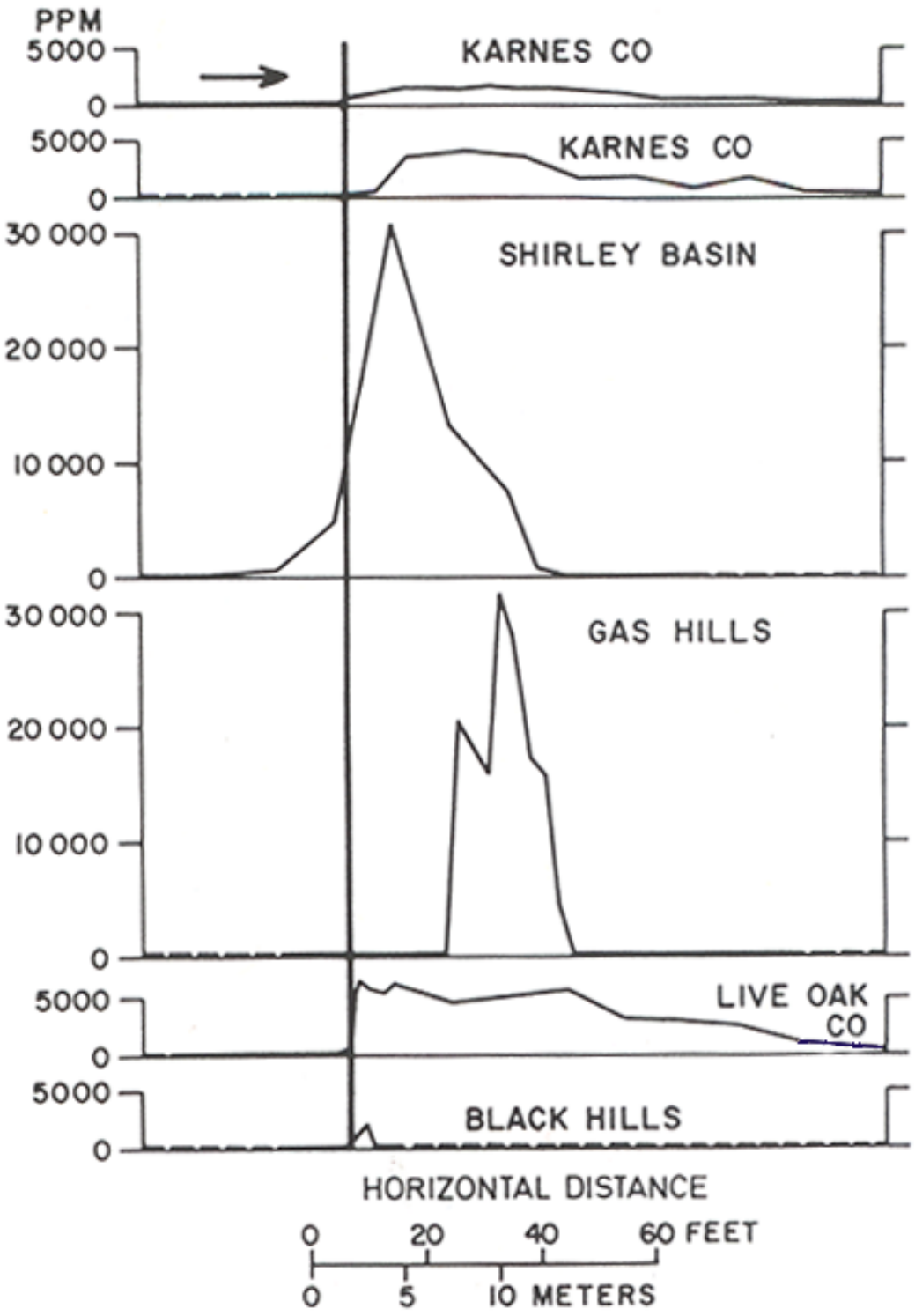

Figure 8. Concentration and distribution of arsenic in various uranium roll front deposits (after Harshman, 1974).

3 AQUEOUS GEOCHEMICAL REACTIONS DURING IN-SITU URANIUM MINING

Geochemical gradients across roll front deposits can be characterized in terms of the major reactions of U, Fe, S, O, and CO_2 (Fig. 3). In the oxidized altered sandstone and oxic groundwater, the significant Fe minerals are hematite and magnetite. Most or all of the pyrite in the original sandstone has been oxidized, along with the reduced forms of uranium(IV) in pitchblende and coffinite. Much of the uranium is dissolved as U(VI) or present in the solid phases as adsorbed U(VI) or in U(VI) minerals. As the oxic water approaches the upgradient edge of the roll front the remaining dissolved oxygen in the groundwater is consumed by oxidation of siderite ($FeCO_3$) and elemental sulfur to form additional hematite and aqueous ferric thiosulfate complexes. The mineral ferroselite may also be found in this upgradient region of the roll front. The aqueous ferric thiosulfate complexes are transported further into the roll front, until conditions are sufficiently reducing to encounter ferrous sulfides (pyrite, marcasite), which reduces the iron back to dissolved Fe(II) and siderite. Further downgradient in the ore zone, the aqueous thiosulfate ions are reduced to sulfides and iron sulfide minerals are formed, as well as elemental selenium, and the dissolved U(VI) is reduced to U(IV), which is precipitated as U(IV) minerals.

The ISL uranium leach mining process involves injecting a lixiviant solution into the roll front ore deposit that will oxidize and dissolve the uranium, pumping the lixiviant and mixed groundwater from the aquifer, and processing the water to remove and recover the uranium that was dissolved. The lixiviant solution should both oxidize and dissolve the uranium in the ore minerals, but must also keep the uranium(VI) in solution by aqueous complexation, so that the removal from the aquifer is not hindered by U(VI) sorption or precipitation. Today, the most commonly used lixiviant solution is a sodium bicarbonate solution saturated with oxygen gas or air. The oxygen oxidizes the U(IV) minerals in the ore, e.g. uraninite and coffinite, and also oxidizes other reduced minerals, such as the iron sulfides. Thus, the chemically reducing conditions that are generally present in the ore zone prior to the mining operation are changed by the oxidation of Fe and S in the mined subsurface region. The reduced iron in sulfide minerals (e.g., pyrite, marcasite) is oxidized to Fe(III) and precipitated as iron oxides and oxyhydroxides. The sulfur is oxidized to sulfate and withdrawn from the aquifer with the lixiviant solution.

It is not well known to what extent the reduced minerals are oxidized in a typical ISL mining operation. Schmidt (1989) stated that 86% of the uranium in the Ruth (Wyoming) ore zone was recovered during an 11-month extraction of the subsurface with sodium bicarbonate solution with oxygen as the oxidant. Dissolved uranium concentrations peaked at 130 mg/liter (as U_3O_8) after 3 months of leaching and steadily declined thereafter to 56.3 mg/liter after 11 months. Dissolved sulfate peaked at 280 mg/liter after 2 months of leaching and declined toward the ambient background concentration of 100 mg/liter after 5 months of leaching (Schmidt, 1989). This suggests that sulfide minerals that were in good hydrologic contact with the groundwater were completely oxidized during the 11-month mining phase of operations. Reduced minerals that were present in low permeability regions may have been oxidized more slowly and incompletely during the mining phase.

4 GROUNDWATER RESTORATION

Groundwater restoration is a major portion of the cost of decommissioning an ISL facility (Table 1). Two widely used techniques for groundwater restoration are "groundwater sweep" and water treatment by reverse osmosis (RO).

Groundwater sweep involves pumping out one or more "pore volumes" from the ore zone region that has been leached and disposing of the groundwater (typically after recovering most of the uranium) to an evaporation pond or a deep disposal well (DOE, 1995). The technique is referred to as "sweeping" because the removed groundwater is replaced by fresh groundwater surrounding the leached ore zone region that moves into the mined ore zone due to the hydrologic depression caused by the pumping (Fig. 9), or uncontaminated water can be injected into the field through wells. The definition of the "pore volume" of water is the volume required to replace the water in the volume of aquifer that was mined. The volume of water required is calculated based on the estimate of porosity for the aquifer and the physical dimensions of ore zone region that was mined. The concept only applies to porous media and assumes that all water in the ore zone region is available for flow (USNRC, 2001). The physical dimensions of the ore zone region are based on the area of well field patterns and the thickness of the mined ore zone. The defined thickness may have some variation in that regulators can decide to consider the full aquifer thickness, the ore zone thickness, or the portion of the aquifer open to the well screens. The thickness used in the definition may depend on what is known about the vertical mixing of the leaching fluids during the mining phase of operations.

Original groundwater quality and regional climate may impact the extent to which groundwater sweep is used. The groundwater quality is poor at many of the ISL facilities in the south Texas plains. Because the regional climate in this portion Texas is characterized by considerable precipitation, pumping out the groundwater by groundwater sweep is acceptable because water use in the area is not significantly impacted. However, in the arid Wyoming basins, regulators are more sensitive to water use, and the use of high-quality, uncontaminated groundwater or surface water to replace the contaminated groundwater may not be approved (DOE, 1995). Typically, with respect to the contaminants associated with the ISL mining operations (uranium, chloride, radium, etc.), groundwater quality improves significantly during the groundwater sweep process (Schmidt, 1989; Rio Algom, 2001).

Groundwater sweep alone is typically insufficient and uneconomical for complete groundwater restoration. Because of heterogeneities in the aquifers, the fresh groundwater that is brought into the ore zone does not completely displace the residual lixiviant, and with increasing volume pumped a greater proportion of the volume pumped is the fresh groundwater (Deutsch et al., 1985). Many pore volumes of groundwater would need to be pumped in order to reach the original baseline conditions, perhaps millions of gallons for a 10-acre leach field. This is particularly true if ammonium ion is used in the lixiviant, because after ion exchange, the ammonium ion desorption is slow to occur. Finally, as described further below, groundwater sweep may cause oxic groundwater from upgradient of the deposit to enter into the mined area, making it more difficult to re-establish chemically reducing conditions.

In order to return the groundwater to baseline or class-of-use conditions, it is usually necessary to use an above-ground treatment method to remove contamination from the mined zone while minimizing the disposal of groundwater in evaporation

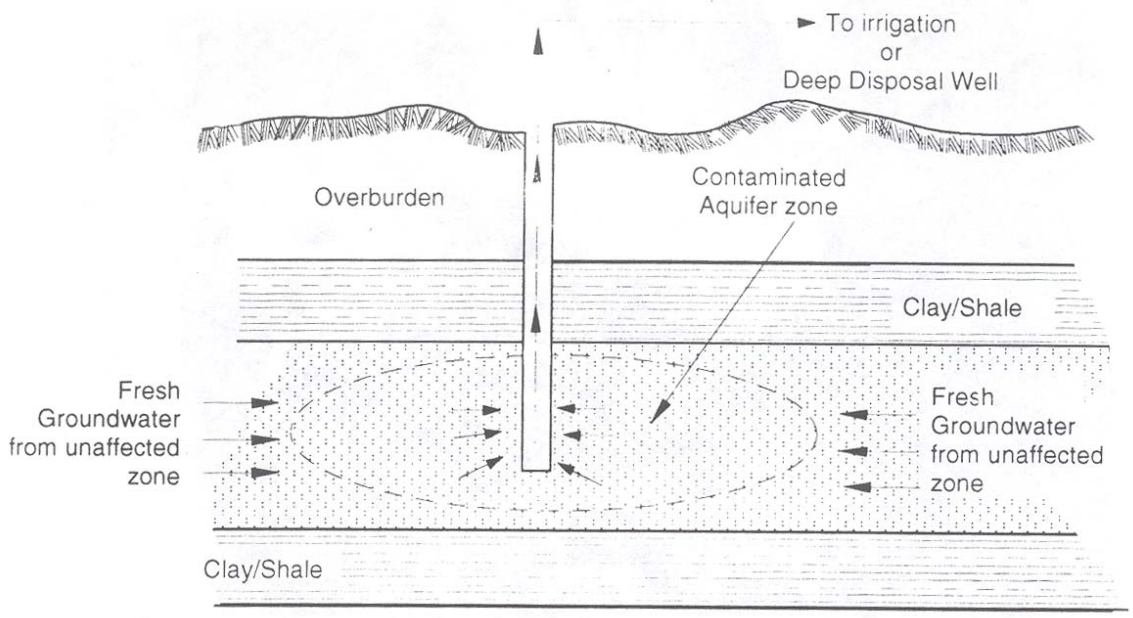

Figure 9. Schematic of the groundwater sweep process, whereby contaminated ground water from the ISL mining operation is removed by pumping (U.S. Department of Energy, 1995).

ponds. Reverse osmosis (RO) is the most common method used to treat the contaminated groundwater, typically after a groundwater sweep of one pore volume. The first pore volume of groundwater cannot be easily treated by reverse osmosis because of the high concentrations of various contaminants that would clog the RO membranes. In addition, during groundwater sweep, the pumped water is processed through the uranium recovery plant to recover additional uranium. A significant portion (>10%) of the uranium mined at a particular location may be recovered during the groundwater restoration process (Schmidt, 1989).

In RO treatment, groundwater is pumped out of the mined zone and filtered, and the pH is usually lowered to prevent calcium carbonate precipitation and plugging of the RO membranes. The water then passes through the RO membranes at high pressure, and the treated water (RO permeate) is re-injected into the contaminated aquifer zone using the same well field system that was used during mining to continue the process of displacing the residual lixiviant. The concentrate liquid waste from the RO units is either fed to evaporation ponds or dried for disposal at a licensed facility. Groundwater recirculation is usually practiced during the RO treatment phase of restoration by alternating which pumps in the well field are used for re-injection and pumping of groundwater.

Many aquifers are characterized by porosity in which relatively immobile groundwater resides in regions of relatively low permeability. Because of this characteristic, it is very difficult to remove all of the lixiviant and its associated contaminants from the subsurface by pumping. Lixiviant in the relatively immobile groundwater and mineral surfaces exposed to that groundwater will continue to provide a source of contamination even after long periods of pumping and treatment.

Because of this residual contamination, chemicals, such as hydrogen sulfide, sodium hydrosulfide, or alkaline solutions, may be added to water injected into the aquifer in

the latter stages of restoration. The purpose of the chemical additions is usually to establish chemically reducing conditions in the aquifer. As will be discussed below, the solubilities of many of the metal and metalloid contaminants of concern (e.g. uranium, selenium, molybdenum, and arsenic) are decreased under reducing conditions.

In general, it can be expected during the groundwater sweep operation that fresh groundwater will enter the ore zone region that has been that mined from regions upgradient and downgradient of the roll front deposit. Because the typical roll front deposit usually has oxic water upgradient of the deposit and reducing water downgradient of the deposit, and the ore zone region has been extensively altered by oxidation during the mining operation, the redox status of the system after groundwater sweep is very difficult to predict. Because the ore zone typically was under chemically reducing conditions prior to mining, it has frequently been argued or assumed that the natural reducing conditions will return after a period of time. However, it is difficult to predict how much time is required or even if the reducing conditions will return via natural processes. The mining disturbance introduces a considerable amount of oxidant to the mined region and may oxidize all of the pyrite associated with the original ore zone.

There are few published studies of evolving water quality during groundwater restoration in the literature. Rio Algom (2001) conducted a pilot scale study of groundwater restoration; the study includes pre-mining baseline data for water quality and water quality data for selected solutes during groundwater sweep, reverse osmosis treatment, and injection of hydrogen sulfide gas. The Crownpoint Uranium Solution Mining Project provided average water quality data for baseline, post-mining, and groundwater stabilization conditions after pumping 16.7 pore volumes (USNRC, 1997). Crow Butte Resources (2000; 2001) has provided water quality data for baseline, post-mining, groundwater restoration phase (including hydrogen sulfide injection), and the groundwater stabilization phase for the Crow Butte Uranium Project (Nebraska). Some groundwater stabilization water quality data are available from the Bison Basin (Wyoming) pilot scale groundwater restoration project (Altair Resources, Inc., 1988; Moxley and Catchpole, 1989; Johnson, 1989).

The study by Schmidt (1989) of the Ruth ISL facility (Wyoming) may provide the most detailed and comprehensive study of evolving temporal water quality conditions during mining and groundwater restoration. Because of the comprehensiveness of this report, it was selected as a test case for geochemical modeling simulations conducted as part of this investigation. The data from Schmidt (1989) suggest that the mined zone remained oxic during the first year of groundwater restoration that included groundwater sweep and reverse osmosis treatment. Only the injection of hydrogen sulfide into the system at the end of one year of treatment (at 0.5 g/liter and total of 113 kg per well) returned the mined zone of the aquifer to reducing conditions (Schmidt, 1989). The hydrogen sulfide was added to the RO permeate during the last two months of the RO treatment phase. Several other ISL facilites have also indicated that hydrogen sulfide gas injection is needed as a part of the groundwater restoration process (Rio Algom, 2001; Crow Butte Resources, 2000; Altair Resources, 1988; and USNRC, 1997).

The effects of the hydrogen sulfide injection into the aquifer were significant at the Ruth ISL for several months (Schmidt, 1989). Hydrogen sulfide gas was injected for six weeks at an average concentration of 500 mg/liter. At the end of the hydrogen sulfide gas injection, the pH in the aquifer had dropped from 8.6 to 6.3, sulfate concentrations had risen from 28 mg/liter to 91 mg/liter, and the dissolved uranium, selenium, arsenic, and vanadium

concentrations decreased markedly (one order of magnitude or more).

After the injection was completed, the recirculation of groundwater/RO permeate was ceased and the aquifer was allowed to stabilize, with monthly groundwater sampling conducted for one year (Schmidt, 1989). The sampling results during the groundwater stabilization period suggest that the reducing conditions may have not been maintained for the entire year. Dissolved iron and manganese concentrations increased during the first 5 months and then abruptly began to decline. As their abrupt decline began, dissolved uranium, arsenic, and radium began to increase. Vanadium concentrations declined and selenium concentrations were not stated.

5 MODELING OF THE GROUNDWATER RESTORATION PROCESS

5.1 Flow Modeling

Hydrologic considerations in the groundwater restoration process for ISL uranium mining facilities and the definition of a pore volume are discussed elsewhere (USNRC, 2001). The focus of this report is on the main geochemical processes that need to be considered, and thus, detailed discussions of flow modeling during groundwater restoration are beyond the scope of the report. Typically, the mined ore zone region is modeled as a well-mixed linear reservoir with homogeneous properties. As a first approximation, results suggest that this may be a reasonable assumption during groundwater sweep of one pore volume, for solutes that have near conservative behavior (Rio Algom, 2001). That is, the solutes that are not significantly retarded by sorption or precipitation processes during the chemical conditions for groundwater sweep, e.g. chloride, bicarbonate, sulfate, sodium, are withdrawn at concentrations expected from a well-mixed linear reservoir as a conceptual model.

It has been observed, however, that lixiviant solutes are not always withdrawn at consistently declining concentrations as expected by the mixed reservoir concept, due to subsurface heterogeneities and minor excursions of lixiviant solution away from the well field. In addition, after the initial pore volume is removed, considerable tailing is observed in the extraction of chemically reactive solutes, such as uranium, arsenic, and selenium, suggesting that retardation is stronger at lower concentrations of lixiviant and that there may be a significant fraction of the porosity that is not well connected hydrologically with the main flow channels (Schmidt, 1989). To consider, these processes, a dual porosity (mobile and immobile fluid) model was considered in this report as part of the reactive transport modeling.

Reactive transport simulations in this report were conducted with the computer code PHREEQC Interactive (Parkhurst and Appelo, 1999), version 2.8.0.0 (released April 15, 2003). A one-dimensional flow model with 10 cells was used, with 5 cells connected with mobile flowing transferred one cell to the next by advective mixing, and with 5 cells containing immobile water that transferred solutes to a mobile cell via a mass transfer relationship (Fig. 10). Total porosity for a hypothetical mined ore zone was assumed to be 20%, with 30% in the mobile cells and 10% in the immobile cells. Water within each cell (mobile and immobile) was assumed to be well mixed by PHREEQC. A time step equivalent to 0.2 pore volumes, and a dimensionless dispersivity value of 0.002 was used in all of the simulations. Values of the dimensionless mass transfer coefficients of 10 and $1.0 \cdot 10^{-4}$ were compared.

5.2. Geochemical Modeling of Groundwater Sweep and Treatment

As a test case, groundwater restoration data (Fig. 11) for the Ruth ISL pilot scale study were used for geochemical modeling (Schmidt, 1989). In all of the simulations, one pore volume was withdrawn first by groundwater sweep. Following that, an additional 3.2 pore volumes was withdrawn with the assumption that the groundwater was treated by RO and that an equal volume of water was re-injected using the same well field as was used during mining. The geochemical data shown in Figure 11 were illustrated versus time in the original report (Schmidt, 1989). It was stated in the report that 4.2 pore volumes (7.2 million gallons) were removed during the 239 days of

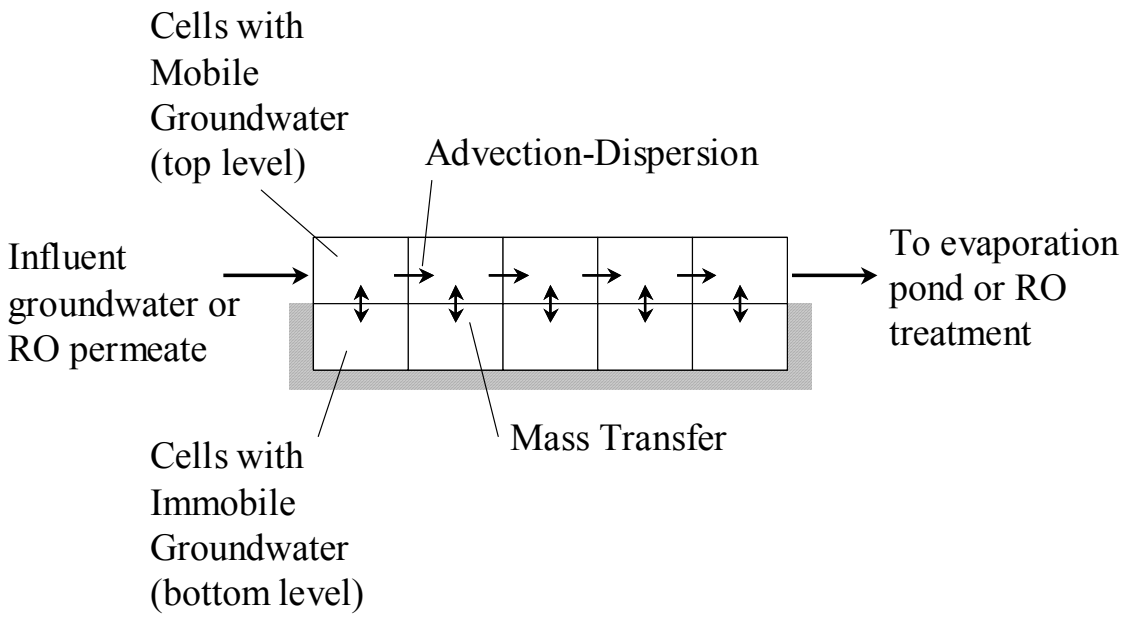

Figure 10. Schematic of the conceptual model used to describe flow within the mined zone during groundwater restoration.

groundwater restoration. Based on an assumption of a uniform pumping rate, the data in Figure 11 were re-plotted from the original report to be shown in terms of pore volumes.

For the re-injected water, it was assumed that the chemical composition was described by a mixture of 25% untreated groundwater and 75% pure water. In several simulations, hydrogen sulfide was added to the re-injected water during pore volumes 3.0 to 3.6, and the RO treatment/re-injection process was simulated up to a total pore volume withdrawal of 100 pore volumes. Table 2 shows a summary of the reactive transport simulations described in detail in this report. PHREEQC has the capability to do kinetic modeling, but only chemical equilibrium simulations were considered for this report. An example PHREEQC input file used for Simulation 8 is given in Appendix A.

Perhaps the most critical aspect of groundwater restoration at ISL uranium mining facilities is the redox status of the mined ore zone. As explained above, the uranium roll front deposits are typically located at a redox boundary in the subsurface. While the conditions within the ore zone are usually chemically reducing before the mining operation begins, it is likely that the conditions are oxidizing by the end of the leaching phase. Uranium recovery during mining is always less than 100%, and so it can be argued that uraninite is still present in the subsurface; however, it is likely that the remaining uraninite is located in regions that are in poor hydrologic contact with the groundwater and lixiviant. Thus, the influence of remaining uraninite and pyrite in the mined ore zone on the redox status of the groundwater may be quite small, and it cannot be assumed that reducing conditions will return to the mined ore zone by "natural" processes. In addition, during groundwater sweep, oxidizing water that is hydrologically upgradient of the mined ore zone or reducing water from downgradient of the ore zone may be drawn into the mined zone.

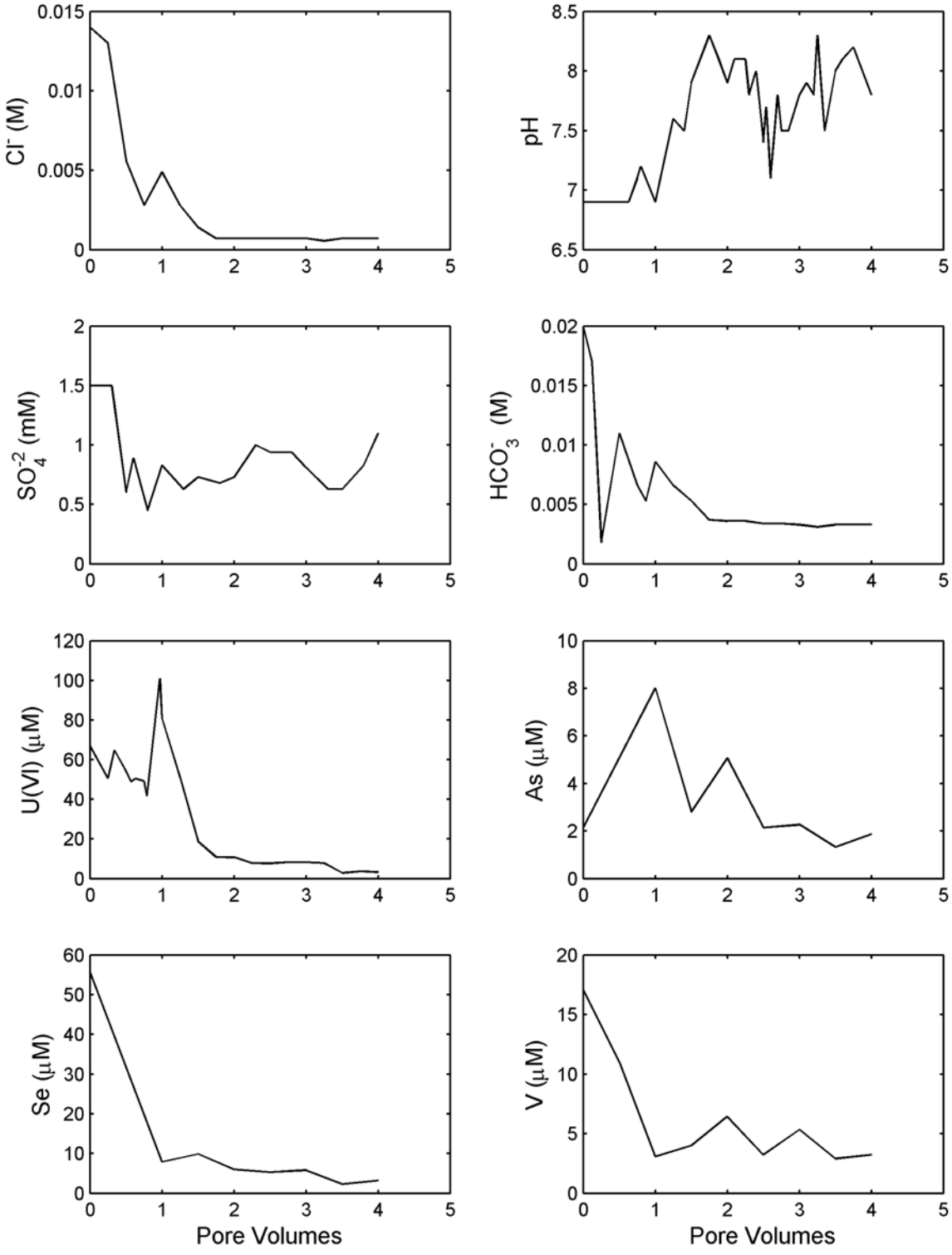

Figure 11. Groundwater chemical data collected during the groundwater sweep and reverse osmosis treatment phases of groundwater restoration at the Ruth (Wyoming) ISL pilot plant; data from Schmidt (1989).

Table 2. Summary of Reactive Transport Simulations for Sweep and Treatment Phases of Groundwater Restoration

			Initial phase concentration[a]			
No.	Injection water amendments during RO treatment	Mineral phases	Mobile zone	Immobile zone	Mass transfer coefficient	Comment
1	1st PV: 9.38×10^{-5} M O_2 After 1st PV[b]: 3.13×10^{-5} M O_2 2.6×10^{-3} M $NaHCO_3$	Calcite Goethite	0.4 0.03	0.4 0.03	10	Aerobic sweep; no H_2S treatment
2	1st PV: 9.38×10^{-5} M O_2 After 1st PV: 3.13×10^{-5} M O_2 2.6×10^{-3} M $NaHCO_3$	Calcite Goethite	0.4 0.03	0.4 0.03	10^{-4}	Same as 1 but slower mass transfer between zones
3	After 1 PV: 3.13×10^{-5} M O_2 2.6×10^{-3} M $NaHCO_3$	Calcite Goethite	0.4 0.03	0.4 0.03	10	Similar to 1 with reducing water influent in first PV
4	1st PV: 9.38×10^{-5} M O_2 After 1st PV: 3.13×10^{-5} M O_2 2.6×10^{-3} M $NaHCO_3$	Calcite Goethite Pyrite Se(s)	0.4 0.03 0.0 0.00253	0.4 0.03 0.0 0.00253	10	Similar to 1 with Se(s) in mobile and immobile zones; pyrite precipitation allowed
5	1st PV: 9.38×10^{-5} M O_2 After 1st PV: 3.13×10^{-5} M O_2 2.6×10^{-3} M $NaHCO_3$	Calcite Goethite Pyrite Se(s) Uraninite Orpiment $FeSe_2$	0.4 0.03 0.0 0.00253 0.0 0.0 0.0	0.4 0.03 0.0668 0.0253 0.0168 0.0 0.0	10	Similar to 4 with pyrite and uraninite present initially in the immobile zone and elemental Se at a higher concentration in the immobile zone
6	1st PV: 9.38×10^{-5} M O_2 After 1st PV: 3.13×10^{-5} M O_2 2.6×10^{-3} M $NaHCO_3$	Calcite Goethite Pyrite Se(s) Uraninite Orpiment $FeSe_2$	0.4 0.03 0.0 0.00253 0.0 0.0 0.0	0.4 0.03 0.0668 0.0253 0.0168 0.0 0.0	10^{-4}	Similar to 5 with smaller mass transfer coefficient

Table 2. Summary of Reactive Transport Simulations for Sweep and Treatment Phases of Groundwater Restoration (continued)

7	1st PV: 9.38x10^{-5} M O_2 1-3 PV: 3.13x10^{-5} M O_2 2.6x10^{-3} M $NaHCO_3$ 3-3.6 PV: 0.0078 M H_2S 1.17x10^{-2} M $NaHCO_3$ 3.6-5 PV: 3.13x10^{-5}M O_2 2.6x10^{-3} M $NaHCO_3$	Calcite Goethite Pyrite Se(s) Uraninite Orpiment $FeSe_2$	0.4 0.03 0.0 0.00253 0.0 0.0 0.0	0.4 0.03 0.0 0.00253 0.0 0.0 0.0	10	Similar to 4 with H_2S added and uraninite, orpiment, and FeS_2 allowed to precipitate.
8	1st PV: 9.38x10^{-5} M O_2 1-3 PV: 3.13x10^{-5} M O_2 2.6x10^{-3} M $NaHCO_3$ 3-3.6 PV: 0.0078 M H_2S 1.17x10^{-2} M $NaHCO_3$ 3.6-5 PV: 3.13x10^{-5}M O_2 2.6x10^{-3} M $NaHCO_3$	Calcite Goethite S(s) Se(s) Uraninite Orpiment $FeSe_2$	0.4 0.03 0.00 0.00253 0.0 0.0 0.0	0.4 0.03 0.00 0.00253 0.0 0.0 0.0	10	Similar to 7 except pyrite was not allowed to precipitate. Elemental sulfur allowed to precipitate.
9	1st PV: 9.38x10^{-5} M O_2 1-3 PV: 3.13x10^{-5} M O_2 2.6x10^{-3} M $NaHCO_3$ 3-3.6 PV: 0.0016 M H_2S 1.17x10^{-2} M $NaHCO_3$ 3.6-5 PV: 3.13x10^{-5}M O_2 2.6x10^{-3} M $NaHCO_3$	Calcite Goethite Se(s) Uraninite Orpiment $FeSe_2$	0.4 0.03 0.00253 0.0 0.0 0.0	0.4 0.03 0.00253 0.0 0.0 0.0	10	Similar to 8 except less H_2S added and elemental sulfur not allowed to precipitate.
10	1st PV: 9.38x10^{-5} M O_2 1-3 PV: 3.13x10^{-5} M O_2 2.6x10^{-3} M $NaHCO_3$ 3-3.6 PV: 0.0078 M H_2S 1.17x10^{-2} M $NaHCO_3$ 3.6-5 PV: 3.13x10^{-5}M O_2 2.6x10^{-3} M $NaHCO_3$	Calcite Goethite Se(s) UO_2(am) Orpiment $FeSe_2$ FeS(ppt)	0.4 0.03 0.00253 0.0 0.0 0.0 0.0	0.4 0.03 0.00253 0.0 0.0 0.0 0.0	10	Similar to 8 except FeS(ppt) and UO_2(am) allowed to precipitate

[a] – Moles of phase per liter of water; a phase concentration equal to zero indicates that the phase can precipitate but is not present initially in the simulations.
[b] – Pore volumes.

However, as will be shown below, it is the presence of reduced minerals (either remaining or precipitated with a reducing agent) that has the greatest influence on the concentrations of elements of greatest concern (e.g., uranium, selenium, arsenic) at the final stage of groundwater restoration.

The thermodynamic database used in the simulations was compiled as a combination of values from other databases and is given in Appendix B. The PHREEQC.DAT database was used, with additional data added for reactions of uranium, selenium, arsenic, and vanadium. Aqueous and mineral phase reactions of selenium, arsenic, and vanadium were added from either the WATEQ4F.DAT or MINTEQ.DAT databases that are distributed with the PHREEQC program,

(http://water.usgs.gov/software/geochemical.html). Aqueous and mineral phase reactions of uranium were modified as needed to be consistent with the uranium database of the Nuclear Energy Agency (NEA) as described in Grenthe et al. (1992) and Silva et al. (1995). These reactions are also given in Davis and Curtis (2003). The stability constants for the adsorption reactions of arsenate, arsenite, and selenite were estimated using selected experimental datasets given in Dzombak and Morel (1990) and for uranium(VI) from selected data given in Waite et al. (1994). The selected experimental adsorption data for each species were fit with a single non-electrostatic surface complexation reaction using a single site model. A key attribute of this modeling approach is that, unlike modeling with a constant retardation factor, U(VI) retardation in the simulations is dependent on the chemical conditions. For example, uranium(VI) retardation will increase as the bicarbonate concentration decreases (Davis and Curtis, 2003). An adsorption constant was also determined for vanadate, V(+5), from data in Dzombak and Morel (1990), but this constant was only used for comparison in Simulation 19, because no sorption constant was available for V(+4), the most stable oxidation state under ordinary conditions. As is shown below, the results were affected significantly by inclusion of V(+5) sorption, and the authors felt the results were incomplete without a consideration of V(+4) sorption.

A non-electrostatic model was used (rather than the diffuse layer model of Dzombak and Morel), because it is expected that the surface charge-pH relationship for natural aquifer materials will be different than that observed for pure hydrous ferric oxide on which the Dzombak and Morel model is based. The experimental data selected for fitting the constants were collected in the pH range 6.5-11, and thus the adsorption stability constants should not be used for simulations outside of this pH range. Stability constants were not determined for selenate or sulfate adsorption because adsorption of these solutes was assumed to be negligible for the chemical conditions that were modeled.

The stability constants were determined using a specific site density of 3.84 μmoles of sites/m^2 of surface area (Dzombak and Morel, 1990; Davis and Kent, 1990), and thermodynamic consistency requires that this surface site density be used in tandem with the stability constants. The surface site concentration is entered as input into the PHREEQC input file; for all simulations given in this report (except Simulations 18 and 19), a site concentration of 4.0×10^{-4} moles/liter was used. This value was chosen based on an assumed porosity (20%), the conversion factor of 3.84 μmoles of sites/m^2 of surface area, and an arbitrary example surface area value of 0.13 m^2/g for the aquifer sediments in the mined zone. To apply this approach to a particular field site, estimates of the relevant porosity and surface area at the site should be used to determine actual surface site concentrations. In addition, it must be noted that the adsorption reaction stability constants used in the example simulations of this report are based on experimental data for adsorption on pure hydrous ferric oxide, which is highly reactive, and therefore, not representative of real aquifer sediments. It is recommended that adsorption experiments be carried out with actual sediments from the field site under consideration, in order to replace the adsorption constants in the database given in Appendix B. The adsorption constants for real sediments may be several orders of magnitude smaller, resulting in greater mobility for uranium, arsenic, selenium, and vanadium. The adsorption constants of Dzombak and Morel (1990) that are normally supplied with PHREEQC were deleted from the database given in Appendix B.

The initial chemical conditions in the groundwater of the mined ore zone (Table 3) were those given for the Ruth ISL pilot plant at the onset of the groundwater restoration (Schmidt, 1989). For most of the

Table 3. Initial Chemical Conditions in the Groundwater of the Mined Zone Prior to the Groundwater Sweep Simulations

Element	Concentration (moles/L)	Concentration (mg/L)	Comments
Sodium	3.63E-2	835	
Potassium	2.56E-4	10	
Calcium	1.13E-3	45.3	Calculated concentration from equilibration with calcite
Magnesium	7.8E-4	19	
Chloride	1.64E-2	581	Calculated concentration based on charge balance
Total sulfur	1.52E-3	146	Sulfate and sulfide concentrations determined from assumed pe
Bicarbonate	2.1E-2	1280	Calculated from alkalinity
Fe(III)	5.33E-14	<0.001	Calculated concentration from equilibration with goethite
Fe(II)	4.55E-21	<0.001	Calculated concentration determined from Fe(III) and assumed pe
Uranium(VI)	6.69E-5	15.9	U(IV) concentration calculated from assumed pe
Total arsenic	2.14E-6	0.16	As(VI) and As(III) determined from assumed pe
Total selenium	5.57E-5	4.4	Se(VI) and Se(IV) determined from assumed pe
Total vanadium	1.7E-5	0.87	V(V), V(IV), V(III), and V(II) determined from assumed pe
pH	7.0		Standard pH units
pe	12.0		Assumed
Temperature	25		Assumed for calculations

simulations, it was assumed that the initial groundwater in the mined ore zone region was oxic, with a pe of 12 and at chemical equilibrium with the mineral phases calcite and goethite. For many of the simulations, it was assumed that elemental selenium was also initially present (at 50 ppm) in the cells with mobile water, which yielded an initial pe of 2.9. In other simulations it was assumed that, in addition to the 50 ppm of elemental selenium, elemental selenium (500 ppm), pyrite (2000 ppm), and uraninite (1000 ppm as U) were initially present in the cells with immobile water, yielding an initial pe of –3.8 in the immobile cells. Preliminary attempts at simulations were made with pyrite or uraninite in the mobile cells as an initial condition. It was not possible using a chemical equilibrium approach for these phases to be present and have a water composition consistent with the initial conditions observed for the Ruth ISL (Table 3). If the presence of pyrite or uraninite was assumed, then the initial dissolved concentrations of uranium, arsenic, selenium, and vanadium were all very low, which is not what was observed. It would be possible to assume that these minerals were initially present using a kinetic modeling approach, but that approach was not tested in the results presented here.

Influent water to the cells during the initial groundwater sweep of one pore volume had the pre-operational baseline chemical conditions for groundwater (Schmidt, 1989) observed for the Ruth ISL (Table 4). The redox status of the groundwater was varied to simulate either oxic or anoxic water entering the mined ore zone region. Most simulations were run with oxic influent water, with $9.4 \cdot 10^{-5}$ moles/liter of dissolved oxygen gas (O_2) added to (mixed into) the water, equivalent to 3 mg/liter and yielding an initial pe of 12 for the influent water. One simulation (Simulation 3) was run with reducing water as influent water, with an initial water composition containing $7 \cdot 10^{-7}$ moles/liter of Fe(II) and $1 \cdot 10^{-8}$ moles/liter of Fe(III). For the anoxic influent case, the pe (-1.5) of the influent groundwater was determined by assumed initial Fe(II)/Fe(III) concentrations.

After the initial pore volume removal by groundwater sweep, the influent water to the column was switched to a mixture of water exiting the column with pure water, in the ratio of 25% effluent and 75% pure water. The purpose of the water mixture was to simulate the recirculation of reverse osmosis permeate and make-up water into the well field (Schmidt, 1989). Any dissolved oxygen in the effluent water remained in the water mixture, but its concentration was diluted by the pure water like other dissolved solutes.

However, it was assumed that some dissolved oxygen would unavoidably enter

Table 4. Chemical Conditions in Oxic Influent Groundwater to the Mined Zone During Groundwater Sweep and Stabilization

Element	Concentration (moles/L)	Concentration (mg/L)	Comments
Sodium	4.78E-3	110	
Potassium	1.1E-4	4.3	
Calcium	6.1E-3	240	Calculated concentration from equilibration with calcite
Magnesium	8.2E-5	2.0	
Chloride	1.25E-3	44.3	Calculated concentration based on charge balance
Total sulfur	1.04E-3	100	Sulfide concentration determined from calculated pe
Bicarbonate	2.62E-3	160	Calculated from alkalinity
O_2(g)	2.2E-4	7.0	Calculated from 0.2 atm O_2(g)
Uranium(VI)	6.0E-8	0.014	U(IV) concentration calculated from calculated pe
Total arsenic	1.3E-7	0.010	As(VI) and As(III) determined from calculated pe
Total selenium	1.3E-7	0.010	Se(VI) and Se(IV) determined from calculated pe
Total vanadium	2.75E-7	0.014	V(V), V(IV), V(III), and V(II) determined from calculated pe
pH	7.0		Standard pH units
Temperature	25		Assumed for calculations

the permeate during the RO operation, and $3.1 \cdot 10^{-5}$ moles/liter of O_2 gas was added to the mixture of permeate and pure water, equivalent to 1 mg/liter, prior to its re-injection into the column. In addition, sodium bicarbonate ($NaHCO_3$) was added to the water mixture at a concentration ($2.6 \cdot 10^{-3}$ moles/liter) equivalent to the pre-operational baseline bicarbonate concentration in order to stabilize the pH near 8.5, its baseline value. In several simulations, hydrogen sulfide gas (H_2S) at a concentration of $7.8 \cdot 10^{-3}$ or $1.56 \cdot 10^{-3}$ moles/liter was added to the mixture of 25% effluent and 75% pure water during pore volumes 3.0 to 3.6, prior to re-injection to the column. In these cases, no dissolved oxygen was mixed into the re-injected water. In four simulations, for those time steps that H_2S was added to the water mixture before re-injection into the column, sodium bicarbonate ($NaHCO_3$) was added to the water mixture at a higher concentration ($1.2 \cdot 10^{-2}$ moles/liter) to stabilize the pH.

5.2.1 Modeling Results

The results for the most oxic conditions (Simulation 1) are given in Figure 12. In this case, the initial conditions in the column were oxic, no reduced mineral phases were initially present, and oxic water entered the column during the groundwater sweep. Note that the pe value peaked at about 13.3 after the groundwater sweep and stayed above 12 throughout the first 4 pore volumes pumped. The pH increased from 7 to about 8.4 during the restoration, in very good agreement with the results (Fig. 11) observed for the Ruth groundwater restoration (Schmidt, 1989). Most of the solutes decreased markedly after the first pore volume was removed by the groundwater sweep, except arsenic. Arsenic was present predominantly in all the column cells as As(V), and its dissolved concentration at pH 7 was very low due to strong sorption. However, after the first pore volume, the pH rose steadily to 8.5, the As concentration peaked at about 10 μM, and then continued to increase after a brief decline. The small delayed peak in the chloride concentration at 2.4 pore volumes was due to the slow transfer of chloride out of the immobile groundwater cells (mass transfer coefficient = 10). Similar small peaks were observed for all the parameters at 2.4 pore volumes (a small valley for pH) except As(V), which appeared near 3 pore volumes due to retardation by sorption. After the 4.2 pore volumes of pumping and treatment, the concentrations of uranium (1.4 μM), arsenic (24 μM), and selenium (0.7 μM) were still considerably above their baseline values (0.06, 0.13, and 0.13 μM, respectively). The arsenic concentrations were still increasing with increasing pore volumes (Fig. 12), however, the dissolved uranium concentration was essentially constant with pore volumes. It appeared it would take many more pore volumes of pumping to achieve the baseline uranium concentration.

The field observations for the Ruth ISL facility (Fig. 11) have some similar characteristics to the prediction. Small secondary peaks in chloride, bicarbonate, and sulfate concentrations were observed just after one estimated pore volume of pumping, possibly due to secondary porosity effects on transport. The pH rose to near 8 at about two pore volumes. After 4 pore volumes, the uranium concentration decreased to about 3 μM, similar to the 1.4 μM simulated. The observed arsenic data had two peaks, one at about 8 μM at one pore volume, and a second peak at 5.1 μM at two pore volumes (Fig. 11). Although the breakthrough was more complex in the field observations, the simulations did predict an increase in dissolved arsenic, which was observed initially. The selenium concentration predicted after 4 pore volumes (0.7 μM) was underestimated from that observed (3 μM).

Simulation 2 (Fig. 13) shows predicted results for the same set of conditions as in Simulation 1 except that the mass transfer coefficient was made 5 orders of magnitude

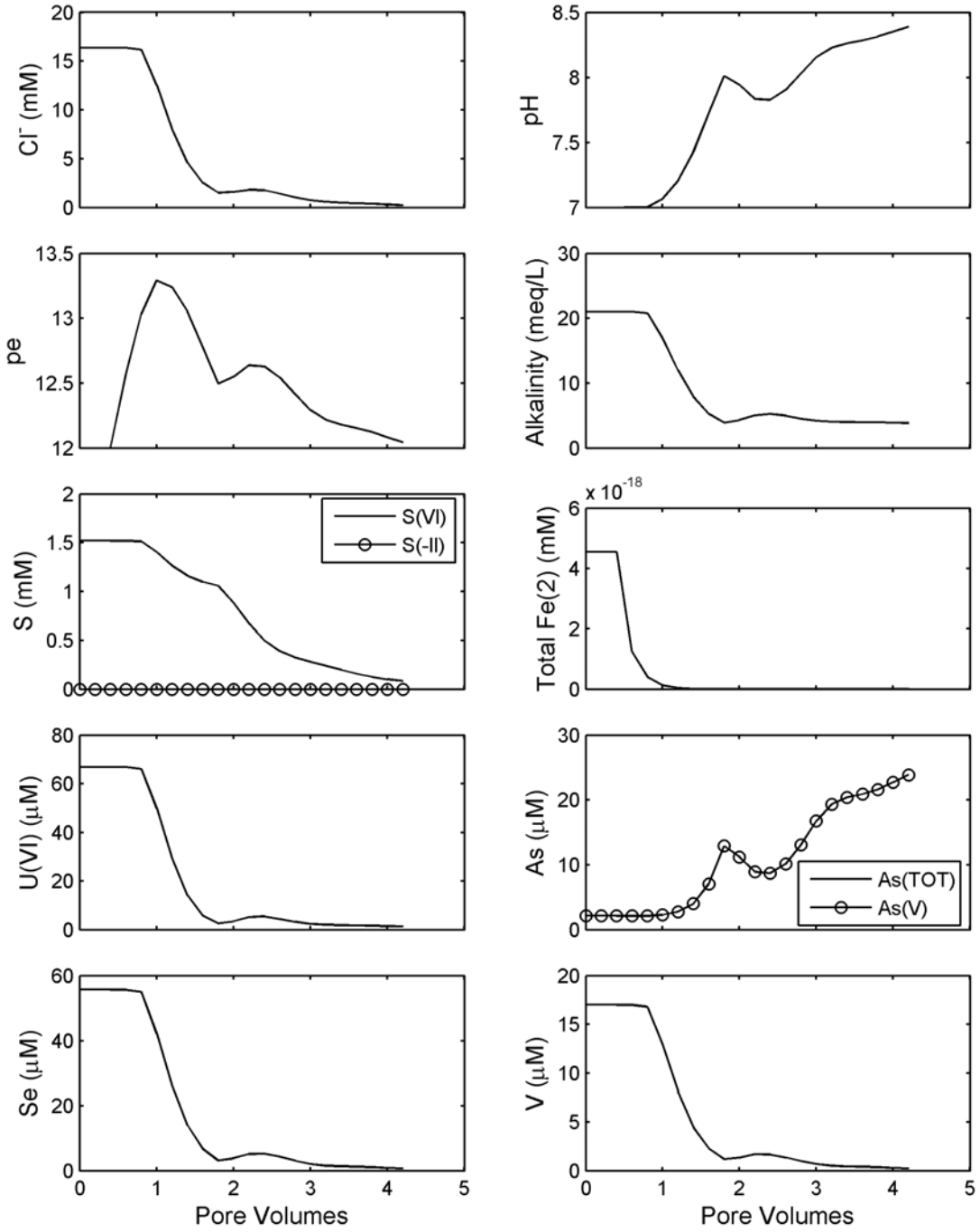

Figure 12. Simulation 1 results. Oxic influent groundwater. Calcite and goethite initially present. Mass transfer coefficient = 10.

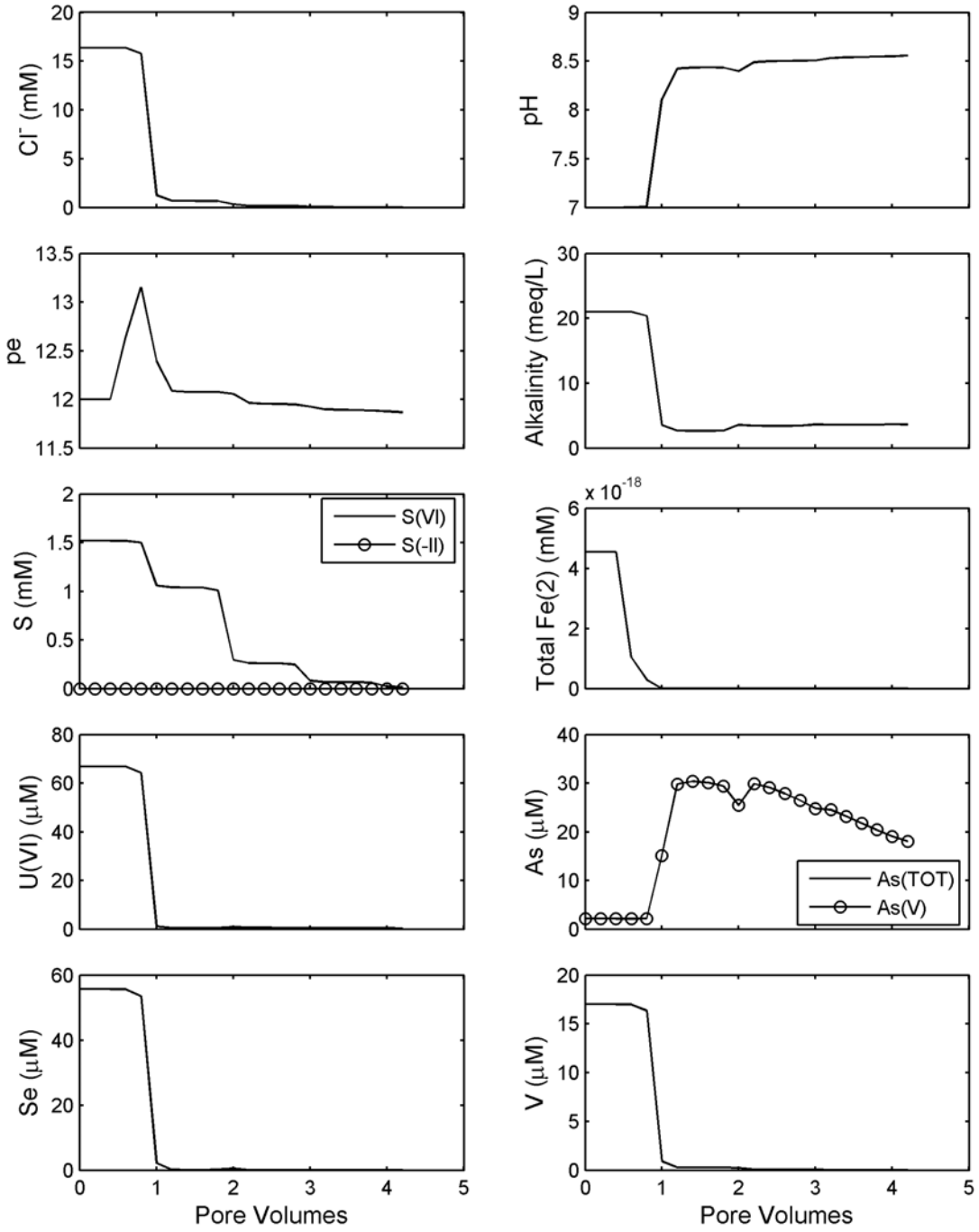

Figure 13. Simulation 2 results. Oxic influent groundwater. Calcite and goethite initially present. Mass transfer coefficient = 10^{-4}.

smaller ($1.0 \cdot 10^{-4}$ instead of 10). Because of the slower mass transfer between the mobile and immobile cells, the effects of the immobile cells on breakthrough are much smaller. For example, the changes in pH and the chloride, bicarbonate, uranium, selenium, and vanadium concentrations are much more abrupt after the first pore volume has been pumped. In addition, the As(V) concentration rises much higher because of the greater change in pH at one pore volume, causing faster and more extensive desorption of As(V) leading to

decreasing As(V) concentration after 2.5 pore volumes. The predicted uranium concentration after 4 pore volumes was again relatively constant at 0.4 μM. The predicted arsenic, selenium, and vanadium concentrations were all considerably smaller after 4 pore volumes than observed in Simulation 1. Comparison of the two predictions with the field observations suggests that Simulation 1 gives a better description of the field data.

Simulation 3 (Fig. 14) presents predicted results for the same conditions as in Simulation 1 except that anoxic groundwater was the influent water to the column during groundwater sweep (the first pore volume). The effects are only seen in the predicted pe of the water leaving the column, especially just after one pore volume. After the first pore volume, the pe begins to rise again because of the dissolved oxygen that is mixed with the permeate before re-injection. However, the difference in pe is too small to observe any significant difference between Simulations 1 and 3. Thus, whether oxic or reducing waters were drawn into the mined ore zone by groundwater sweep was relatively unimportant in the Ruth ISL case for the early pore volume predictions. It could be more important if the water was more reducing and contained dissolved sulfide, but this was not tested.

Simulation 4 (Fig. 15) presents predicted results for the same conditions as in Simulation 1 except that 50 ppm of elemental selenium were assumed to be present in the column as an initial condition. Essentially no difference from Simulation 1 was observed in the breakthrough curves for pH and the chloride and bicarbonate concentrations. However, the pe of water exiting the column was considerably lower than in Simulation 1, due to the presence of the elemental selenium. The assumed conditions for Simulation 4 had very little effect on the breakthrough curves for uranium, arsenic, or vanadium. The conditions were not sufficiently reducing to form a meaningful quantity of U(IV) or As(III) in the column. However, the effect on the breakthrough curve for selenium was very significant. In Simulation 1, dissolved Se decreased from 56 to 3.8 μM at 4 pore volumes. In Simulation 4, dissolved Se increased from an initial value of 44 μM to 50 μM at 1.8 pore volumes and then decreased to 39 μM at 4 pore volumes. The initially lower dissolved selenium concentration in Simulation 4 resulted because selenium solubility was controlled by elemental selenium. The subsequent increase in dissolved selenium was due to the oxidation of elemental selenium by oxygen entering the column with the re-injected water. The pe did not increase, but the pe is also dependent on pH, which was increasing.

The observed breakthrough of selenium in the field was complex. In general, a decrease was observed from the initial value, but some increases in dissolved selenium during breakthrough also occurred, and the final concentration at 4 pore volumes was intermediate between that of Simulations 1 and 4, suggesting that a smaller amount of elemental selenium may have been present or that selenium was controlled by a non-equilibrium process. A simulation was also run with reducing water entering the column during groundwater sweep and elemental selenium present as an initial condition. Essentially no difference from Simulation 4 was observed (prediction not shown).

Simulation 5 (Fig. 16) presents predicted results for the same conditions as in Simulation 4 except that elemental selenium was present at a higher concentration (500 ppm), along with pyrite (2000 ppm), and uraninite (1000 ppm as U) in the cells with immobile water, as an initial condition. The presence of the reducing minerals lowered the pe of the water exiting the column, especially at the later pore volumes. The effect was significant on the breakthrough curves for uranium, selenium, and arsenic. Uranium decreased much more quickly to

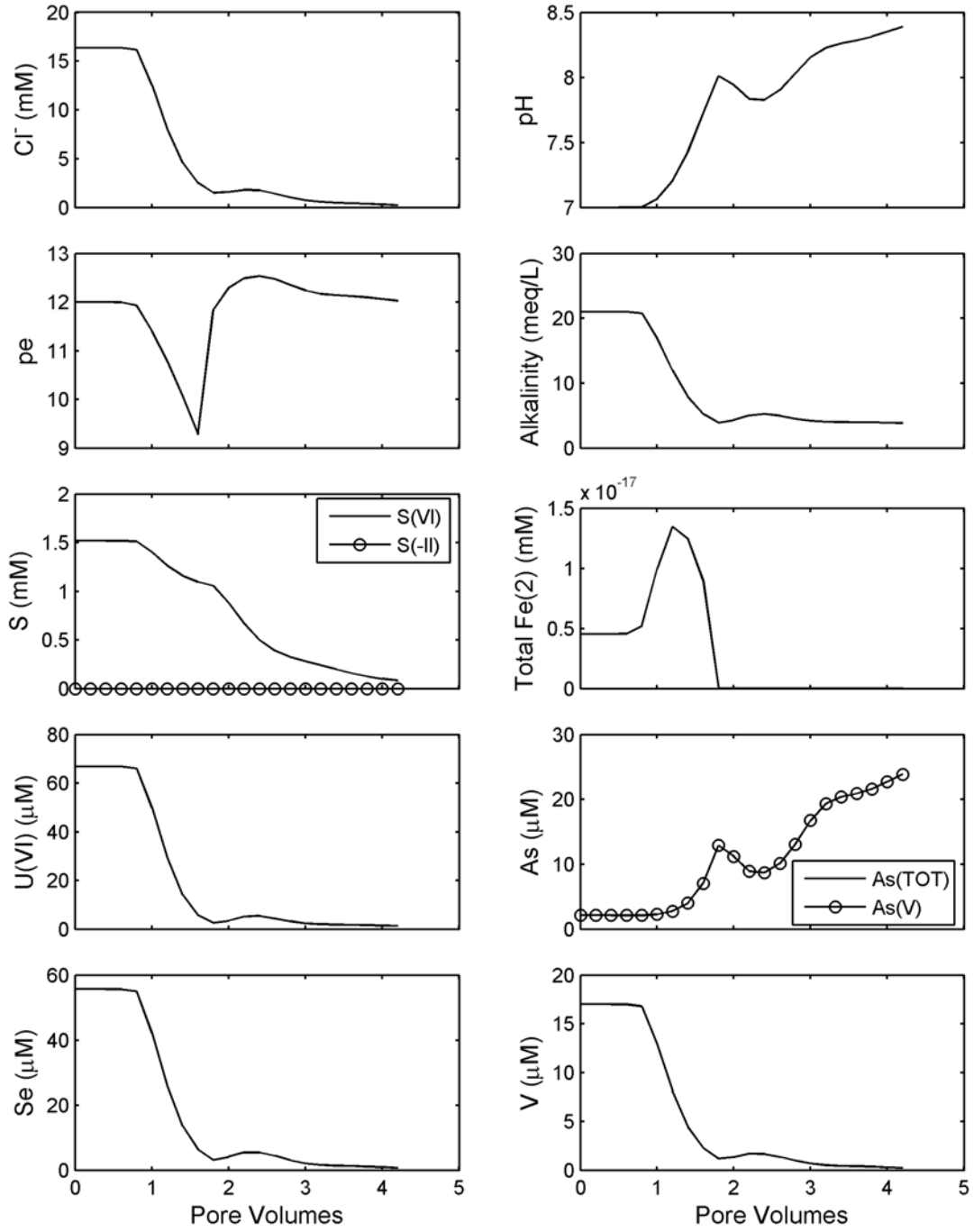

Figure 14. Simulation 3 results. Reducing influent groundwater. Calcite and goethite initially present. Mass transfer coefficient = 10.

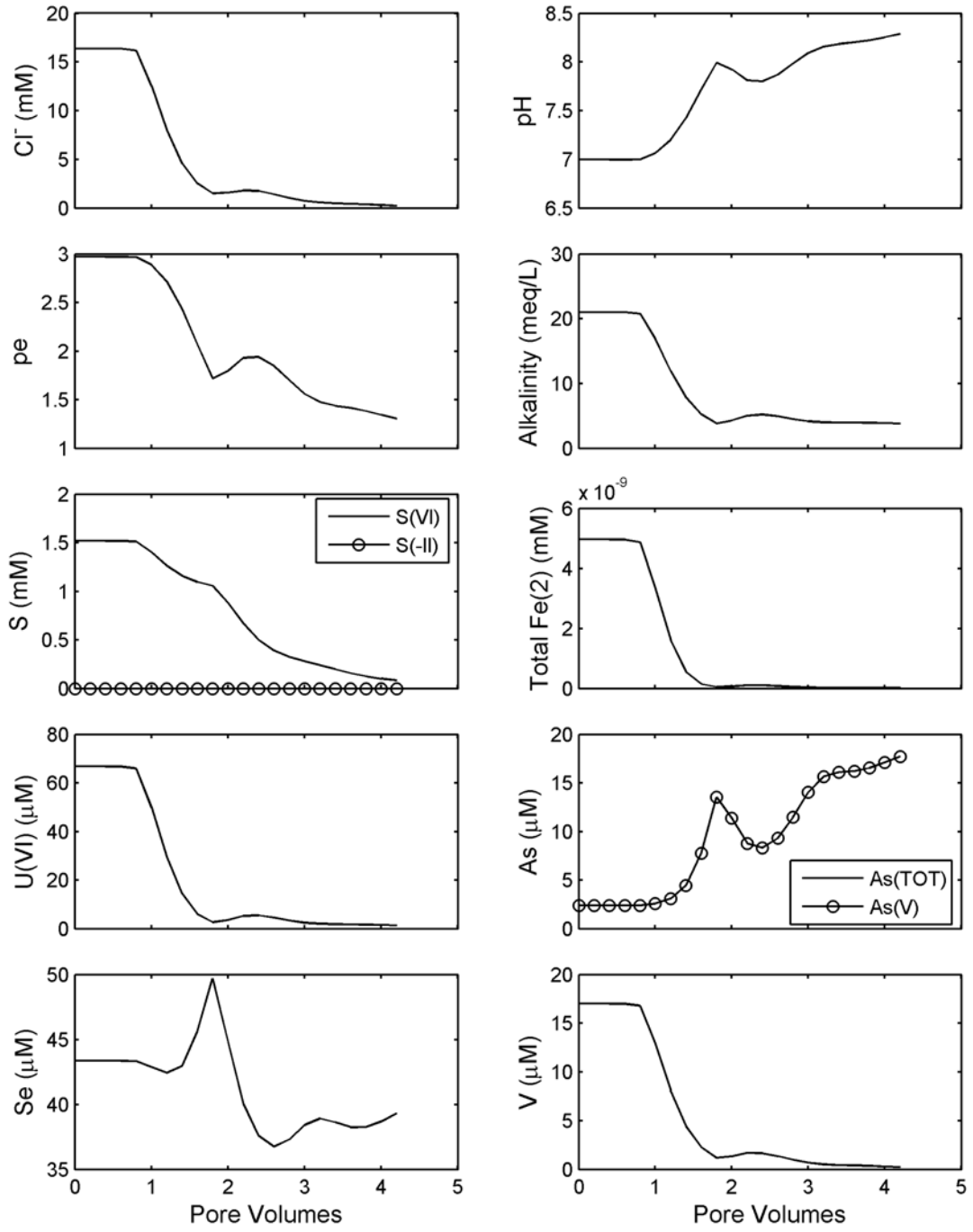

Figure 15. Simulation 4 results. Oxic influent groundwater. Calcite, goethite, and elemental Se (50 ppm) initially present. Mass transfer coefficient = 10.

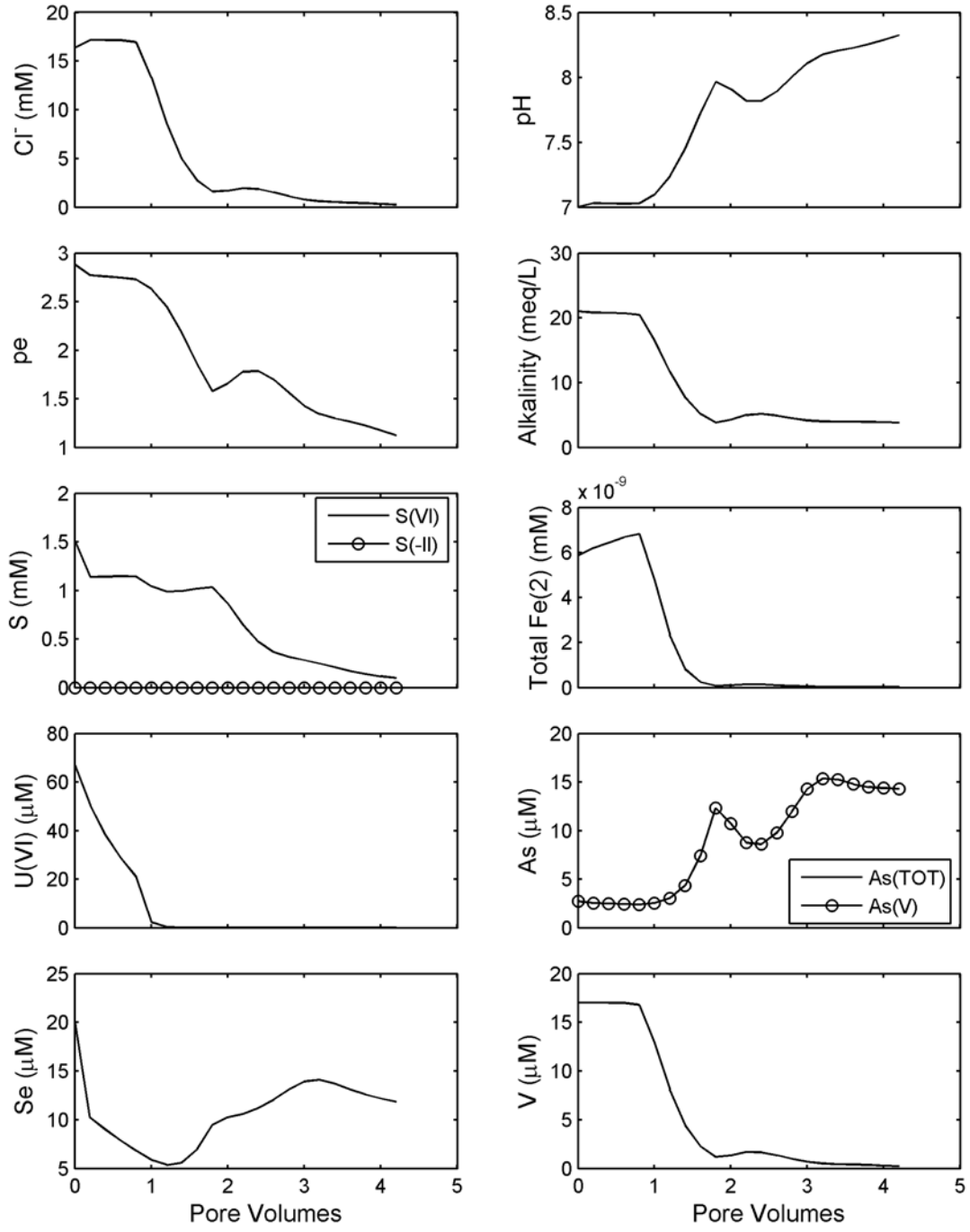

Figure 16. Simulation 5 results. Oxic influent groundwater. Calcite and goethite initially present in all cells. Elemental Se initially present at 50 ppm in the mobile cells. Elemental Se (500 ppm), pyrite (2000 ppm), and uraninite (1000 ppm) initially present in the immobile cells. Mass transfer coefficient = 10.

low concentrations in Simulation 5, because essentially all the uranium in the immobile cells was converted to U(IV) and precipitated as uraninite. Dissolved uranium exiting the column after 4 pore volumes approached a lower value of about 0.002 μM. The selenium concentration also initially decreased in the first pore volume because of reduction to form elemental selenium. With increasing time, elemental selenium is oxidized to Se(IV), whose transport is retarded by sorption, but Se(IV) is eventually transported out of the column. Dissolved arsenic in the immobile cells was present primarily as As(V) with a few percent present as As(III); conditions were not sufficiently reducing for the precipitation of orpiment (As_2S_3).

Simulation 6 (Fig. 17) was conducted with the same conditions as in Simulation 5, except that the mass transfer coefficient was made 5 orders of magnitude smaller ($1.0 \cdot 10^{-4}$ instead of 10). As was observed before, the effect decreases the influence of the immobile cells on the breakthrough curves.

Simulations 5 and 6 were not particularly consistent with the field observations. The uranium concentrations during groundwater restoration were maintained at higher values than predicted here with these simulations, and the observed selenium did not illustrate the initial decrease shown in the simulations.

Simulation 7 (Fig. 18) was conducted with conditions similar to those of Simulation 4, except that hydrogen sulfide gas (H_2S) at a concentration of $7.8 \cdot 10^{-3}$ moles/liter was added to the mixture of 25% effluent and 75% pure water during pore volumes 3.0 to 3.6, prior to re-injection to the column. No dissolved oxygen was mixed into the re-injected water as H_2S was added. Uraninite, orpiment and $FeSe_2$ were allowed to precipitate in Simulation 7. Precipitation of minerals prior to the water entering the column was not allowed. The predictions show that the pe dropped below –6 in the water leaving the column at about 4.5 pore volumes, and the pH rose to about 8.9 at the same time. The pe of –6 is similar to the very reducing conditions that develop in the front of the column in the first cell, where pyrite, uraninite, and more elemental selenium are precipitated. The precipitation of pyrite (and the excess goethite present as the source of iron for the pyrite) prevents much of the sulfide from being transported further down the column. The pH increase is caused by the net result of pyrite and elemental selenium precipitation and goethite dissolution. The rise in pH causes desorption of U(VI) and Se(IV) from the sediments in the tail end of the column, where the pe values are in the range of 0 to 0.5.

The increase in pH and selenium and uranium concentrations predicted in Simulation 7 were not observed in the groundwater at the Ruth ISL after hydrogen sulfide addition (Schmidt, 1989). The reason for this may be that the formation of pyrite is kinetically hindered under the field conditions by the supply of iron; rapid precipitation of pyrite would require rapid dissolution of goethite, which probably does not occur. Schmidt (1989) reported that elemental sulfur was observed in the groundwater after hydrogen sulfide addition, and that little dissolved sulfide broke through to the wells withdrawing groundwater.

Simulation 8 (Fig. 19) shows the results for the same conditions as in Simulation 7, except that pyrite precipitation was not allowed and precipitation of elemental sulfur was allowed. Most of the sulfide added to the column was precipitated as elemental sulfur in the column. The solubility of the elemental sulfur with respect to sulfide ion is much greater, and this allowed sulfide to be transported down the column and into the effluent, greatly decreasing the effluent pe and the concentrations of dissolved uranium, arsenic, selenium, and vanadium (by orders of magnitude).

At approximately 4.2 pore volumes, the simulations clearly illustrate the effects of

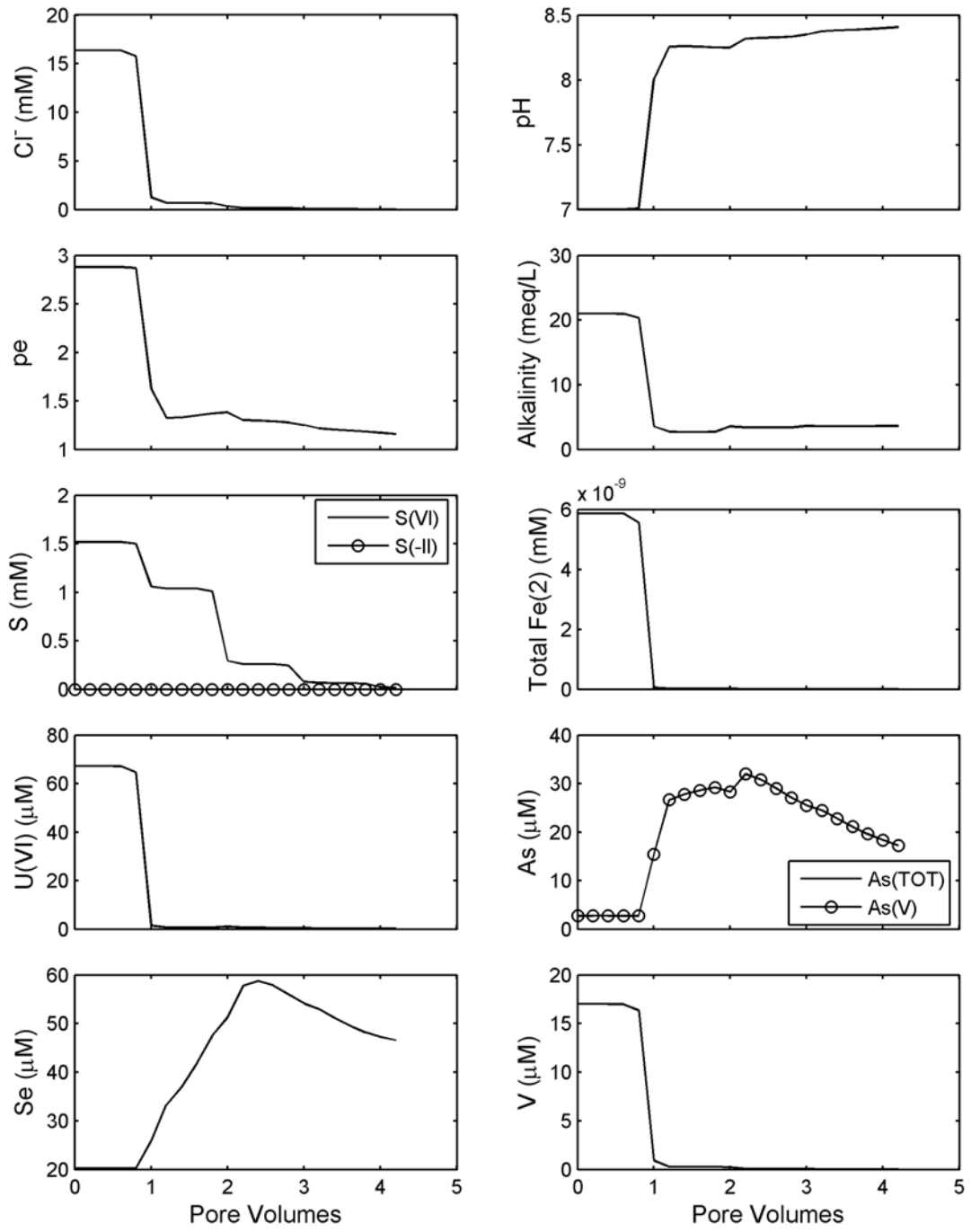

Figure 17. Simulation 6 results. Oxic influent groundwater. Calcite and goethite initially present in all cells. Elemental Se initially present at 50 ppm in the mobile cells. Elemental Se (500 ppm), pyrite (2000 ppm), and uraninite (1000 ppm) initially present in the immobile cells. Mass transfer coefficient = 10^{-4}.

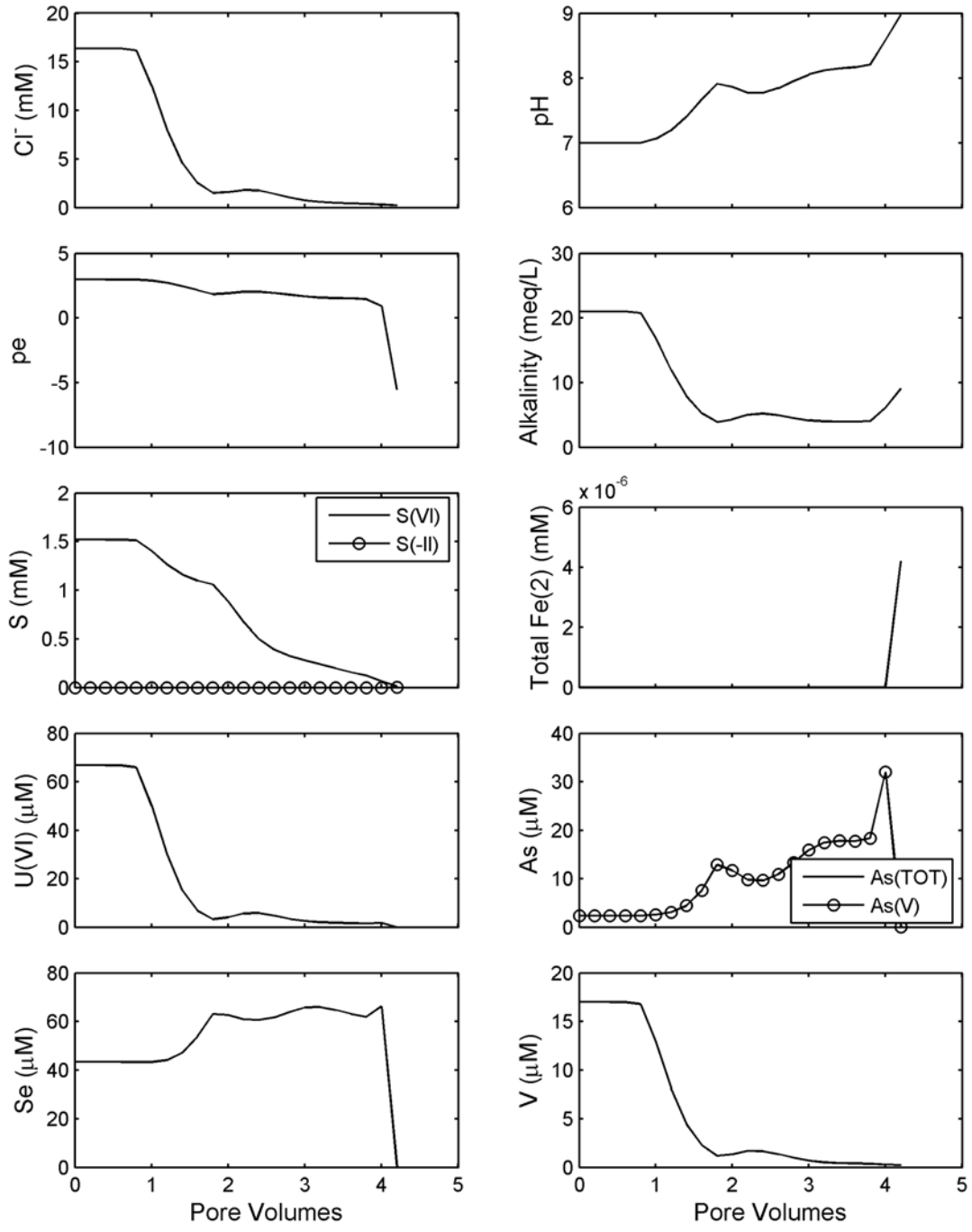

Figure 18. Simulation 7 results. Oxic influent groundwater. Calcite, goethite, and elemental Se (50 ppm) initially present. 265 mg/L of H_2S(g) added to the influent water during pore volumes 3.0 to 3.6. Mass transfer coefficient = 10.

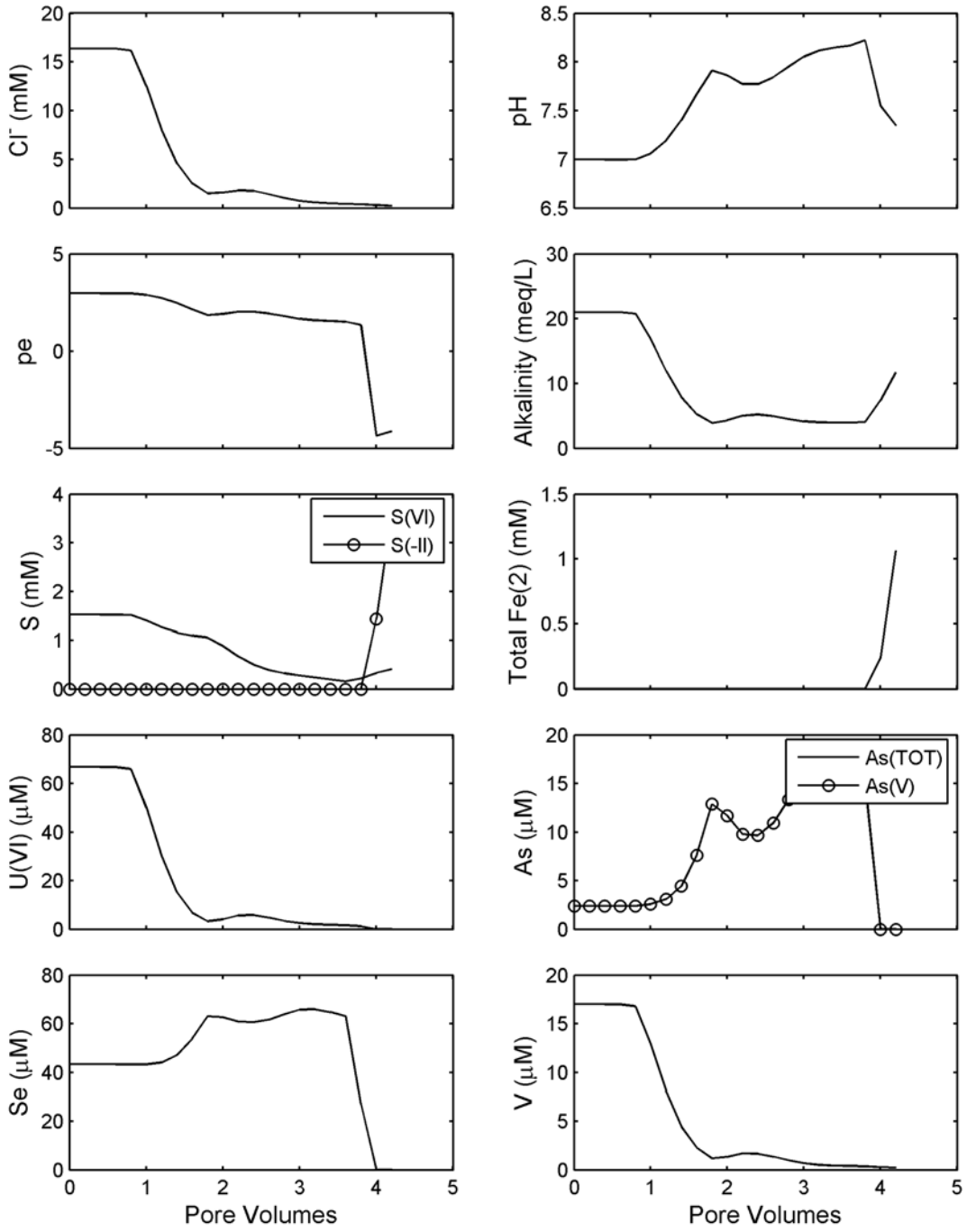

Figure 19. Simulation 8 results. Oxic influent groundwater. Calcite, goethite, and elemental Se (50 ppm) initially present. 265 mg/L of $H_2S(g)$ added to the influent water during pore volumes 3.0 to 3.6. Pyrite precipitation not allowed. Elemental sulfur precipitation allowed. Mass transfer coefficient = 10.

the H_2S addition. Sulfate increases because H_2S is oxidized by goethite, which also causes Fe(II) to increase. Small amounts of the H_2S were also consumed by the precipitation of orpiment (As_2S_3), but the extent of this reaction was limited by the amount of As. The dissolved U(VI) concentration decreased to approximately 10^{-10} M because of uraninite precipitation; the uraninite concentrations were up to 25 □M throughout the column. These results are in much better agreement with the field observations of Schmidt (1989) after hydrogen sulfide addition.

Simulation 9 (Fig. 20) is similar to Simulation 8, except the concentration of H_2S added between 3.2 and 3.6 pore volumes was decreased by a factor of 5, and elemental sulfur was not allowed to precipitate. Although reducing conditions were formed in the inlet to the column, the H_2S was completely consumed by the goethite and oxidized to sulfate. The conditions at the end of the column remained relatively oxidizing, as indicated by the moderate pe values and the small Fe(II) and S(-II) concentrations. Also, there was no decrease in U, Se or As after 4.2 pore volumes, because there was insufficient reductant added.

Simulation 10 (Fig. 21) is similar to Simulation 8, except amorphous FeS was allowed to form in the simulations. In addition, uraninite was not considered, and instead amorphous UO_2 was allowed to precipitate. Even though a relatively high concentration of H_2S was added, reducing conditions were not simulated at the end of the column. Reducing conditions did occur in the inlet of the column: both amorphous FeS and amorphous UO_2 formed in that region, and the simulated pe was –4.4. However, the precipitation of FeS consumed H_2S, and therefore less was oxidized to sulfate. The reducing conditions at the entrance of the column caused dissolved Se and As to decrease because of precipitation of reduced phases. In contrast, U(VI) increased slightly after 4.2 pore volumes, probably because of the increase in alkalinity that resulted from the oxidation of H_2S.

5.3 Geochemical Modeling of Groundwater Stabilization

The stabilization of chemical conditions in the leached zone in response to an influx of native groundwater was considered by conducting simulations for 96 pore volumes, under natural gradient conditions, after the groundwater sweep and treatment. A complete description of groundwater flow characteristics, including the mean groundwater velocity, is beyond the scope of this report. Consequently, it is not possible to make an accurate factor for converting pore volumes as used in this report to an actual time relevant to regulatory framework. The groundwater velocity is proportional to both the hydraulic conductivity and hydraulic gradient, both of which can vary substantially at field sites. Nevertheless, for illustrative purposes, the time for one pore volume to flow through an in-situ mining zone was crudely estimated by assuming that the length of the in-situ leaching zone was 100 m with a relatively high velocity of 1 m/d. For these conditions, one pore volume corresponds to 0.27 years. Conversely, if it is assumed that the groundwater velocity was 1 m/year, then one pore volume corresponds to 100 years.

Simulations were also conducted to compare with Simulation 10 for various scenarios that considered native groundwaters of differing composition and different properties of the porous medium (Table 5). The baseline composition of the influent groundwater is given in Table 4; most simulations were conducted with oxic groundwater, but three simulations were conducted with the mildly reducing groundwater conditions that existed prior to mining at the Ruth ISL. For these simulations, the influent groundwater had an initial water composition containing $7 \cdot 10^{-7}$ moles/liter of Fe(II), $1 \cdot 10^{-8}$ moles/liter of Fe(III), and a pe of -1.5.

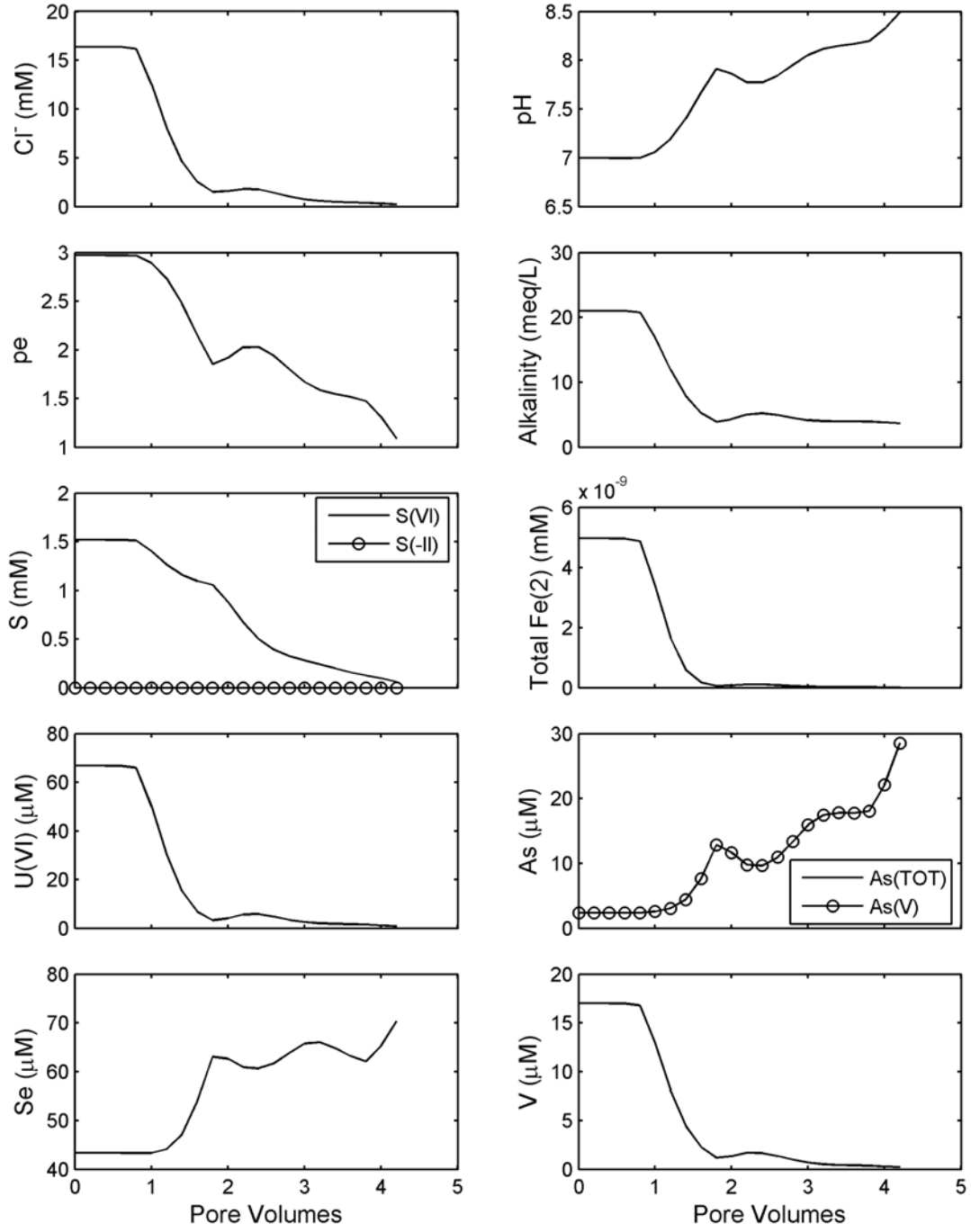

Figure 20. Simulation 9 results. Oxic influent groundwater. Calcite, goethite, and elemental Se (50 ppm) initially present. 53 mg/L of H_2S(g) added to the influent water during pore volumes 3.0 to 3.6. Pyrite precipitation not allowed. Mass transfer coefficient = 10.

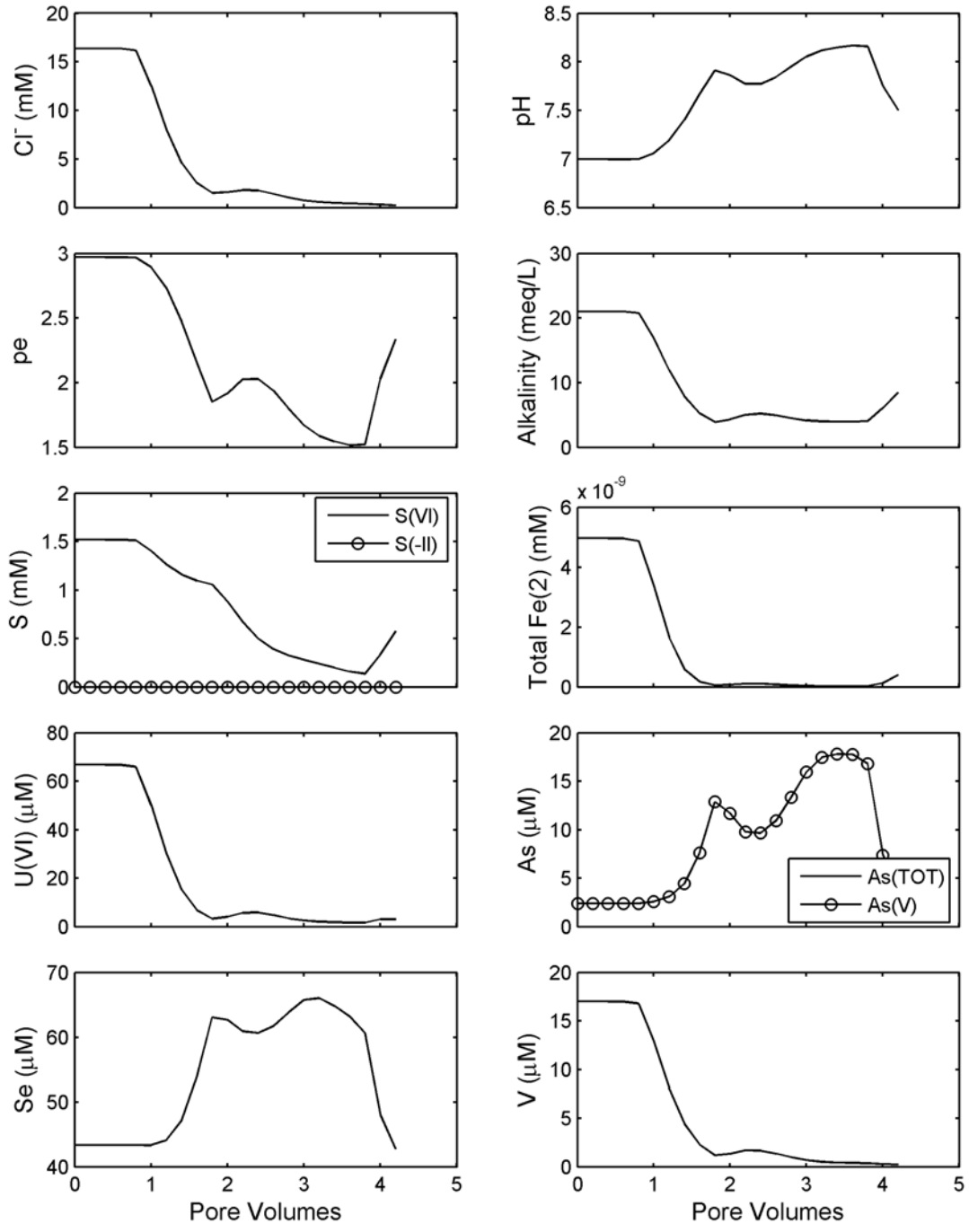

Figure 21. Simulation 10 results. Oxic influent groundwater. Calcite, goethite, and elemental Se (50 ppm) initially present. 265 mg/L of H_2S(g) added to the influent water during pore volumes 3.0 to 3.6. Pyrite and uraninite precipitation not allowed. Amorphous FeS and UO_2 precipitation allowed. Mass transfer coefficient = 10.

Table 5. Summary of Additional Variables Considered in Oxic Groundwater Stabilization Simulations

No.[a]	Mass Transfer Coefficient	Immobile Zone Porosity	Influent Groundwater pH	Influent Groundwater alkalinity (meq/L)	Calcite in Mined Zone (moles/L)	Ion Exchange Capacity (meq/L)	Site Concentration (moles/L)	V Adsorption
10	10	0.1	7	2.5	0.4	0	$4x10^{-4}$	no
11	0.01	0.1	7	2.5	0.4	0	$4x10^{-4}$	no
12	10	0.5	7	2.5	0.4	0	$4x10^{-4}$	no
13	10	0.1	7.5	2.5	0.4	0	$4x10^{-4}$	no
14	10	0.1	7	10	0.4	0	$4x10^{-4}$	no
15	10	0.1	7	10	0.004	0	$4x10^{-4}$	no
16	10	0.1	7	10	0.4	1	$4x10^{-4}$	no
17	10	0.1	7 (PV<30) 7.5 (PV>30)	2.5 (PV<30) 10 (PV>30)	.4	0	$4x10^{-4}$	no
18	10	0.1	7	2.5	0.4	0	$4x10^{-2}$	no
19	10	0.1	7	2.5	0.4	0	$4x10^{-2}$	yes

[a] Simulation number.

The local velocities during the in situ leaching activities are likely much larger than the velocities present under natural gradient conditions. However, the difference in velocities did not affect the simulations because of the local equilibrium assumption.

5.3.1 Stabilization Modeling Results with Oxic Influent Groundwater

Figures 22-26 show results for Simulations 1, 5, 8, 9 and 10, respectively, except that a total of 100 pore volumes were simulated, with an end to RO treatment at 4.2 pore volumes, followed by stabilization with oxic influent groundwater. The simulated concentrations are shown on a log scale so that small concentrations present in tailing peaks can be seen.

In Simulation 1 (Fig. 22), the concentrations of U, As, and V all reached a plateau equal to background values at approximately 6 pore volumes. In contrast, As(V) continued to decrease during the stabilization phase because its concentration was controlled by desorption.

In Simulation 5 (Fig. 23), the elemental Se in the mobile cells was gradually oxidized by the incoming oxic groundwater, first oxidizing to Se(IV) and then to Se(VI), raising the dissolved Se to very high levels between 20 and 40 pore volumes. Uranium, As, and V concentrations remained low for the long-term simulation.

In Simulation 8 (Fig. 24), pe decreased to –5 because of the H_2S addition, and then increased to nearly 15 in a stepwise fashion. Each step in the pe value corresponds to the complete oxidation and dissolution of a reduced phase in the column. For example, at approximately 8.8 pore volumes, uraninite and orpiment that formed in the column are completely oxidized, and all of As in the system is oxidized to As(V). At 8.8 pore volumes, the U(VI) concentration increased to 7 μM (1670 ppb) as the uraninite disappears, and the pe increases from –5 to 0. U(VI) decreased to background values within 5 additional pore volumes because of adsorption-desorption equilibrium. At 22 pore volumes all the Se(s) was oxidized, and between 22 and 30 pore volumes the Se(IV) is adsorbed and then oxidized to Se(VI).

In Simulation 9 (Fig. 25), like Simulation 5, the oxidation of elemental Se in the column eventually caused very high dissolved Se concentrations between 20 and 40 pore volumes. The concentrations of U, As, and V remained low during the long-term stabilization.

Simulation 10 (Fig. 26) considered the formation of amorphous FeS and amorphous UO_2. In this simulation, the reduced phases formed at the inlet of the column, but the exit of the column remained moderately oxidizing for the first 9.6 pore volumes. The pe increase that started at 44 pore volumes corresponds to the oxidation of FeS at the inlet of the column. Between 44 and 47 pore volumes, uraninite and orpiment are oxidized and dissolved. The pe increase at 60 pore volumes corresponds to the oxidation of elemental selenium. The U(VI) concentration in the effluent shows a gradual decline in the initial 10 pore volumes. Because influent U(VI) was precipitated in the upgradient cell, initial adsorbed U(VI) in the 4 downgradient cells was slowly depleted via U(VI) desorption, causing a slow decrease in U(VI) concentration at the outlet in the initial 10 pore volumes. At the inlet of the column, the concentration of FeS(am) at the end of H_2S treatment was 15 mM, whereas the UO_2(am) concentration was 7.5 μM. The FeS(am) was slowly reoxidized by O_2 in the groundwater after the H_2S treatment was completed. The FeS(am) was completely oxidized at 44 pore volumes. Once the FeS(am) is oxidized at the inlet of the column, the relatively small concentration of UO_2(am) is rapidly oxidized and this releases a pulse of U(VI) into the groundwater. Thus, the second U(VI) peak occurs because of the oxidation of amorphous UO_2 that formed in the

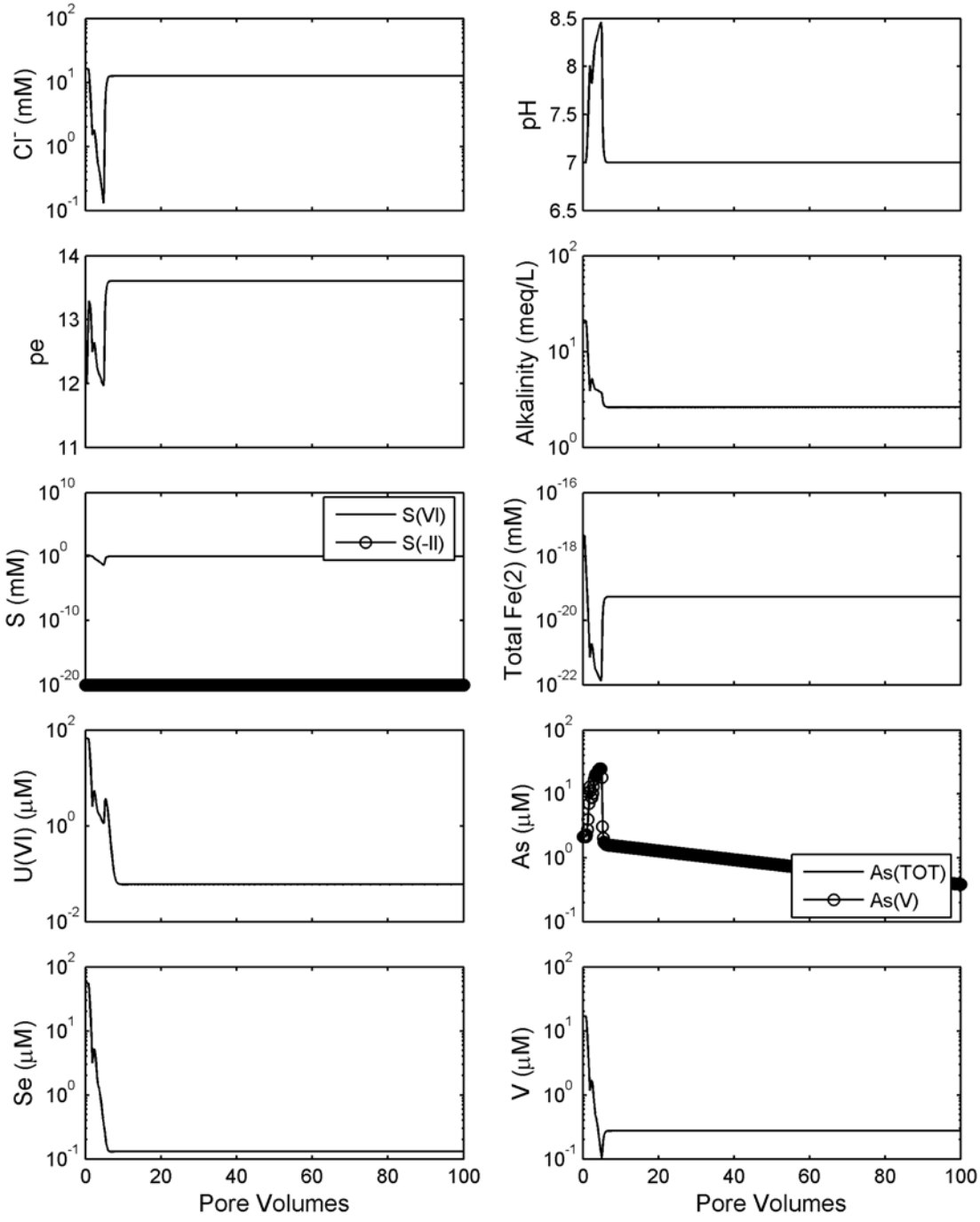

Figure 22. Simulation 1 results, including groundwater stabilization with oxic influent groundwater. Calcite and goethite initially present. Mass transfer coefficient = 10. Total sulfide ≤ $1x10^{-20}$ M in plot.

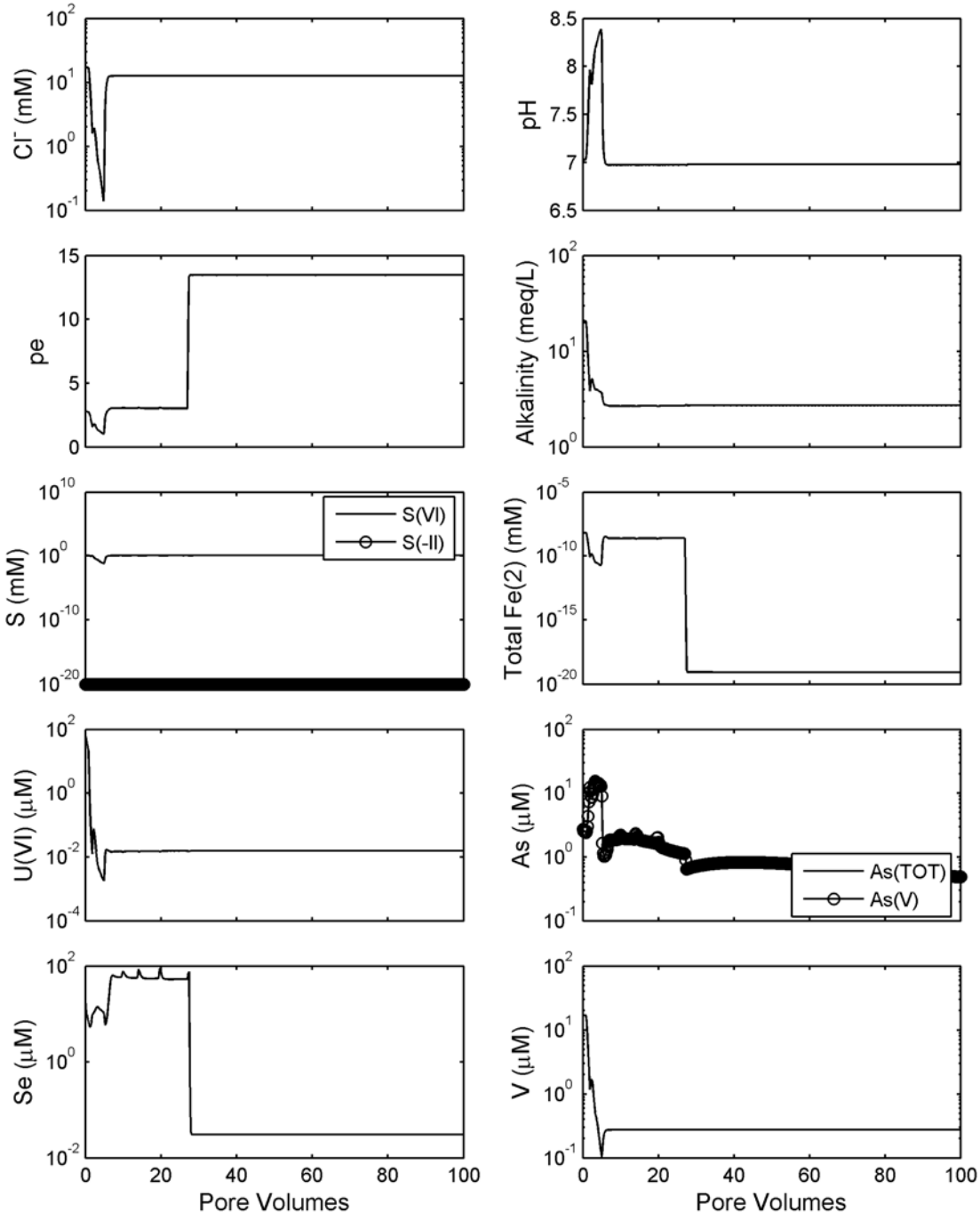

Figure 23. Simulation 5 results, including groundwater stabilization with oxic influent groundwater. Calcite and goethite initially present in all cells. Elemental Se initially present at 50 ppm in the mobile cells. Elemental Se (500 ppm), pyrite (2000 ppm), and uraninite (1000 ppm) initially present in the immobile cells. Mass transfer coefficient = 10. Total sulfide ≤ $1x10^{-20}$ M in plot.

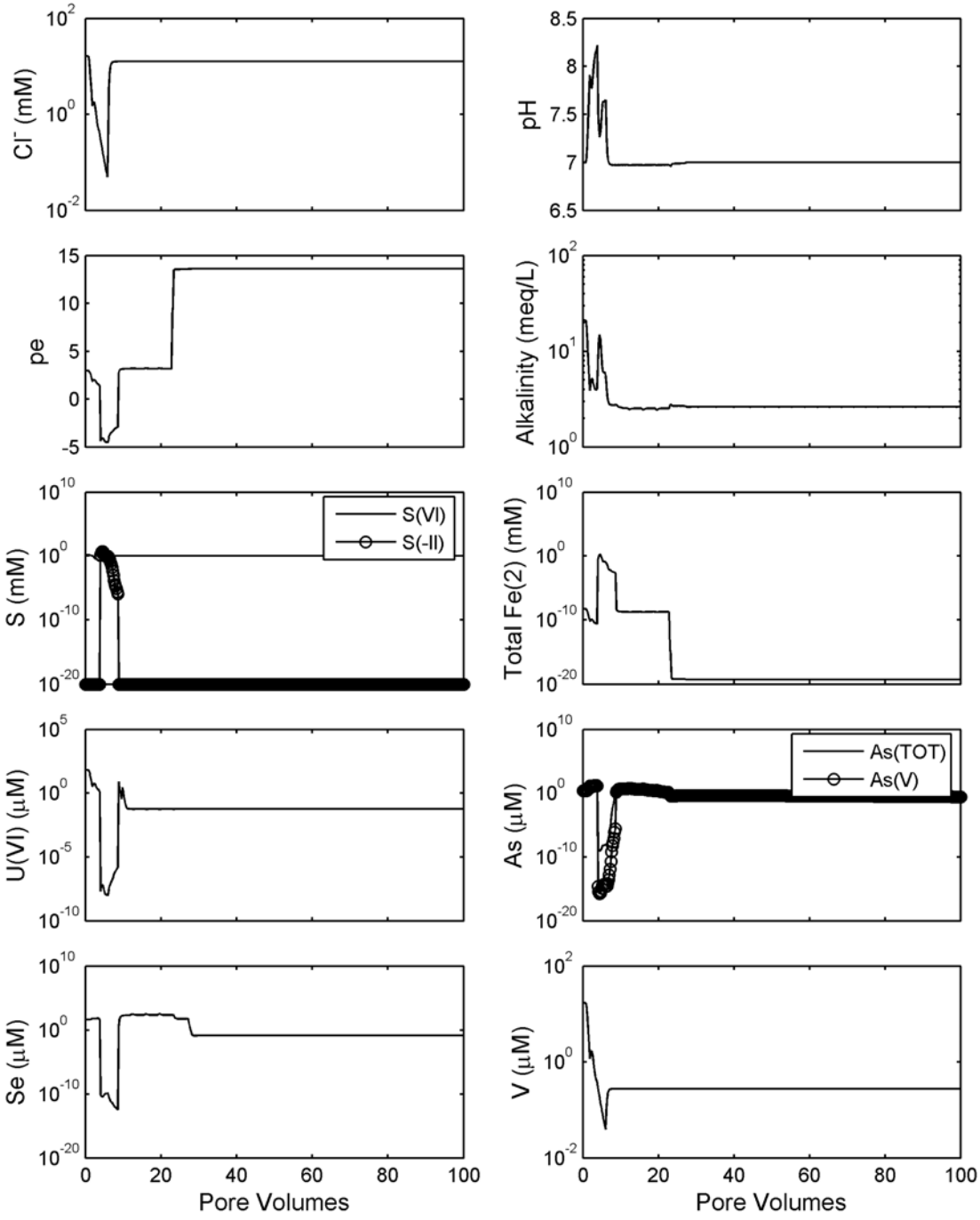

Figure 24. Simulation 8 results, including groundwater stabilization with oxic influent groundwater. Calcite, goethite, and elemental Se (50 ppm) initially present. 265 mg/L of $H_2S(g)$ added to the influent water during pore volumes 3.0 to 3.6. Pyrite precipitation not allowed. Elemental sulfur precipitation allowed. Mass transfer coefficient = 10. Sulfide concentration indicated at $1x10^{-20}$ M is actually $\leq 1x10^{-20}$ M in plot.

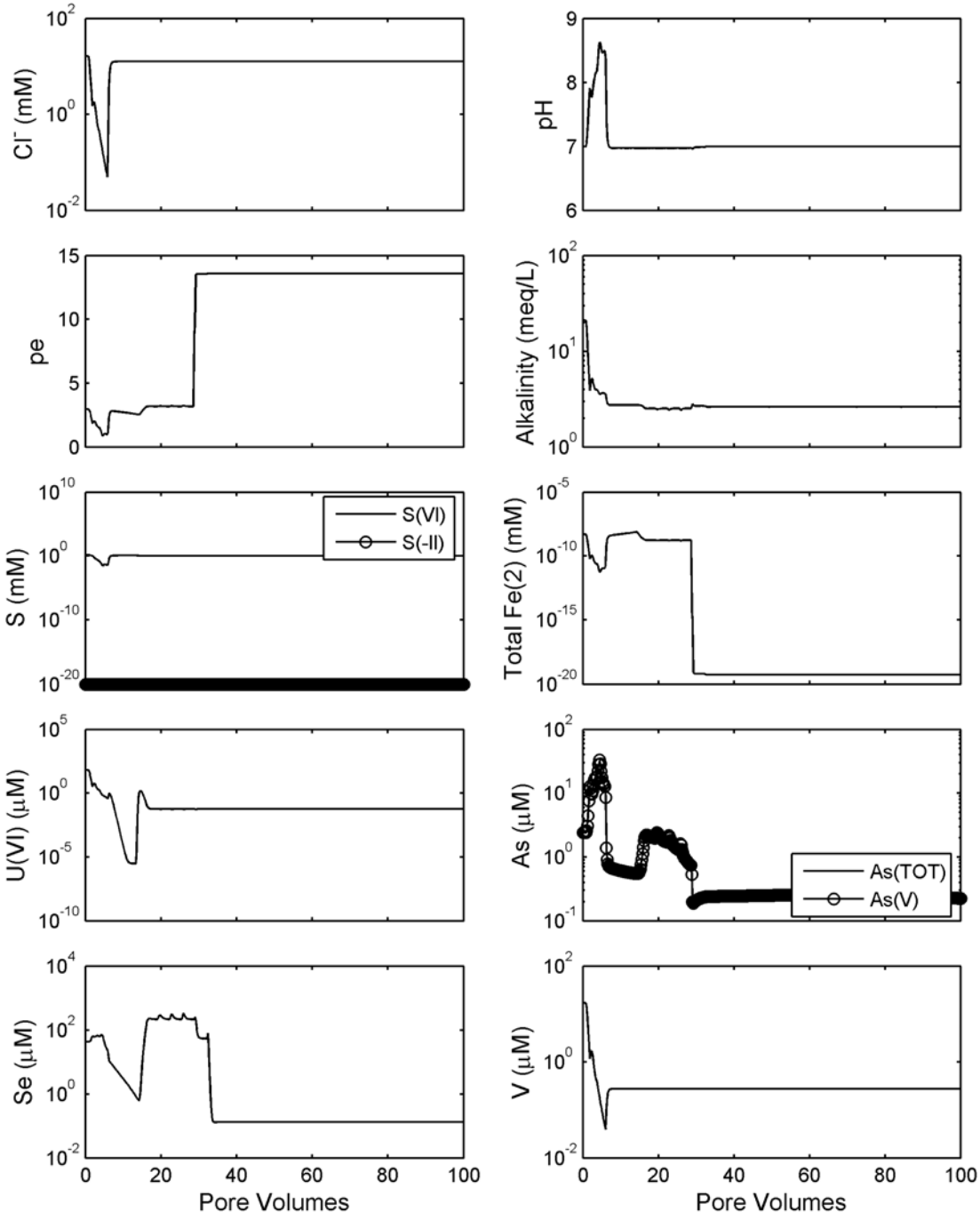

Figure 25. Simulation 9 results, including groundwater stabilization with oxic influent groundwater. Calcite, goethite, and elemental Se (50 ppm) initially present. 53 mg/L of $H_2S(g)$ added to the influent water during pore volumes 3.0 to 3.6. Pyrite and elemental sulfur precipitation not allowed. Mass transfer coefficient = 10. Total sulfide ≤ $1x10^{-20}$ M in plot.

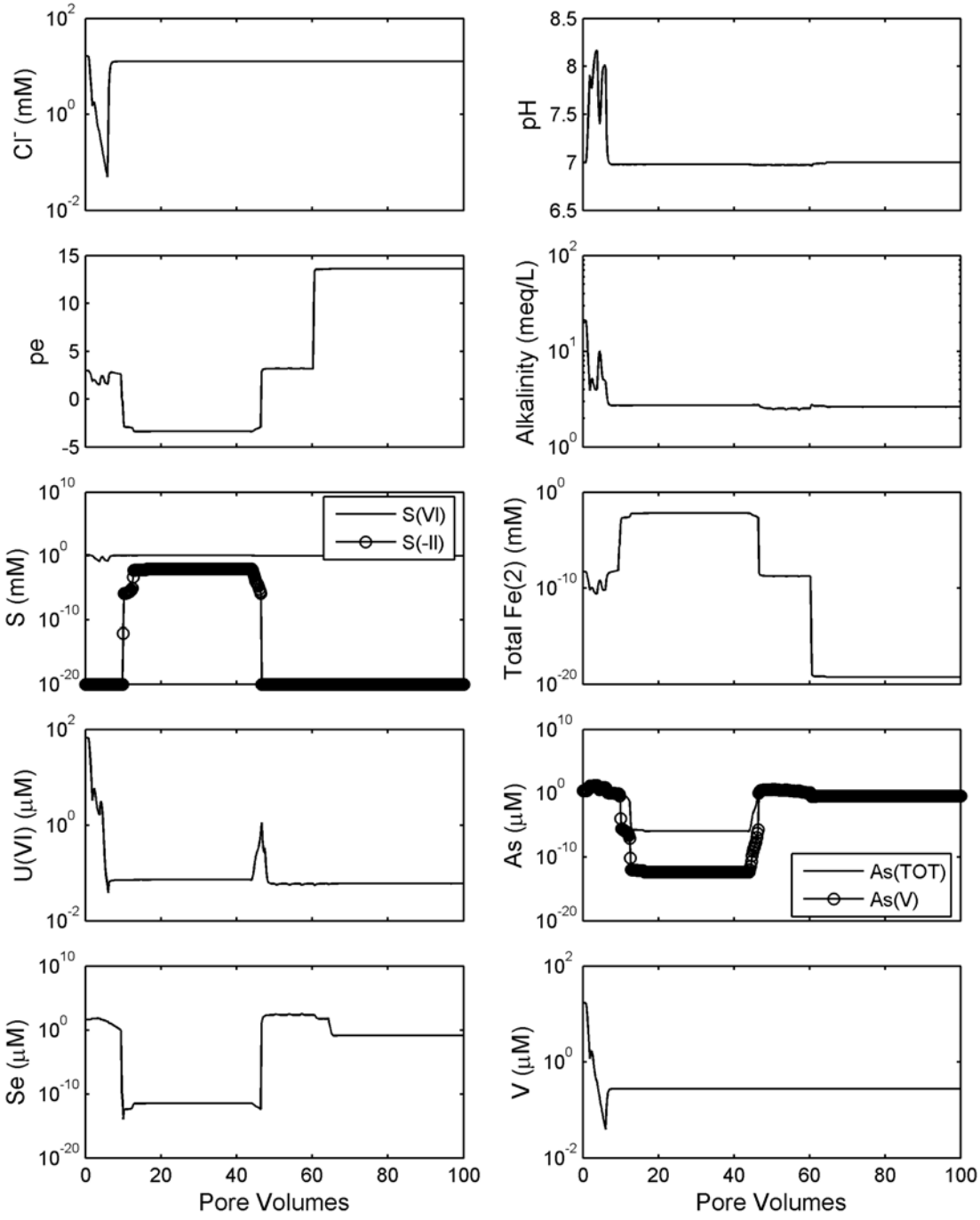

Figure 26. Simulation 10 results, including groundwater stabilization with oxic influent groundwater. Calcite, goethite, and elemental Se (50 ppm) initially present. 265 mg/L of $H_2S(g)$ added to the influent water during pore volumes 3.0 to 3.6. Pyrite and uraninite precipitation not allowed. Amorphous FeS and UO_2 precipitation allowed. Mass transfer coefficient = 10. Sulfide concentration indicated at $1x10^{-20}$ M is actually ≤ $1x10^{-20}$ M in plot.

column during the H_2S treatment, and the peak shape is controlled by U(VI) adsorption and desorption.

Figure 27 illustrates the concentration of 10 species along the length of the column after 6, 41, 45, and 55 pore volumes for Simulation 10. These concentration profiles show that after 6 pore volumes, goethite at the inlet of the column was reduced by the H_2S to FeS(ppt), which was not present initially but was allowed to precipitate in the simulation. Orpiment and UO_2(am) were also precipitated at the inlet of the column. After 41 pore volumes, approximately 1 mM of FeS(ppt) remained at the inlet of the column, although most of the Fe was reoxidized to goethite. The small amount of FeS(ppt) present after 41 pore volumes still created reducing conditions, such that small concentrations of orpiment and UO_2(am) were also still present at the column inlet. Between 41 and 45 pore volumes, the remaining FeS(ppt)was oxidized, as was the orpiment and UO_2(am). After 45 pore volumes, a small amount of UO_2(am) formed at a normalized distance of 0.7, whereas dissolved U(VI) had a maximum concentration at a normalized distance of 0.5. The peak in U(VI) concentration was caused by the sequential oxidation of U(IV) to U(VI) in the oxidizing zone, followed by reduction of U(VI) to U(IV) in the reducing zones. The oxidizing zone was created by the influent oxic water, while the reducing zone was controlled by the concentrations of Fe^{+2}, Se(s) and orpiment. Finally, after 55 pore volumes, Se(s) was the only reduced phase remaining in the system and was present only near the exit of the column. As the Se(s) was oxidized, As(III), which was primarily adsorbed to surfaces, was oxidized to As(V). The combination of oxidation and desorption accounts for the increase in As(V) concentration simulated at the end of the column at 60 pore volumes.

The remaining simulations to be presented in this section are variations of the initial conditions for Simulation 10, as shown in Table 5. Simulation 11 only differed in the value of the mass transfer coefficient (10^{-2} instead of 10). The results (Fig. 28) are very similar to those shown in Figure 26 for Simulation 10. The main difference is that the peaks are somewhat sharper and the uranium peak at 44 pore volumes is higher.

In Simulation 12, the porosity of the immobile zone was increased to 0.5 (Fig. 29). This value is relatively high but was selected as a rough approximation of the case where the flow is dominated by a relatively few number of preferential flow paths. The peak in U(VI) concentration at 44 pore volumes is 8 μM, which is approximately the same as the value shown in Figure 26 for Simulation 10. The double uranium peak at 44 pore volumes is likely due to modest numerical oscillations at the sharp redox boundary.

In Simulation 13, the influent groundwater was assumed to have a higher pH (7.5 instead of 7). The main difference in the results occurs for the U(VI) and As concentrations, shown in Figure 30. Between 10 and 44 pore volumes, the U(VI) concentration was smaller than in Simulation 10 (Fig. 26), because the oxidation of UO_2(am), which supplies U(VI) to the groundwater at a nearly constant rate, is slightly less favorable at the higher pH value.

The alkalinity of the influent groundwater was increased fourfold in Simulation 14 (Fig. 31). The increase in alkalinity makes the oxidation and dissolution of UO_2(am) more favorable, and the adsorption of U(VI) is less favorable. Thus, a flat plateau in U(VI) concentration was formed between 6 and 12 pore volumes.

Simulation 15 (Fig. 32) considers a groundwater that was not in equilibrium with calcite (Saturation Index = -1.3), and the porous medium had a calcite concentration that was only 1% of the base case value in Simulation 10. The dissolution of calcite increased the pH and the alkalinity until the calcite was exhausted after 13 pore

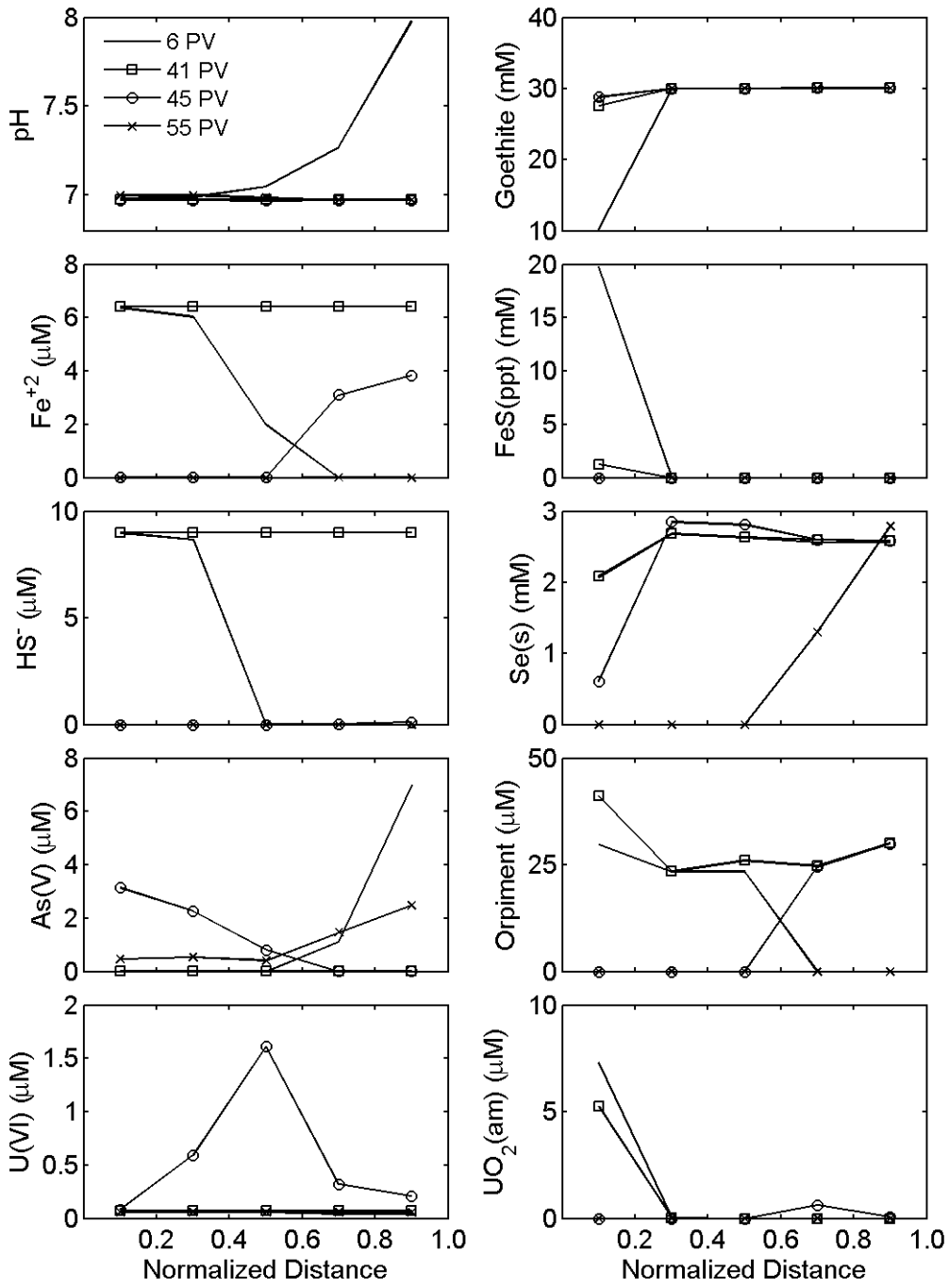

Figure 27. Concentration profiles along the column length for Simulation 10 corresponding to the time at which 6, 41, 45, or 55 pore volumes have entered the column.

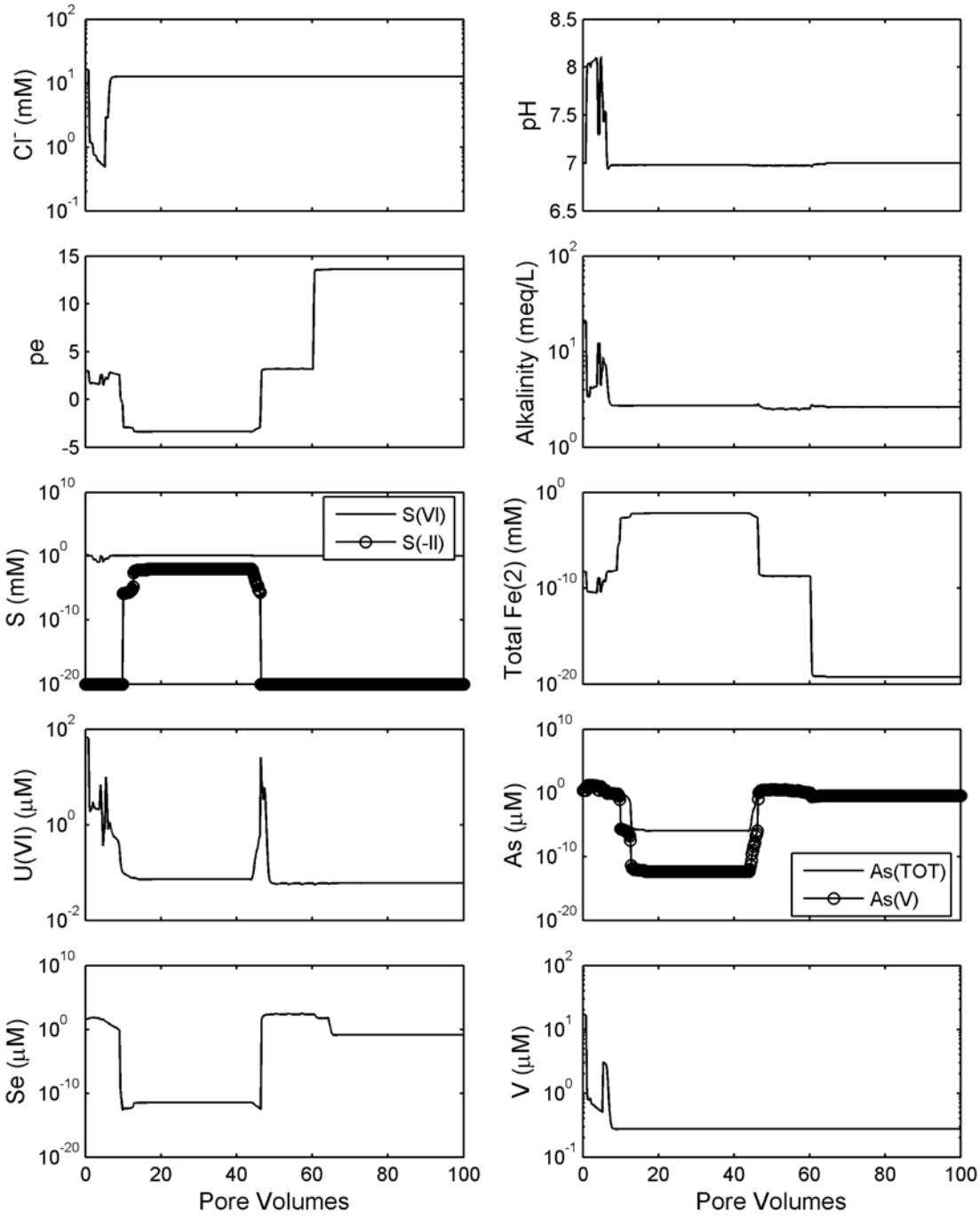

Figure 28. Simulation 11 results. Mass transfer coefficient changed to 10^{-2}. Oxic influent groundwater. Calcite, goethite, and elemental Se (50 ppm) initially present. 265 mg/L of H_2S(g) added to the influent water during pore volumes 3.0 to 3.6. Pyrite and uraninite precipitation not allowed. Amorphous FeS and UO_2 precipitation allowed. Sulfide concentration indicated at $1x10^{-20}$ M is actually ≤ $1x10^{-20}$ M in plot.

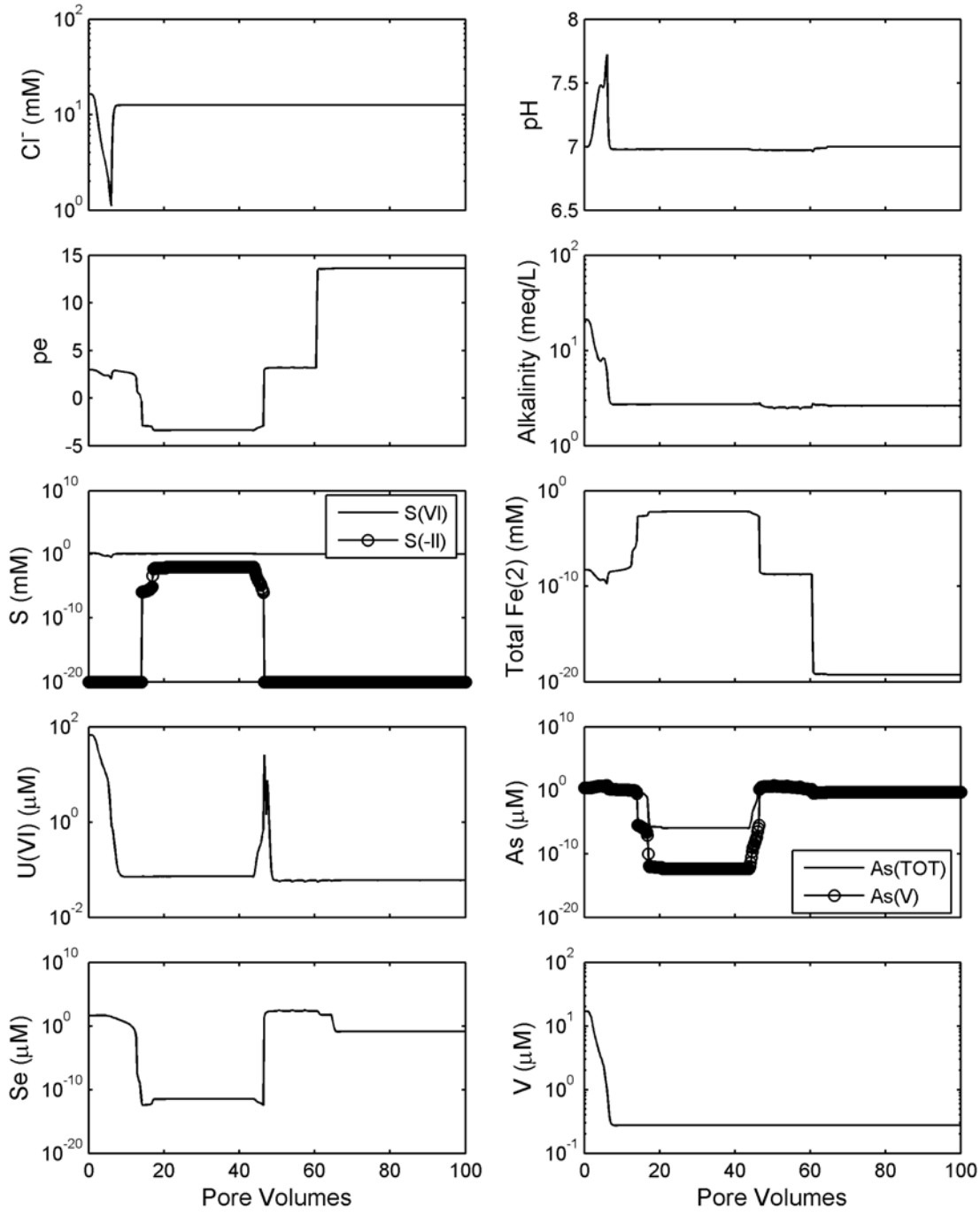

Figure 29. Simulation 12 results. Porosity of immobile zone changed to 50% to create a greater reservoir of immobile water. Oxic influent groundwater. Calcite, goethite, and elemental Se (50 ppm) initially present. 265 mg/L of $H_2S(g)$ added to the influent water during pore volumes 3.0 to 3.6. Pyrite and uraninite precipitation not allowed. Amorphous FeS and UO_2 precipitation allowed. Mass transfer coefficient = 10. Sulfide concentration indicated at $1x10^{-20}$ M is actually ≤ $1x10^{-20}$ M in plot.

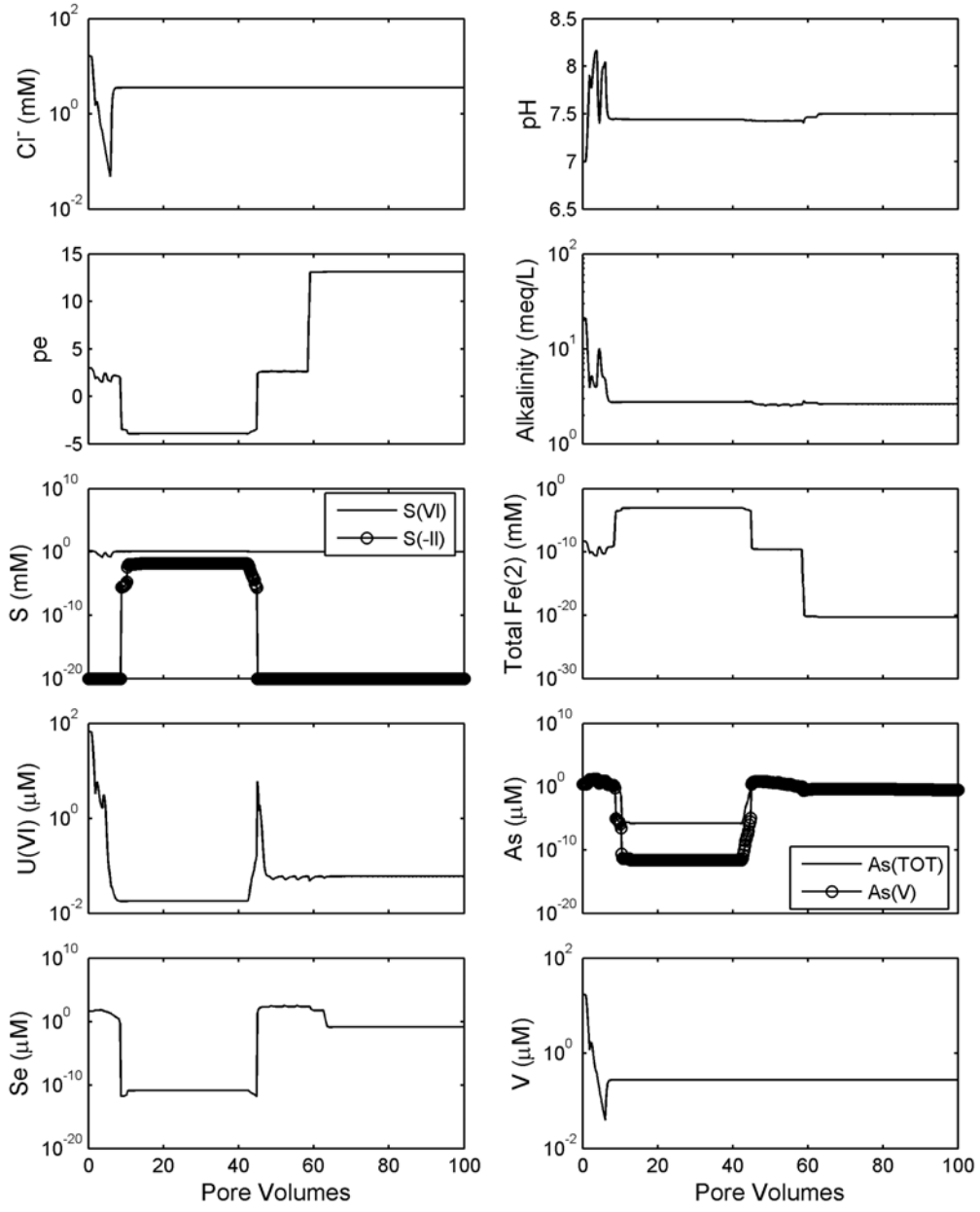

Figure 30. Simulation 13 results. Influent groundwater pH changed to 7.5. Oxic influent groundwater. Calcite, goethite, and elemental Se (50 ppm) initially present. 265 mg/L of $H_2S(g)$ added to the influent water during pore volumes 3.0 to 3.6. Pyrite and uraninite precipitation not allowed. Amorphous FeS and UO_2 precipitation allowed. Mass transfer coefficient = 10. Sulfide concentration indicated at $1x10^{-20}$ M is actually ≤ $1x10^{-20}$ M in plot.

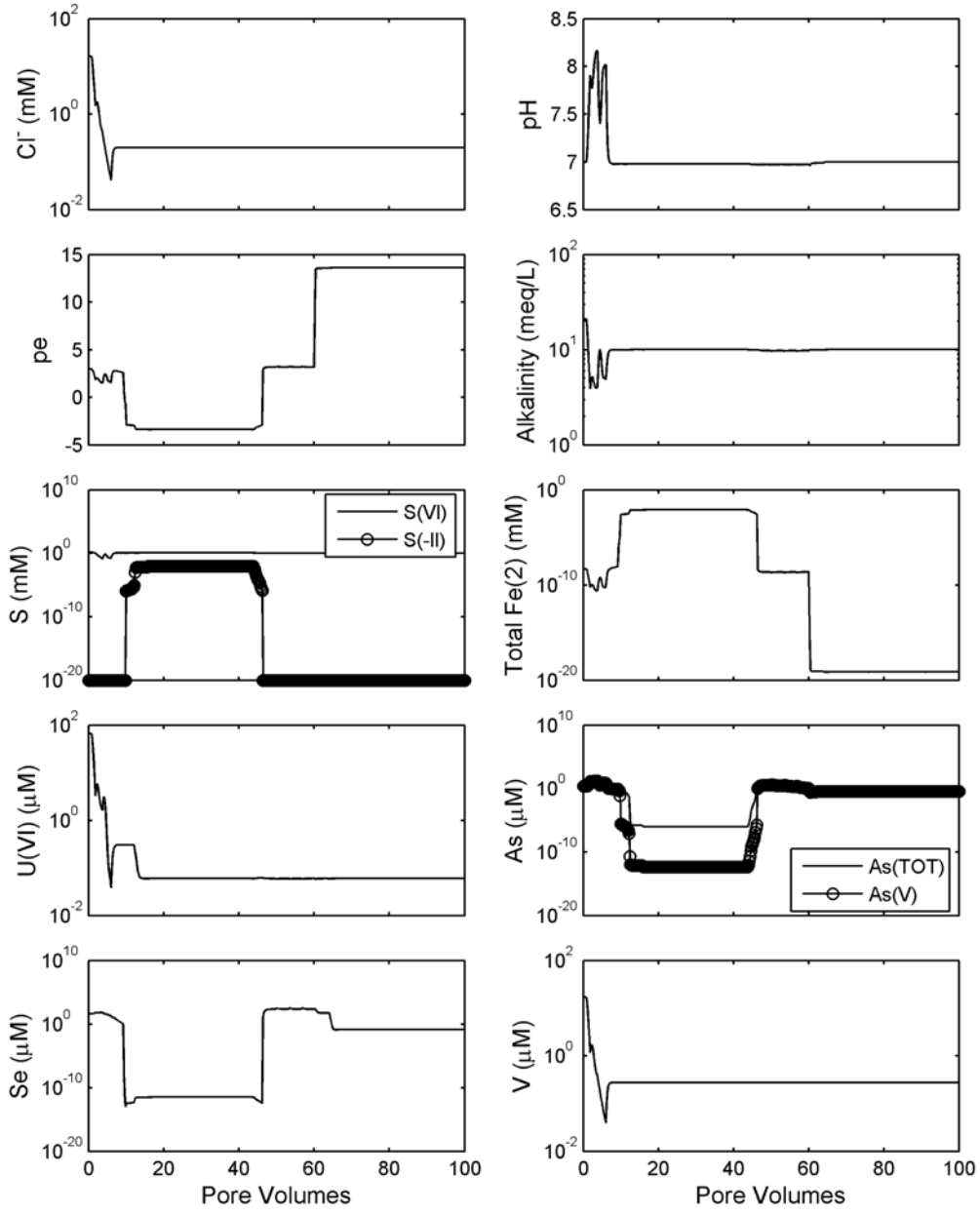

Figure 31. Simulation 14 results. Influent groundwater alkalinity changed to 10 meq/L. Oxic influent groundwater. Calcite, goethite, and elemental Se (50 ppm) initially present. 265 mg/L of $H_2S(g)$ added to the influent water during pore volumes 3.0 to 3.6. Pyrite and uraninite precipitation not allowed. Amorphous FeS and UO_2 precipitation allowed. Mass transfer coefficient = 10. Sulfide concentration indicated at $1x10^{-20}$ M is actually ≤ $1x10^{-20}$ M in plot.

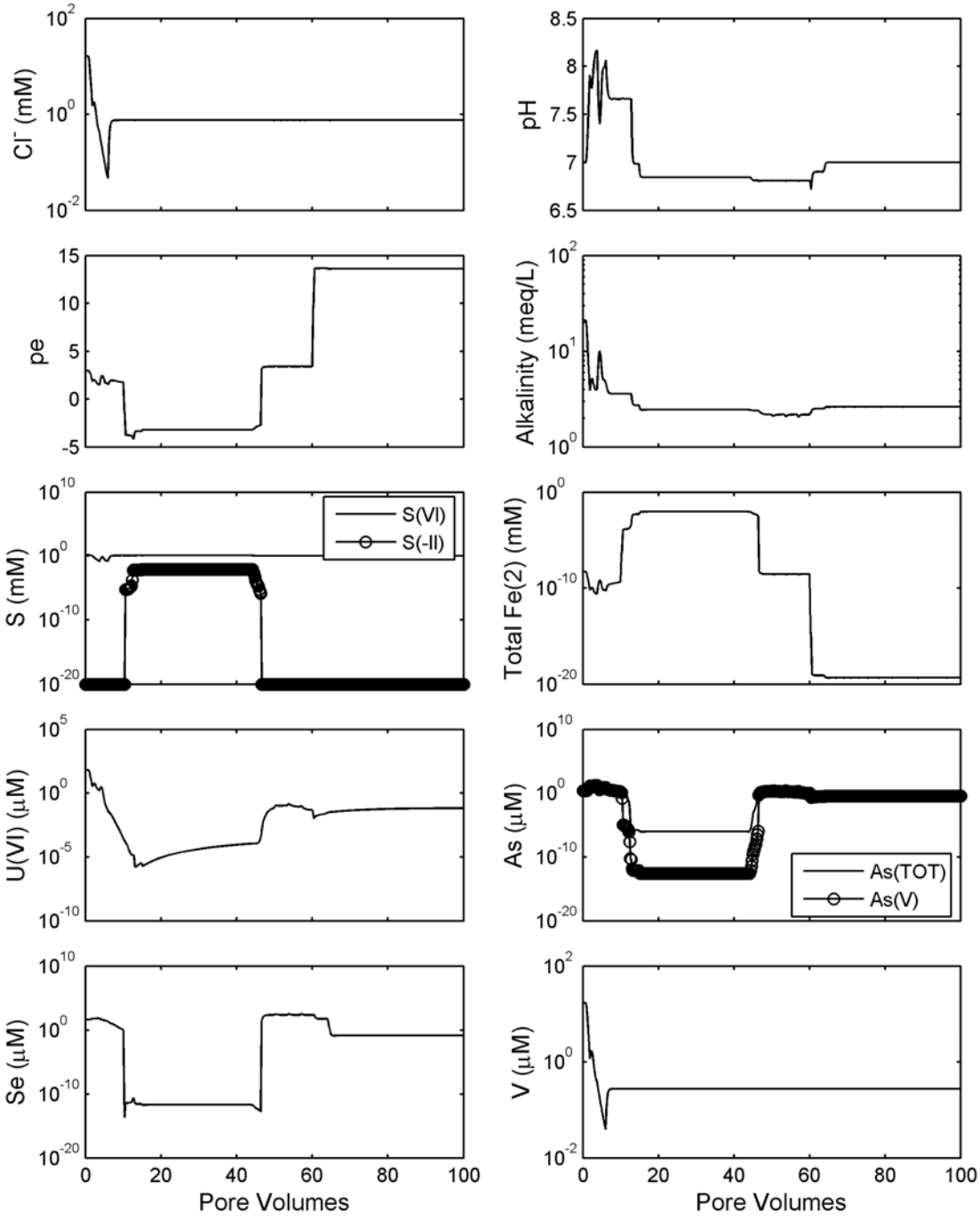

Figure 32. Simulation 15 results. Influent groundwater changed to be undersaturated with respect to calcite, and calcite abundance in the mined zone decreased to 4 mmoles/L. Oxic influent groundwater. Calcite, goethite, and elemental Se (50 ppm) initially present. 265 mg/L of $H_2S(g)$ added to the influent water during pore volumes 3.0 to 3.6. Pyrite and uraninite precipitation not allowed. Amorphous FeS and UO_2 precipitation allowed. Mass transfer coefficient = 10. Sulfide concentration indicated at $1x10^{-20}$ M is actually ≤ $1x10^{-20}$ M in plot.

volumes. The increased alkalinity favored UO_2(am) dissolution, and U(VI) was not adsorbed significantly at the elevated pH values and alkalinities. Therefore, the second peak at approximately 40 pore volumes did not occur as was observed in Simulation 10.

Simulation 16 (Fig. 33) considered the effect of the presence of an ion exchanging clay mineral in the porous medium. The total exchange capacity was set at 1 meq/L of water. The presence of the ion exchanger had a negligible effect on the simulation, because the exchanger was dominated by the Ca exchange complex due to the presence of calcite.

In Simulation 17 (Fig. 34), the chemistry of the influent groundwater was assumed to change after 30 pore volumes. It was assumed that the pH of the groundwater increased from 7 to 7.5, and the alkalinity increased from 2.5 to 10 meq/L. At 31 pore volumes, there was a small peak in the U(VI) concentration which resulted from desorption.

The adsorption site concentration was increased by a factor of 100 in Simulation 18 (Fig. 35). The higher adsorption site concentration caused an increase in the initial concentration of adsorbed Se(IV) to approximately 10 mM. Some of the adsorbed Se(IV) is reduced when the H_2S is added, but because the total Se(IV) concentration was larger than the added H_2S (7.6mM), there was not enough H_2S added to achieve reducing conditions at the end of the column. Consequently, the concentrations of dissolved uranium, arsenic, and selenium did not decrease below background concentrations between 3 and 6 pore volumes. Between 6 and 100 pore volumes, the concentration of dissolved uranium decreased gradually from 3 □M to 0.03 □M. The concentration of dissolved selenium was relatively constant between 6 and 70 pore volumes, but then increased by a factor of 25 as elemental selenium was completely dissolved and oxidized. A comparison of Figures 26 and 35 also shows that the time required to achieve oxidizing conditions in the aquifer increased with increasing adsorption site concentration. This occurred results because of the higher Se(IV) concentrations initially associated with the adsorption sites. Even after 100 pore volumes, some Se(IV) is adsorbed, and the pe had not increased as much as in the previous simulation (Fig. 26). This clearly shows that the adsorption site concentration can have a significant effect on the simulated concentration histories.

Adsorption of vanadium was included in Simulation 19 (Fig. 36). Of all of the adsorbing solutes considered, i.e., As(III), As(V), Se(IV), U(VI), and V(V), vanadium(V) is by far the most strongly adsorbed. For example, in the initial conditions for Simulation 19, more than 99 percent of the surface sites were occupied by V(V). The remaining 1 percent of the adsorption sites were either unoccupied or bound to the remaining adsorbates.

The results illustrated in Figure 36 show very large concentrations of vanadium between 4 and 29 pore volumes. This high vanadium concentration results because H_2S that was added in groundwater treatment, and the FeS that formed in the first cell, reduced V(V) to V(III) and V(IV), and adsorption of these species is not included in the simulations because of a lack of constants. However, because of the limited H_2S concentrations in the simulations, not all of the V(V) was reduced; the V(V) that was reduced was primarily adsorbed V(V) in the first cell. Adsorbed vanadium in cells 2-5 was nearly constant. At 29 pore volumes, there were uranium and arsenic peaks that result from the dissolution of uraninite and orpiment from the first cell. The increase in vanadium concentrations between 35 and 44 pore volumes coincides with the oxidation of Se(s) and elution of As(V) from the column.

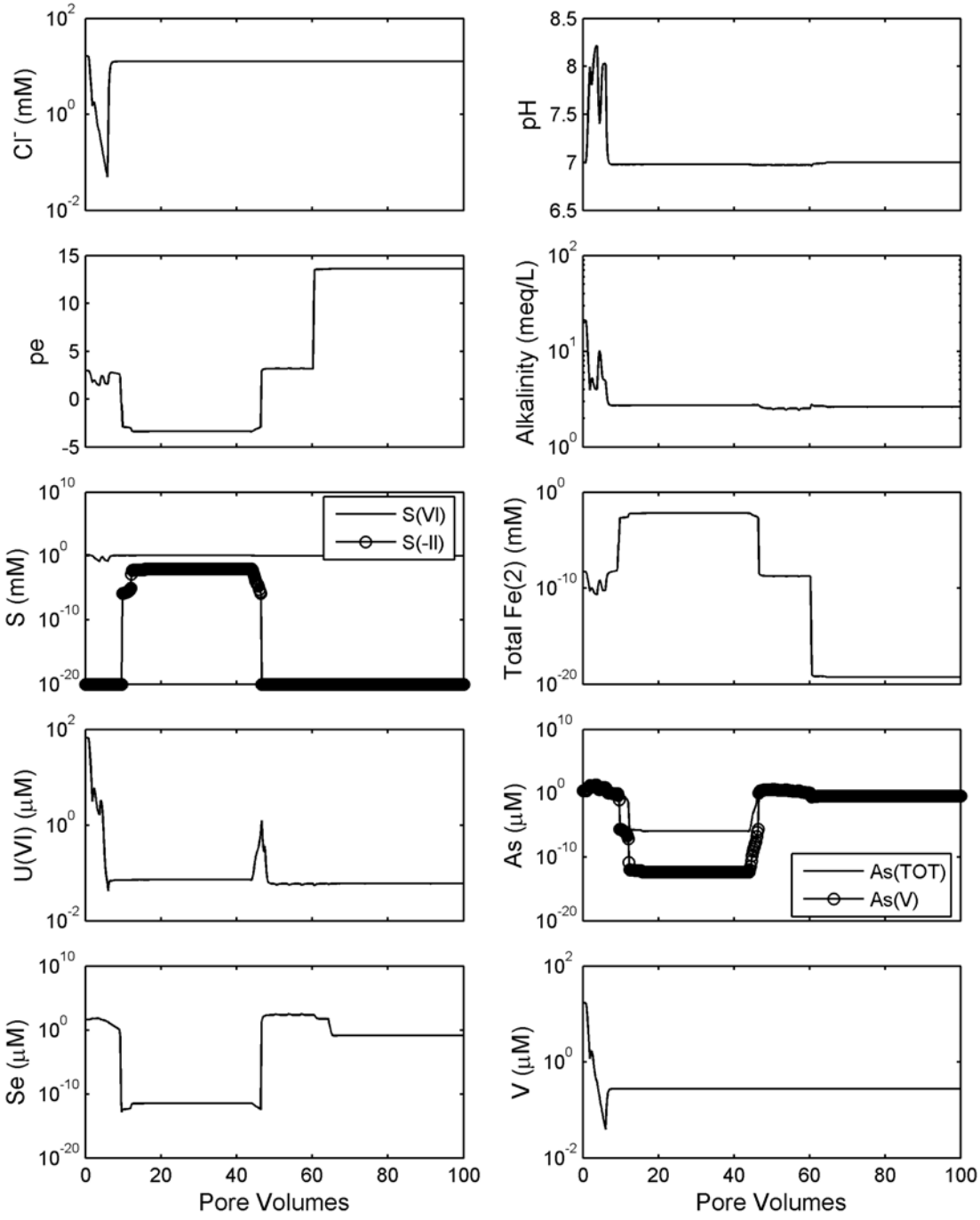

Figure 33. Simulation 16 results. Consideration of the effect of an ion exchanging clay mineral. Oxic influent groundwater. Calcite, goethite, and elemental Se (50 ppm) initially present. 265 mg/L of H_2S(g) added to the influent water during pore volumes 3.0 to 3.6. Pyrite and uraninite precipitation not allowed. Amorphous FeS and UO_2 precipitation allowed. Mass transfer coefficient = 10. Sulfide concentration indicated at $1x10^{-20}$ M is actually ≤ $1x10^{-20}$ M in plot.

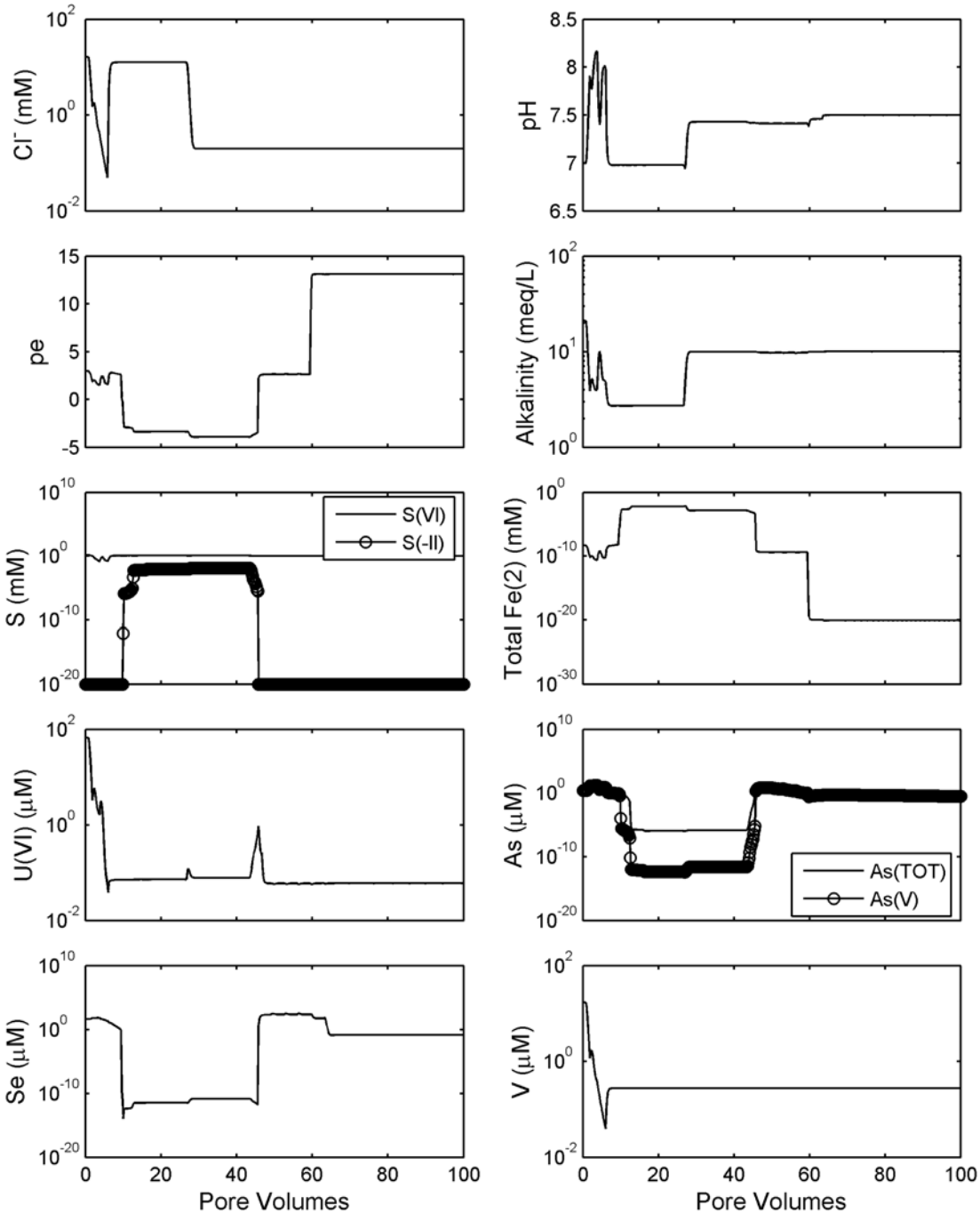

Figure 34. Simulation 17 results. Consideration of the effect of an increase in the pH and alkalinity of the influent groundwater at 30 pore volumes. Oxic influent groundwater. Calcite, goethite, and elemental Se (50 ppm) initially present. 265 mg/L of $H_2S(g)$ added to the influent water during pore volumes 3.0 to 3.6. Pyrite and uraninite precipitation not allowed. Amorphous FeS and UO_2 precipitation allowed. Mass transfer coefficient = 10. Sulfide concentration indicated at $1x10^{-20}$ M is actually ≤ $1x10^{-20}$ M in plot.

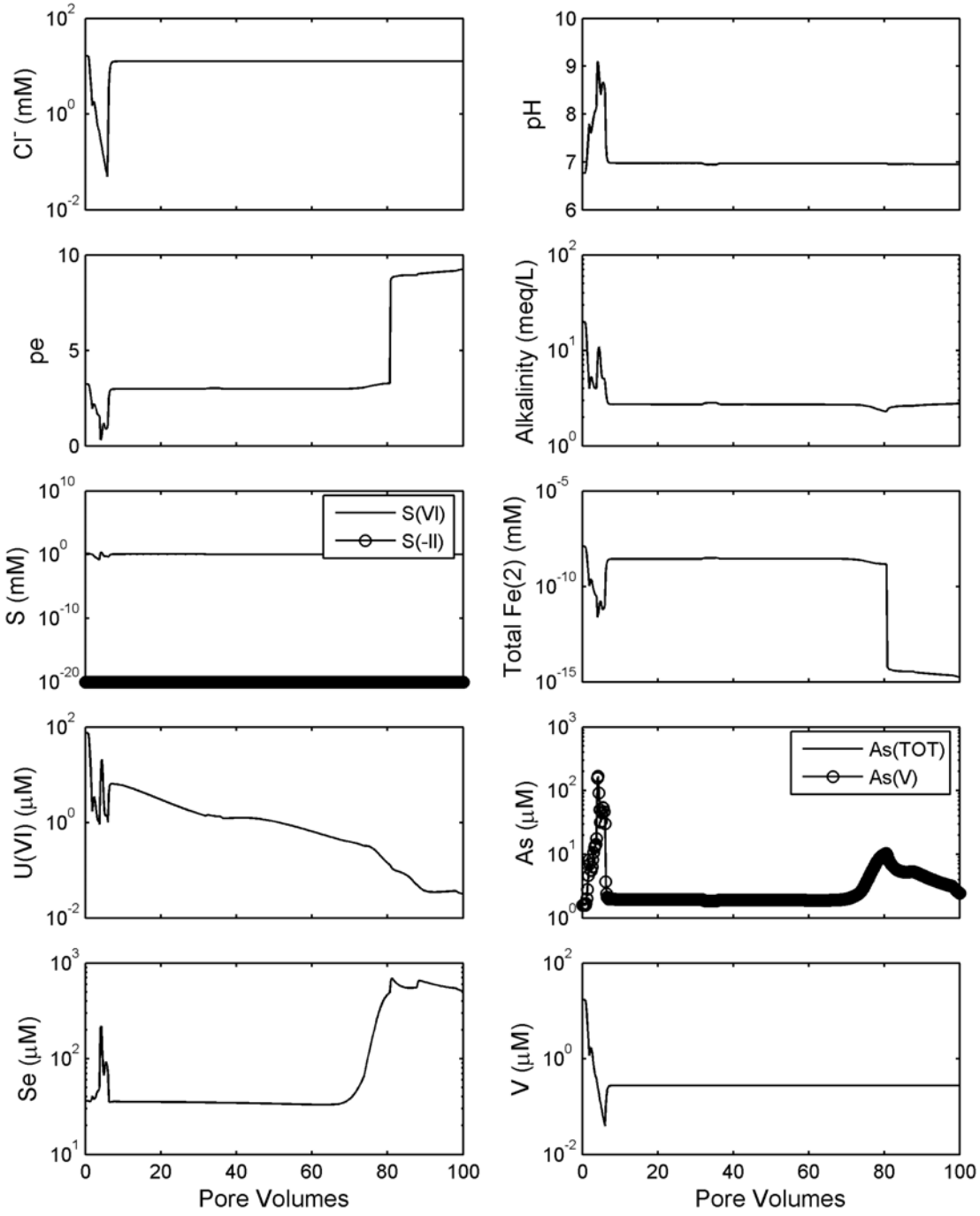

Figure 35. Simulation 18 results. Consideration of the effect of an increase in adsorption site density by a factor of 100. Oxic influent groundwater. Calcite, goethite, and elemental Se (50 ppm) initially present. 265 mg/L of $H_2S(g)$ added to the influent water during pore volumes 3.0 to 3.6. Pyrite and uraninite precipitation not allowed. Amorphous FeS and UO_2 precipitation allowed. Mass transfer coefficient = 10. Total sulfide ≤ $1x10^{-20}$ M in plot.

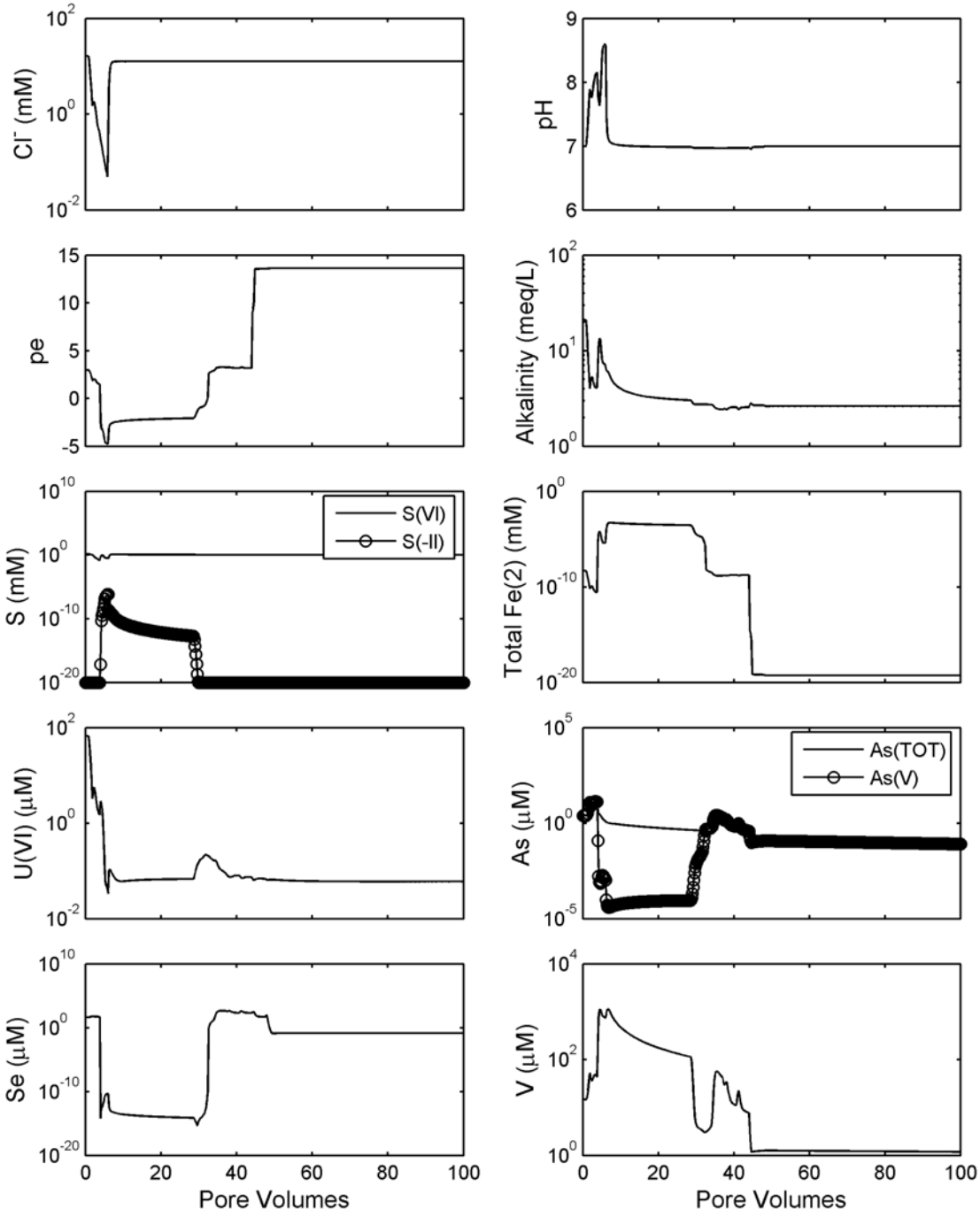

Figure 36. Simulation 19 results. Consideration of the effect of an increase in adsorption site density by a factor of 100 and including the effects of vanadium adsorption. Oxic influent groundwater. Calcite, goethite, and elemental Se (50 ppm) initially present. 265 mg/L of $H_2S(g)$ added to the influent water during pore volumes 3.0 to 3.6. Pyrite and uraninite precipitation not allowed. Amorphous FeS and UO_2 precipitation allowed. Mass transfer coefficient = 10. Sulfide concentration indicated at $1x10^{-20}$ M is actually ≤ $1x10^{-20}$ M in plot.

5.3.2 Stabilization Modeling Results with Mildly Reducing Influent Groundwater

Three simulations were conducted to examine the predicted long term behavior of groundwater stabilization when mildly reducing groundwater flowed into the mined zone after the groundwater sweep and treatment phases.

Simulation 20 (Fig. 37) was similar to Simulation 3, except that the groundwater flowing into the mined zone was equivalent to the initial mildly reducing groundwater present before mining activities started. The groundwater had a pH of 8.5, contained no dissolved oxygen, had an Fe(II) concentration of 0.7 □M, a SO_4 concentration of 1 mM, but no S(-II). As in Simulation 3, there was no H_2S treatment. The initial pe was approximately 12 because of the in situ leaching activities and because some oxygen was introduced into the system by the reverse osmosis treatment. After approximately 10 pore volumes, all of the dissolved oxygen had been removed from the mobile and immobile cells, and then the remaining Se(VI) was reduced to Se(IV), which displaced U(VI) from the adsorption sites. After 20 pore volumes, there were no significant changes in the simulation results.

Simulation 21 was similar to Simulation 8, except that instead of oxic groundwater flowing into the mined zone during stabilization, the same mildly reducing water considered in Simulation 20 was assumed to enter the mined zone. In this simulation, the groundwater at the end of the groundwater sweep and treatment was relatively reducing because of the H_2S addition. Figure 38 illustrates that after 5 pore volumes, the reducing groundwater decreased the pe to approximately –5, and then there were no significant changes in the predicted water quality out to 100 pore volumes.

Simulation 22 was the same as Simulation 21, except that the pH of the mildly reducing influent groundwater was assumed to equal 7. The results for this case are shown in Figure 39. Again, there were no significant changes after 10 pore volumes.

In all cases in which reducing groundwater flowed into the mined region during groundwater stabilization, the concentrations of U, Se, As, and V were predicted to remain very low, in contrast to the various cases in which oxic influent groundwater was introduced during groundwater stabilization.

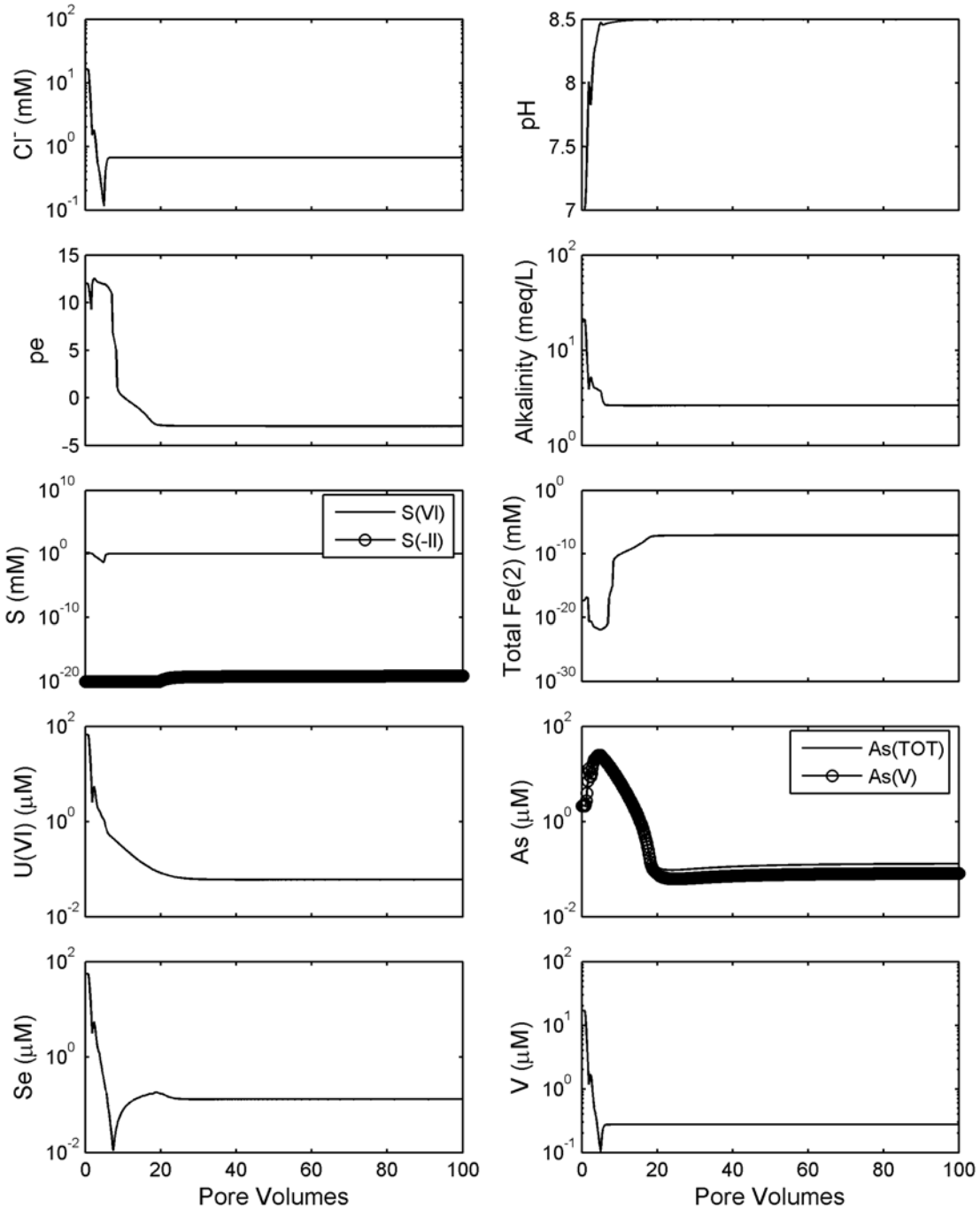

Figure 37. Simulation 20 results, similar to Simulation 3, except with groundwater stabilization with mildly reducing influent groundwater at pH 8.5. Calcite and goethite initially present in all cells. Mass transfer coefficient = 10. Sulfide concentration indicated at $1x10^{-20}$ M is actually ≤ $1x10^{-20}$ M in plot.

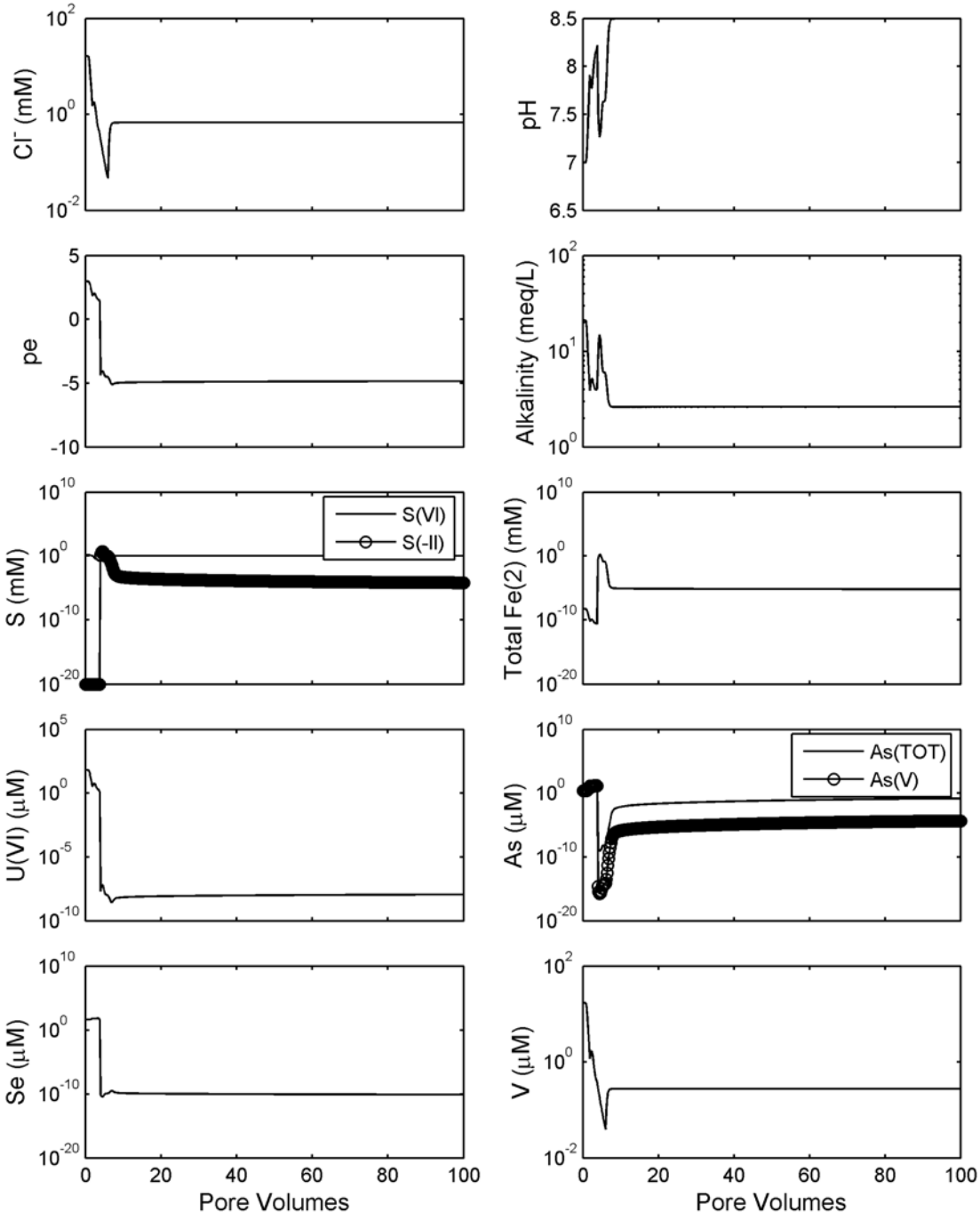

Figure 38. Simulation 21 results, similar to Simulation 8, except with groundwater stabilization with anoxic influent groundwater at pH 8.5. Calcite, goethite, and elemental Se (50 ppm) initially present. 265 mg/L of $H_2S(g)$ added to the influent water during pore volumes 3.0 to 3.6. Pyrite precipitation not allowed. Elemental sulfur precipitation allowed. Mass transfer coefficient = 10. Sulfide concentration indicated at $1x10^{-20}$ M is actually ≤ $1x10^{-20}$ M in plot.

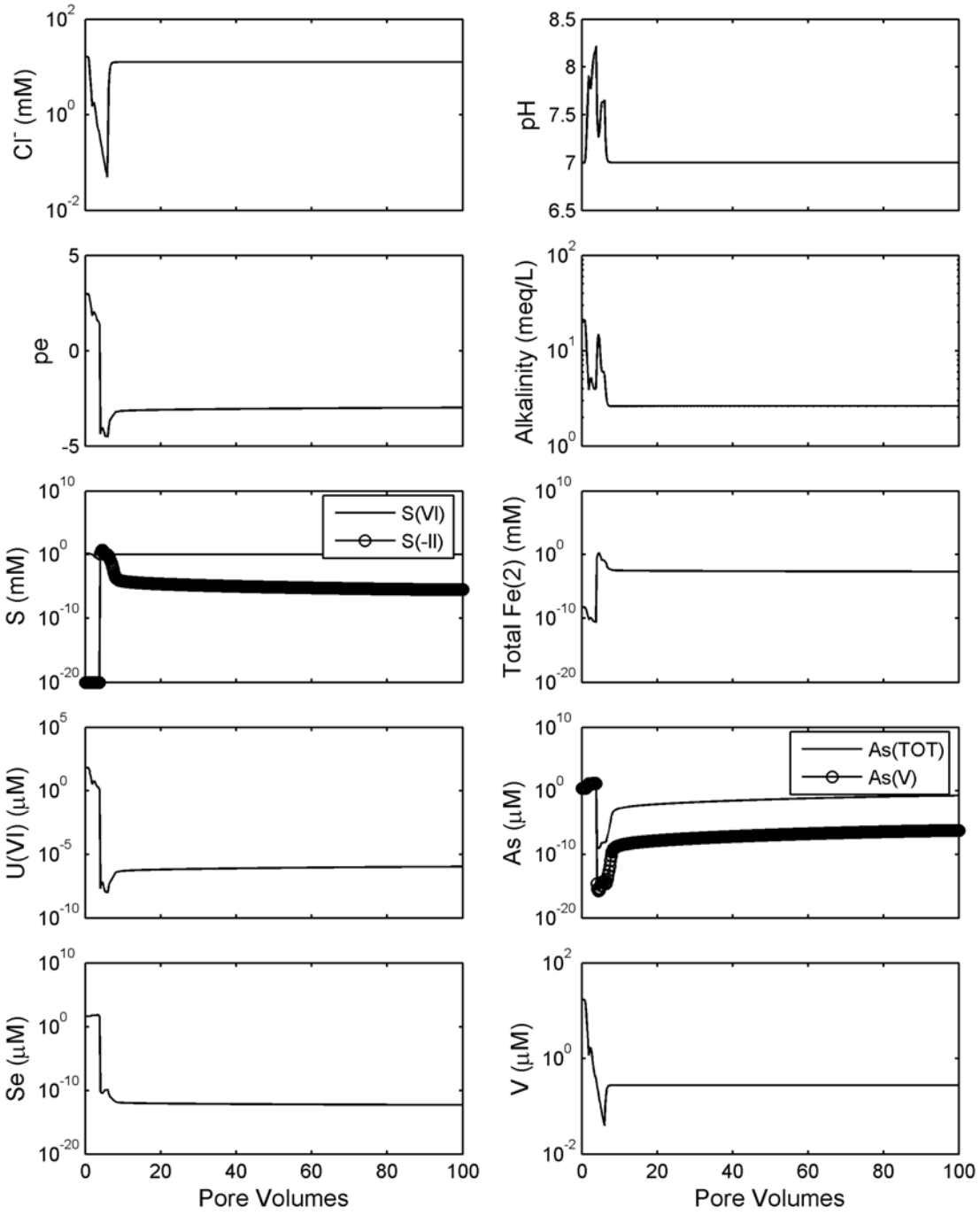

Figure 39. Simulation 22 results, similar to Simulation 21, except with groundwater stabilization with anoxic influent groundwater at pH 7. Calcite, goethite, and elemental Se (50 ppm) initially present. 265 mg/L of $H_2S(g)$ added to the influent water during pore volumes 3.0 to 3.6. Pyrite precipitation not allowed. Elemental sulfur precipitation allowed. Mass transfer coefficient = 10. Sulfide concentration indicated at $1x10^{-20}$ M is actually ≤ $1x10^{-20}$ M in plot.

6 CONCLUSIONS

Modeling the geochemical aspects of groundwater restoration at uranium ISL facilities is complex. The modeling requires a detailed knowledge of the redox environment within the leached zone during the restoration process, which may be affected by many factors. With respect to the restoration of groundwater quality to baseline conditions, the model results were sensitive to two major factors: 1) whether oxic or reducing groundwater flowed into the mined zone during stabilization, and 2) which reduced mineral phases were initially present or precipitated in the mined zone during hydrogen sulfide addition.

In the generic case where hydrogen sulfide treatment is used and reducing groundwater enters the mined zone by natural gradient processes after treatment, the concentrations of dissolved U, Se, As, and V are predicted to remain at low concentrations near or below baseline, i.e, their concentrations are indeed stabilized.

Most of the simulations in this report consider cases where oxic groundwater enters the mined zone by natural gradient processes after treatment, in order to identify potential problems in water quality that could occur under this scenario. This scenario also appears more likely unless there has been a reversal in groundwater flow direction between the deposition of the uranium roll front and the present time.

The modeling of groundwater quality evolution during the first few pore volumes of groundwater sweep (pore volume 1) and RO treatment was in reasonable agreement with the results observed in the field at the Ruth ISL. The pH increased from 7 to about 8.4, in very good agreement with the field results, and the concentrations of most solutes decreased markedly after the first pore volume, with the exception of arsenic.

In the most oxic case considered (no hydrogen sulfide treatment), arsenic was present predominantly as As(V), and its dissolved concentration at pH 7 was initially very low due to strong sorption. Although the arsenic concentration evolution was more complex in the field observations than in the model, the simulations did predict an increase in dissolved arsenic that was observed. Although the concentrations of U, Se, and V decreased rapidly during the first few pore volumes in the oxic case, their concentrations were still maintained above baseline levels for tens of pore volumes by desorption from the sediments.

The modeling results show that the presence of residual reducing mineral phases in the mined zone had a big effect on predicted water quality during groundwater stabilization (without hydrogen sulfide treatment). For example, the presence of elemental Se caused a big increase in the dissolved Se concentrations during stabilization, because more Se was available to be oxidized, leading to higher dissolved Se concentrations after many pore volumes. Assumed residual pyrite and uraninite in immobile groundwater zones resulted in a large decrease in the predicted concentrations of dissolved U, Se, and As. However, these modeling results were not consistent with the field observations at Ruth ISL, which showed elevated concentrations of these elements until hydrogen sulfide treatment was applied.

It is clear from the modeling and from field observations that hydrogen sulfide treatment greatly reduces the concentrations of dissolved U, Se, As, and V. Once hydrogen sulfide treatment ends, however, the modeling suggests that the long-term effectiveness of the treatment may depend on which reduced mineral phases formed in the subsurface if oxic groundwater infiltrates the mined zone during the stabilization phase. In particular, the modeling results are very sensitive to the fate of the introduced

sulfide. If sulfide is assumed to be oxidized to sulfate by iron oxides, and there is an excess of iron oxides, then the results are not dramatically different from the oxic cases without hydrogen sulfide treatment. If the most thermodynamically stable phase, pyrite, is allowed to form and chemical equilibrium is assumed, then sulfide is mostly precipitated as pyrite in the region of the aquifer near the well at which the hydrogen sulfide is introduced. This means that much of the mined zone does not become reducing, and the predicted concentrations of U and Se remain high in withdrawal wells. This type of behavior was not observed at the Ruth ISL after hydrogen sulfide treatment.

It was reported in the field observations at the Ruth ISL that elemental sulfur was observed in the groundwater after hydrogen sulfide treatment and that very little sulfide ion broke through to the withdrawal wells. If the modeling was constrained to let metastable elemental sulfur precipitate, but not pyrite, then the reducing conditions spread throughout the modeling domain, and the concentrations of dissolved U, Se, As, and V, were dramatically reduced in the modeling results, as observed in the field after hydrogen sulfide treatment. Thus, Simulation 8 in this report was probably closest to the field observations at the Ruth ISL during the first few pore volumes.

It is important to note that the decrease in the concentrations of dissolved U, Se, and As that are predicted to occur as a result of the hydrogen sulfide treatment are due to the precipitation of reduced mineral phases, such as uraninite, orpiment, and ferrous selenide. Thus, these elements are still present in the mined zone and can potentially be re-oxidized by influent oxic groundwater.

The long-term stabilization simulations suggest that if oxic groundwater enters the mined zone by natural-gradient groundwater flow, the reducing conditions that cause the precipitation of these phases will eventually be overcome, the reduced mineral phases will be re-oxidized, and U, Se, and As will be mobilized again after many pore volumes of groundwater have passed. However, the actual concentrations of these elements and the timing of the mobilization would depend on numerous factors, such as the concentration of oxygen in the influent groundwater, the amount of hydrogen sulfide treatment, the rate of groundwater flow, the rate of mineral oxidation, and many other variables.

7 REFERENCES

Altair Resources, Inc., *Bison Basin Decommissioning Project, Phase 1, Final Report*, Altair Resources, Casper, Wyoming, 1988.

Crow Butte Resources, Inc., *Mine Unit 1 Restoration Report, Crow Butte Uranium Project,* Source Materials License Application SUA-1534, Crow Butte Resources, Inc., Crawford, Nebraska, 2000.

Crow Butte Resources, Inc., *Response to U. S. Nuclear Regulatory Commission Request for Additional Information, Mine Unit 1 Restoration Report, Crow Butte Uranium Project,* Source Materials License Application SUA-1534, Crow Butte Resources, Inc., Crawford, Nebraska, 2001.

Dahlkamp, F.J., *Uranium Ore Deposits*, Springer-Verlag, Berlin, Germany, 1993.

Davis, J.A. and Curtis, G.P. (2003) *Application of Surface Complexation Modeling to Describe Uranium(VI) Adsorption and Retardation at the Uranium Mill Tailings Site at Naturita, Colorado*, Report NUREG CR-6820, U. S. Nuclear Regulatory Commission, Rockville, MD.

Davis, J.A., and D.B. Kent, "Surface Complexation Modeling in Aqueous Geochemistry," *Mineral-Water Interface Geochemistry*, Reviews in Mineralogy Series, Mineralogical Society of America, Vol. 23, 177-260, 1990.

Department of Energy, *Decommissioning of U.S. Uranium Production Facilities*, DOE-EIA-0592, 1995.

Deutsch, W.J., W.J. Martin, L.E. Eary, and R.J. Serne, *Methods of Minimizing Ground-Water Contamination from In situ Leach Uranium Mining*, NUREG/CR-3709, U. S. Nuclear Regulatory Commission, Washington, D.C., 1985.

Dzombak, D.A. and Morel, F.M.M. *Surface Complexation Modeling: Hydrous Ferric Oxide*, John Wiley & Sons, New York, NY, 1990.

Granger, H.C. and Warren, C.G., Zoning in the altered tongue associated with roll-type uranium deposits, in *Formation of Uranium Ore Deposits,* International Atomic Energy Agency, Vienna, Austria, p. 185-199.

Grenthe, I. et al., *Chemical Thermodynamics of Uranium*, Elsevier, Amsterdam, 1992.

Harshman, E.N., Distribution of some elements in some roll-type uranium deposits, in *Formation of Uranium Ore Deposits,* International Atomic Energy Agency, Vienna, Austria, p. 169-183, 1974.

Johnson, S., Summary document on the groundwater restoration for the Bison Basin Decommissioning Project, Wyoming Dept. of Environmental Quality, Land Quality Division, 1989.

Kasper, D.R., H.W. Martin, L.D. Munsey, R.B. Bhappu, and C.K. Chase, *Environmental Assessment of In-situ Mining*, Open File Rept. 101-80. Bureau of Mines, Washington, D.C., 1979.

Langmuir, D.L., *Aqueous Environmental Geochemistry*, Prentice-Hall, 1997.

Moxley, M. and G. Catchpole, *Aquifer Restoration at the Bison Basin In Situ Uranium Mine*, Proceedings, In Situ Minerals Symposium, Casper, Wyoming, May 22-24, 1989.

Parkhurst, D.L., *User's Guide to PHREEQ – A Computer Program for Speciation, Reaction-path, Advective-Transport, and Inverse Geochemical Calculations*, U. S. Geological Survey, Water Resources Investigation Rept., 95-4227, Washington, D.C., 1995.

Parkhurst, D.L. and Appelo, C.A.J., *User's Guide to PHREEQC (Version 2) – A Computer Program for Speciation, Reaction-path, Advective-Transport, and Inverse Geochemical Calculations*, U. S. Geological Survey, Water Resources Investigation Rept., 99-4259, Washington, D.C., 1999.

Potter, R.W., M.A. Clynne, J.M. Thompson, V.L. Thurmond, R.C. Erd, N.L. Nehring, K.A. Smith, P.J. Lamothe, J.L. Seeley, D.R. Tweeton, G.R. Anderson, and W.H. Engelmann, *Chemical Monitoring of the In-Situ Leaching of a South Texas Uranium Orebody*, Open File Rept. 79-1144, U. S. Geological Survey, Washington, D.C., 1979.

Rio Algom, Amendment 1 to Source Material License SUA-1548, Flare Factor Estimate and Justification, Smith Ranch Facility, Source: U. S. Nuclear Regulatory Commission, 2001.

Rojas, J.L., Introduction to in situ leaching or uranium, In: *In Situ Leaching of Uranium: Technical, Environmental, and Economic Aspects,* IAEA-TECDOC-492, International Atomic Energy Agency, Vienna, Austria, p. 7-20, 1989.

Schmidt, C., Groundwater restoration and stabilization at the Ruth ISL test site in Wyoming, USA, In: *In Situ Leaching of Uranium: Technical, Environmental, and Economic Aspects,* IAEA-TECDOC-492, International Atomic Energy Agency, Vienna, Austria, p. 97-126, 1989.

Silva, R.J. et al., "Thermodynamics 2; Chemical Thermodynamics of Americium," with an appendix on "Chemical Thermodynamics of Uranium," Nuclear Energy Agency, OECD, North-Holland, Elsevier, 1995.

U. S. Department of Energy, *Decommissioning of U.S. Uranium Production Facilities,* DOE-EIA-0592, 1995.

U. S. Nuclear Regulatory Commission, *Standard Review Plan for In Situ Leach Uranium Extraction License Applications*, NUREG-1569, U. S. Nuclear Regulatory Commission, Washington, D.C., 2003.

U. S. Nuclear Regulatory Commission, *Final Environmental Impact Statement to Construct and Operate the Crownpoint Solution Mining Project, Crownpoint, New Mexico*, NUREG-1508, U. S. Nuclear Regulatory Commission, Washington, D.C., 1997.

U. S. Nuclear Regulatory Commission, *A Baseline Risk-Informed, Performance-Based Approach for In Situ Leach Uranium Extraction Licensees*, NUREG/CR-6733, U. S. Nuclear Regulatory Commission, Washington, D.C., 2001.

Waite, T.D. et al., "Uranium(VI) Adsorption to Ferrihydrite; Application of a Surface Complexation Model," *Geochim. Cosmochim. Acta*, Vol. 58, No. 24, 5465-5478, 1994.

8 APPENDIX A: EXAMPLE PHREEQC INPUT FILE FOR SIMULATION 8

The listing below is the PHREEQC input file for Simulation 8.

```
DATABASE D:\NRC\Simulations\database\phreeqcU.dat
TITLE water quality evolution at Ruth ISL during gw restoration
#
# Authors: James A. Davis  (jadavis@usgs.gov) and
#          Gary P. Curtis  (gpcurtis@usgs.gov)
#
# Beginning of gw sweep phase in January 1984
# one pore volume, then RO unit for 3.2 PV
# Mass transfer coefficient of 10; pyrite can ppt. but not dissolve;
# 50 ppm Se(s) present
# 250 mg/L sulfide added during pore volumes 3.0 to 3.6 with
# neutralizing HCO3 and Br tracer
# After 5 PV, aerobic (PO2=.2atm) water at pH 7 enters to column
SOLUTION 0  Background water conditions - oxic upgrad water, December 1983
   # NOTES:
   units   mmol/kgw
   pH       8.5
   pe       6.5
   redox    Fe(2)/Fe(3)
   temp     25.0
   Na       4.78
   K        0.11
   Ca       0.2      Calcite
   Mg       0.082
   Cl       0.2      Charge
   S        1.04
   Br       0.001
   Fe(2)   0.0007
   Fe(3)   1.0E-5
   As      1.3E-4
   Se      1.3E-4
   V       2.75E-4
   Alkalinity 2.62
   U        0.00006
REACTION 0
   O2(g)   1.0
   9.375E-5  #3 ppm O2 added
SAVE solution 0
END
SOLUTION 1-11  Initial solution for column
   units   mmol/kgw
   pH       7.0
   pe      -0.4
   temp     25.0
   Na       36.3
   K        0.256
   Ca       0.65       Calcite
   Mg       0.78
   Cl       15.9      Charge
   S       1.52
   Br       0.00001
   Fe      1.0E-7
   As      2.14E-3
   Se      5.57E-2
   V       1.70E-2
```

```
    Alkalinity 21.0
    U       6.69E-2
  EQUILIBRIUM_PHASES 1-11
    Calcite 0.0   0.400  #1.0% calcite
    Goethite 0.0  0.03
    FeS(ppt)  0.0   0.00  #pyrite can ppt., but not dissolve
    Se(s)   0.0   0.00253  #50 ppm Se (leftover Se)
    UO2(am) 0.0 0.0
    Orpiment  0.0 0.0
    FeSe2     0.0 0.0
    Sulfur    0.0 0.0
  SURFACE 1-11
    # This equilibrates the solutions in the domain with
    # a nonelectrostatic surface complexation model
    # adsorption constants for U(6), As(5), As(3), and Se(4) in database
    -no_edl
    equilibrate 1
    Sfo_w    3.795E-02  1  1     # The " 1  1" are used in edl calcs
    #Sfo_s    2.8445e-005
    #Sfo_z    2.8445e-006
  END
  # If the following 2 lines are uncommented, less output is written
  PRINT
     -reset  false
SELECTED_OUTPUT
    -file               breakthru.out
    -reset              false
    -solution           true
    -distance           true
    -time               true
    -pH                 true
    -pe                 true
    -alkalinity         true
    -equilibrium_phases   Calcite  Goethite  FeS(ppt)  Se(s) UO2(am)  Orpiment  FeSe2 Sulfur
    -molalities          UO2+2  HCO3-  Cl-  Na+ Ca+2  HS-
                       Fe+2   SO4-2  O2 Sfo_wOUO2+

  USER_PUNCH
    -head Fe2_mmol SO4_mmol HS_mmol As(V)_umol As(III)_umol U(VI)_umol Se_umol V_umol
  10 PUNCH TOT("Fe(2)")*1.0E3 TOT("S(6)")*1.0E3 TOT("S(-2)")*1.0E3 TOT("As(5)")*1.0E6
  TOT("As(3)")*1.0E6 TOT("U(6)")*1.0E6 TOT("Se")*1.0E6 TOT("V")*1.0E6

  TRANSPORT
     -cells  5
     -shifts 5
     -lengths     5*0.2
     -timest 0.2
     -bcon   3  3
     -diffc  0.0e-9
     -disp   0.002
     -punch  1
     -punch  5
     -stag        1  1.0E01    0.3        0.1
  #    -stag       1  6.8e-16  0.3        0.001
  #   1 stagnant layer^, ^alpha, ^theta(m), ^theta(im)
  END
  #Begin RO cycling after 1 PV - uranium removed ion exchanger not simulated
  #Assume dilution of water extracted from ground by 75% pure water
  USE SOLUTION 5
  SOLUTION 12
    units   mmol/kgw
    pH        7.0
```

```
   pe        12
   temp    25.0
MIX 0
     5      0.25
     12     0.75
SAVE SOLUTION 0
REACTION 0
   O2(g)   1.0   NaHCO3  83.8
   3.125E-5  #1 ppm O2 added  background HCO3 added
EQUILIBRIUM_PHASES 0
   Calcite 10.0   0.000
   Goethite 100.0  0.00
SAVE SOLUTION 0
END
SELECTED_OUTPUT
   #-file              breakthru.out
   -reset              false
   -solution           true
   -distance           true
   -time               true
   -pH                 true
   -pe                 true
   -alkalinity         true
   -equilibrium_phases   Calcite  Goethite  FeS(ppt)  Se(s) UO2(am)  Orpiment  FeSe2 Sulfur
   -molalities          UO2+2  HCO3-  Cl-  Na+ Ca+2   HS-
                      Fe+2   SO4-2  O2 Sfo_wOUO2+

USER_PUNCH
       -head Fe2_mmol SO4_mmol HS_mmol As(V)_umol As(III)_umol U(VI)_umol Se_umol V_umol
10 PUNCH TOT("Fe(2)")*1.0E3 TOT("S(6)")*1.0E3 TOT("S(-2)")*1.0E3 TOT("As(5)")*1.0E6
TOT("As(3)")*1.0E6 TOT("U(6)")*1.0E6 TOT("Se")*1.0E6 TOT("V")*1.0E6

TRANSPORT
    -cells  5
    -shifts 1
    -lengths     5*0.2
    -timest 0.2
    -bcon   3  3
    -diffc  0.0e-9
    -disp   0.002
    -punch  1
    -punch  5
    -stag        1  1.0E01    0.3        0.1
#     -stag       1  6.8e-16  0.3        0.001
#   1 stagnant layer^, ^alpha, ^theta(m), ^theta(im)
END
#RO cycling after 1.2 PV
#Assume dilution of water extracted from ground by 75% pure water
USE SOLUTION 5
MIX 0
     5      0.25
     12     0.75
SAVE SOLUTION 0
REACTION 0
   O2(g)   1.0   NaHCO3  83.8
   3.125E-5  #1 ppm O2 added  background HCO3 added
EQUILIBRIUM_PHASES 0
   Calcite 10.0   0.000
   Goethite 100.0  0.00
SAVE SOLUTION 0
END
SELECTED_OUTPUT
```

```
   #-file              breakthru.out
   -reset              false
   -solution           true
   -distance           true
   -time               true
   -pH                 true
   -pe                 true
   -alkalinity         true
   -equilibrium_phases  Calcite  Goethite  FeS(ppt)  Se(s) UO2(am)  Orpiment  FeSe2 Sulfur
   -molalities          UO2+2  HCO3-  Cl-  Na+ Ca+2   HS-
                      Fe+2   SO4-2  O2 Sfo_wOUO2+

USER_PUNCH
      -head Fe2_mmol SO4_mmol HS_mmol As(V)_umol As(III)_umol U(VI)_umol Se_umol V_umol
10 PUNCH TOT("Fe(2)")*1.0E3 TOT("S(6)")*1.0E3 TOT("S(-2)")*1.0E3 TOT("As(5)")*1.0E6
TOT("As(3)")*1.0E6 TOT("U(6)")*1.0E6 TOT("Se")*1.0E6 TOT("V")*1.0E6

TRANSPORT
    -cells  5
    -shifts 1
    -lengths     5*0.2
    -timest 0.2
    -bcon   3  3
    -diffc  0.0e-9
    -disp   0.002
    -punch  1
    -punch  5
    -stag        1  1.0E01    0.3        0.1
#    -stag       1  6.8e-16  0.3        0.001
#   1 stagnant layer^, ^alpha, ^theta(m), ^theta(im)
END
#RO cycling after 1.4 PV
#Assume dilution of water extracted from ground by 75% pure water
USE SOLUTION 5
MIX 0
     5       0.25
     12      0.75
SAVE SOLUTION 0
REACTION 0
   O2(g)   1.0   NaHCO3  83.8
   3.125E-5  #1 ppm O2 added  background HCO3 added
EQUILIBRIUM_PHASES 0
   Calcite 10.0   0.000
   Goethite 100.0  0.00
SAVE SOLUTION 0
END
SELECTED_OUTPUT
   #-file              breakthru.out
   -reset              false
   -solution           true
   -distance           true
   -time               true
   -pH                 true
   -pe                 true
   -alkalinity         true
   -equilibrium_phases  Calcite  Goethite  FeS(ppt)  Se(s) UO2(am)  Orpiment  FeSe2 Sulfur
   -molalities          UO2+2  HCO3-  Cl-  Na+ Ca+2   HS-
                      Fe+2   SO4-2  O2 Sfo_wOUO2+

USER_PUNCH
      -head Fe2_mmol SO4_mmol HS_mmol As(V)_umol As(III)_umol U(VI)_umol Se_umol V_umol
```

```
10 PUNCH TOT("Fe(2)")*1.0E3 TOT("S(6)")*1.0E3 TOT("S(-2)")*1.0E3 TOT("As(5)")*1.0E6
TOT("As(3)")*1.0E6 TOT("U(6)")*1.0E6 TOT("Se")*1.0E6 TOT("V")*1.0E6

TRANSPORT
    -cells  5
    -shifts 1
    -lengths     5*0.2
    -timest 0.2
    -bcon   3  3
    -diffc  0.0e-9
    -disp   0.002
    -punch  1
    -punch  5
    -stag        1  1.0E01    0.3        0.1
#     -stag       1  6.8e-16  0.3        0.001
#   1 stagnant layer^, ^alpha, ^theta(m), ^theta(im)
END
#RO cycling after 1.6 PV
#Assume dilution of water extracted from ground by 75% pure water
USE SOLUTION 5
MIX 0
     5       0.25
     12      0.75
SAVE SOLUTION 0
REACTION 0
   O2(g)   1.0   NaHCO3  83.8
   3.125E-5  #1 ppm O2 added  background HCO3 added
EQUILIBRIUM_PHASES 0
   Calcite 10.0   0.000
   Goethite 100.0  0.00
SAVE SOLUTION 0
END
SELECTED_OUTPUT
   #-file              breakthru.out
   -reset              false
   -solution             true
   -distance             true
   -time               true
   -pH                 true
   -pe                true
   -alkalinity           true
   -equilibrium_phases   Calcite Goethite FeS(ppt)  Se(s) UO2(am)  Orpiment  FeSe2 Sulfur
   -molalities           UO2+2  HCO3-  Cl-  Na+ Ca+2   HS-
                      Fe+2   SO4-2  O2 Sfo_wOUO2+

USER_PUNCH
       -head Fe2_mmol SO4_mmol HS_mmol As(V)_umol As(III)_umol U(VI)_umol Se_umol V_umol
10 PUNCH TOT("Fe(2)")*1.0E3 TOT("S(6)")*1.0E3 TOT("S(-2)")*1.0E3 TOT("As(5)")*1.0E6
TOT("As(3)")*1.0E6 TOT("U(6)")*1.0E6 TOT("Se")*1.0E6 TOT("V")*1.0E6

TRANSPORT
    -cells  5
    -shifts 1
    -lengths     5*0.2
    -timest 0.2
    -bcon   3  3
    -diffc  0.0e-9
    -disp   0.002
    -punch  1
    -punch  5
    -stag        1  1.0E01    0.3        0.1
#     -stag       1  6.8e-16  0.3        0.001
```

```
#   1 stagnant layer^, ^alpha, ^theta(m), ^theta(im)
END
#RO cycling after 1.8 PV
#Assume dilution of water extracted from ground by 75% pure water
USE SOLUTION 5
MIX 0
     5       0.25
     12      0.75
SAVE SOLUTION 0
REACTION 0
   O2(g)   1.0   NaHCO3  83.8
   3.125E-5  #1 ppm O2 added  background HCO3 added
EQUILIBRIUM_PHASES 0
   Calcite 10.0   0.000
   Goethite 100.0  0.00
SAVE SOLUTION 0
END
SELECTED_OUTPUT
   #-file              breakthru.out
   -reset              false
   -solution             true
   -distance             true
   -time               true
   -pH                 true
   -pe                true
   -alkalinity           true
   -equilibrium_phases   Calcite  Goethite  FeS(ppt)  Se(s) UO2(am)  Orpiment  FeSe2 Sulfur
   -molalities           UO2+2  HCO3-  Cl-  Na+ Ca+2   HS-
                      Fe+2   SO4-2  O2 Sfo_wOUO2+

USER_PUNCH
       -head Fe2_mmol SO4_mmol HS_mmol As(V)_umol As(III)_umol U(VI)_umol Se_umol V_umol
10 PUNCH TOT("Fe(2)")*1.0E3 TOT("S(6)")*1.0E3 TOT("S(-2)")*1.0E3 TOT("As(5)")*1.0E6
TOT("As(3)")*1.0E6 TOT("U(6)")*1.0E6 TOT("Se")*1.0E6 TOT("V")*1.0E6

TRANSPORT
    -cells  5
    -shifts 1
    -lengths     5*0.2
    -timest 0.2
    -bcon   3  3
    -diffc  0.0e-9
    -disp   0.002
    -punch  1
    -punch  5
    -stag        1  1.0E01    0.3        0.1
#     -stag       1  6.8e-16  0.3        0.001
#   1 stagnant layer^, ^alpha, ^theta(m), ^theta(im)
END
#RO cycling after 2.0 PV
#Assume dilution of water extracted from ground by 75% pure water
USE SOLUTION 5
MIX 0
     5       0.25
     12      0.75
SAVE SOLUTION 0
REACTION 0
   O2(g)   1.0   NaHCO3  83.8
   3.125E-5  #1 ppm O2 added  background HCO3 added
EQUILIBRIUM_PHASES 0
   Calcite 10.0   0.000
   Goethite 100.0  0.00
```

```
SAVE SOLUTION 0
END
SELECTED_OUTPUT
   #-file              breakthru.out
   -reset              false
   -solution           true
   -distance           true
   -time               true
   -pH                 true
   -pe                 true
   -alkalinity         true
   -equilibrium_phases  Calcite  Goethite  FeS(ppt)  Se(s) UO2(am)  Orpiment  FeSe2 Sulfur
   -molalities          UO2+2  HCO3-  Cl-  Na+ Ca+2   HS-
                      Fe+2   SO4-2  O2 Sfo_wOUO2+

USER_PUNCH
      -head Fe2_mmol SO4_mmol HS_mmol As(V)_umol As(III)_umol U(VI)_umol Se_umol V_umol
10 PUNCH TOT("Fe(2)")*1.0E3 TOT("S(6)")*1.0E3 TOT("S(-2)")*1.0E3 TOT("As(5)")*1.0E6
TOT("As(3)")*1.0E6 TOT("U(6)")*1.0E6 TOT("Se")*1.0E6 TOT("V")*1.0E6

TRANSPORT
    -cells  5
    -shifts 1
    -lengths    5*0.2
    -timest 0.2
    -bcon   3  3
    -diffc  0.0e-9
    -disp   0.002
    -punch  1
    -punch  5
    -stag       1  1.0E01    0.3       0.1
#    -stag      1  6.8e-16  0.3       0.001
#   1 stagnant layer^, ^alpha, ^theta(m), ^theta(im)
END
#RO cycling after 2.2 PV
#Assume dilution of water extracted from ground by 75% pure water
USE SOLUTION 5
MIX 0
     5      0.25
     12     0.75
SAVE SOLUTION 0
REACTION 0
   O2(g)   1.0   NaHCO3  83.8
   3.125E-5  #1 ppm O2 added  background HCO3 added
EQUILIBRIUM_PHASES 0
   Calcite 10.0   0.000
   Goethite 100.0  0.00
SAVE SOLUTION 0
END
SELECTED_OUTPUT
   #-file              breakthru.out
   -reset              false
   -solution           true
   -distance           true
   -time               true
   -pH                 true
   -pe                 true
   -alkalinity         true
   -equilibrium_phases  Calcite  Goethite  FeS(ppt)  Se(s) UO2(am)  Orpiment  FeSe2 Sulfur
   -molalities          UO2+2  HCO3-  Cl-  Na+ Ca+2   HS-
                      Fe+2   SO4-2  O2 Sfo_wOUO2+
```

```
USER_PUNCH
      -head Fe2_mmol SO4_mmol HS_mmol As(V)_umol As(III)_umol U(VI)_umol Se_umol V_umol
10 PUNCH TOT("Fe(2)")*1.0E3 TOT("S(6)")*1.0E3 TOT("S(-2)")*1.0E3 TOT("As(5)")*1.0E6
TOT("As(3)")*1.0E6 TOT("U(6)")*1.0E6 TOT("Se")*1.0E6 TOT("V")*1.0E6

TRANSPORT
    -cells  5
    -shifts 1
    -lengths     5*0.2
    -timest 0.2
    -bcon   3  3
    -diffc  0.0e-9
    -disp   0.002
    -punch  1
    -punch  5
    -stag        1  1.0E01    0.3        0.1
#     -stag       1  6.8e-16  0.3        0.001
#   1 stagnant layer^, ^alpha, ^theta(m), ^theta(im)
END
#RO cycling after 2.4 PV
#Assume dilution of water extracted from ground by 75% pure water
USE SOLUTION 5
MIX 0
     5       0.25
     12      0.75
SAVE SOLUTION 0
REACTION 0
   O2(g)   1.0   NaHCO3  83.8
   3.125E-5  #1 ppm O2 added  background HCO3 added
EQUILIBRIUM_PHASES 0
   Calcite 10.0   0.000
   Goethite 100.0  0.00
SAVE SOLUTION 0
END
SELECTED_OUTPUT

   #-file              breakthru.out
   -reset             false
   -solution            true
   -distance            true
   -time              true
   -pH                true
   -pe                true
   -alkalinity          true
   -equilibrium_phases   Calcite  Goethite  FeS(ppt)  Se(s) UO2(am)  Orpiment  FeSe2 Sulfur
   -molalities          UO2+2  HCO3-  Cl-  Na+ Ca+2  HS-
                      Fe+2   SO4-2  O2 Sfo_wOUO2+

USER_PUNCH
      -head Fe2_mmol SO4_mmol HS_mmol As(V)_umol As(III)_umol U(VI)_umol Se_umol V_umol
10 PUNCH TOT("Fe(2)")*1.0E3 TOT("S(6)")*1.0E3 TOT("S(-2)")*1.0E3 TOT("As(5)")*1.0E6
TOT("As(3)")*1.0E6 TOT("U(6)")*1.0E6 TOT("Se")*1.0E6 TOT("V")*1.0E6

TRANSPORT
    -cells  5
    -shifts 1
    -lengths     5*0.2
    -timest 0.2
    -bcon   3  3
    -diffc  0.0e-9
    -disp   0.002
    -punch  1
```

```
    -punch  5
    -stag        1  1.0E01    0.3       0.1
#    -stag       1  6.8e-16  0.3       0.001
#   1 stagnant layer^, ^alpha, ^theta(m), ^theta(im)
END
#RO cycling after 2.6 PV
#Assume dilution of water extracted from ground by 75% pure water
USE SOLUTION 5
MIX 0
     5       0.25
     12      0.75
SAVE SOLUTION 0
REACTION 0
   O2(g)   1.0   NaHCO3  83.8
   3.125E-5  #1 ppm O2 added  background HCO3 added
EQUILIBRIUM_PHASES 0
   Calcite 10.0   0.000
   Goethite 100.0  0.00
SAVE SOLUTION 0
END
SELECTED_OUTPUT
   #-file              breakthru.out
   -reset              false
   -solution           true
   -distance           true
   -time               true
   -pH                 true
   -pe                 true
   -alkalinity         true
   -equilibrium_phases   Calcite  Goethite  FeS(ppt)  Se(s) UO2(am)  Orpiment  FeSe2 Sulfur
   -molalities         UO2+2  HCO3-  Cl-  Na+ Ca+2   HS-
                     Fe+2   SO4-2  O2 Sfo_wOUO2+

USER_PUNCH
      -head Fe2_mmol SO4_mmol HS_mmol As(V)_umol As(III)_umol U(VI)_umol Se_umol V_umol
10 PUNCH TOT("Fe(2)")*1.0E3 TOT("S(6)")*1.0E3 TOT("S(-2)")*1.0E3 TOT("As(5)")*1.0E6
TOT("As(3)")*1.0E6 TOT("U(6)")*1.0E6 TOT("Se")*1.0E6 TOT("V")*1.0E6

TRANSPORT
    -cells  5
    -shifts 1
    -lengths    5*0.2
    -timest 0.2
    -bcon   3  3
    -diffc  0.0e-9
    -disp   0.002
    -punch  1
    -punch  5
    -stag        1  1.0E01    0.3       0.1
#    -stag       1  6.8e-16  0.3       0.001
#   1 stagnant layer^, ^alpha, ^theta(m), ^theta(im)
END
#RO cycling after 2.8 PV
#Assume dilution of water extracted from ground by 75% pure water
USE SOLUTION 5
MIX 0
     5       0.25
     12      0.75
SAVE SOLUTION 0
REACTION 0
   O2(g)   1.0   NaHCO3  83.8
```

```
   3.125E-5  #1 ppm O2 added  background HCO3 added
EQUILIBRIUM_PHASES 0
   Calcite 10.0   0.000
   Goethite 100.0  0.00
SAVE SOLUTION 0
END
SELECTED_OUTPUT
   #-file              breakthru.out
   -reset              false
   -solution           true
   -distance           true
   -time               true
   -pH                 true
   -pe                 true
   -alkalinity         true
   -equilibrium_phases   Calcite  Goethite  FeS(ppt)  Se(s) UO2(am)  Orpiment  FeSe2 Sulfur
   -molalities          UO2+2  HCO3-  Cl-  Na+ Ca+2   HS-
                      Fe+2   SO4-2  O2 Sfo_wOUO2+

USER_PUNCH
      -head Fe2_mmol SO4_mmol HS_mmol As(V)_umol As(III)_umol U(VI)_umol Se_umol V_umol
10 PUNCH TOT("Fe(2)")*1.0E3 TOT("S(6)")*1.0E3 TOT("S(-2)")*1.0E3 TOT("As(5)")*1.0E6
TOT("As(3)")*1.0E6 TOT("U(6)")*1.0E6 TOT("Se")*1.0E6 TOT("V")*1.0E6

TRANSPORT
    -cells  5
    -shifts 1
    -lengths    5*0.2
    -timest 0.2
    -bcon   3  3
    -diffc  0.0e-9
    -disp   0.002
    -punch  1
    -punch  5
    -stag       1  1.0E01    0.3       0.1
#    -stag      1  6.8e-16  0.3       0.001
#   1 stagnant layer^, ^alpha, ^theta(m), ^theta(im)
END
#RO cycling after 3.0 PV
#Assume dilution of water extracted from ground by 75% pure water
USE SOLUTION 5
MIX 0
     5      0.25
     12     0.75
SAVE SOLUTION 0
REACTION 0
   H2S   1.0   NaHCO3  1.5   NaBr   0.01
   0.0078  #250 mg/L sulfide added added  neutralizing HCO3 added  Br tracer added
EQUILIBRIUM_PHASES 0
   Calcite 100.0   0.000
   Goethite 100.0  0.00
SAVE SOLUTION 0
END
SELECTED_OUTPUT
   #-file              breakthru.out
   -reset              false
   -solution           true
   -distance           true
   -time               true
   -pH                 true
   -pe                 true
   -alkalinity         true
```

```
   -equilibrium_phases   Calcite  Goethite  FeS(ppt)  Se(s) UO2(am)  Orpiment  FeSe2 Sulfur
   -molalities          UO2+2  HCO3-  Cl-  Na+ Ca+2   HS-
                      Fe+2   SO4-2  O2 Sfo_wOUO2+

USER_PUNCH
       -head Fe2_mmol SO4_mmol HS_mmol As(V)_umol As(III)_umol U(VI)_umol Se_umol V_umol
10 PUNCH TOT("Fe(2)")*1.0E3 TOT("S(6)")*1.0E3 TOT("S(-2)")*1.0E3 TOT("As(5)")*1.0E6
TOT("As(3)")*1.0E6 TOT("U(6)")*1.0E6 TOT("Se")*1.0E6 TOT("V")*1.0E6

TRANSPORT
    -cells  5
    -shifts 1
    -lengths     5*0.2

    -timest 0.2
    -bcon   3  3
    -diffc  0.0e-9
    -disp   0.002
    -punch  1
    -punch  5
    -stag        1  1.0E01    0.3        0.1
#     -stag       1  6.8e-16  0.3        0.001
#   1 stagnant layer^, ^alpha, ^theta(m), ^theta(im)
END
#RO cycling after 3.2 PV
#Assume dilution of water extracted from ground by 75% pure water
USE SOLUTION 5
MIX 0
      5       0.25
      12      0.75
SAVE SOLUTION 0
REACTION 0
    H2S   1.0   NaHCO3  1.5   NaBr   0.01
    0.0078  #250 mg/L sulfide added added  neutralizing HCO3 added
EQUILIBRIUM_PHASES 0
   Calcite 100.0   0.000
   Goethite 100.0  0.00
SAVE SOLUTION 0
END
SELECTED_OUTPUT
   #-file              breakthru.out
   -reset              false
   -solution           true
   -distance           true
   -time               true
   -pH                 true
   -pe                 true
   -alkalinity         true
   -equilibrium_phases   Calcite  Goethite  FeS(ppt)  Se(s) UO2(am)  Orpiment  FeSe2 Sulfur
   -molalities          UO2+2  HCO3-  Cl-  Na+ Ca+2   HS-
                      Fe+2   SO4-2  O2 Sfo_wOUO2+

USER_PUNCH
       -head Fe2_mmol SO4_mmol HS_mmol As(V)_umol As(III)_umol U(VI)_umol Se_umol V_umol
10 PUNCH TOT("Fe(2)")*1.0E3 TOT("S(6)")*1.0E3 TOT("S(-2)")*1.0E3 TOT("As(5)")*1.0E6
TOT("As(3)")*1.0E6 TOT("U(6)")*1.0E6 TOT("Se")*1.0E6 TOT("V")*1.0E6

TRANSPORT
    -cells  5
    -shifts 1
    -lengths     5*0.2
    -timest 0.2
```

```
    -bcon   3  3
    -diffc  0.0e-9
    -disp   0.002
    -punch  1
    -punch  5
    -stag        1  1.0E01    0.3        0.1
#     -stag      1  6.8e-16  0.3        0.001
#   1 stagnant layer^, ^alpha, ^theta(m), ^theta(im)
END
#RO cycling after 3.4 PV
#Assume dilution of water extracted from ground by 75% pure water
USE SOLUTION 5
MIX 0
     5       0.25
     12      0.75
SAVE SOLUTION 0
REACTION 0
   H2S   1.0   NaHCO3  1.5    NaBr  0.01
   0.0078  #250 mg/L sulfide added added  neutralizing HCO3 added
EQUILIBRIUM_PHASES 0
   Calcite 100.0   0.000
   Goethite 100.0  0.00
SAVE SOLUTION 0
END
SELECTED_OUTPUT
   #-file              breakthru.out
   -reset              false
   -solution           true
   -distance           true
   -time               true
   -pH                 true
   -pe                 true
   -alkalinity         true
   -equilibrium_phases   Calcite  Goethite  FeS(ppt)  Se(s) UO2(am)  Orpiment  FeSe2 Sulfur
   -molalities          UO2+2  HCO3-  Cl-  Na+ Ca+2  HS-
                      Fe+2   SO4-2  O2 Sfo_wOUO2+

USER_PUNCH
       -head Fe2_mmol SO4_mmol HS_mmol As(V)_umol As(III)_umol U(VI)_umol Se_umol V_umol
10 PUNCH TOT("Fe(2)")*1.0E3 TOT("S(6)")*1.0E3 TOT("S(-2)")*1.0E3 TOT("As(5)")*1.0E6
TOT("As(3)")*1.0E6 TOT("U(6)")*1.0E6 TOT("Se")*1.0E6 TOT("V")*1.0E6

TRANSPORT
    -cells  5
    -shifts 1
    -lengths     5*0.2
    -timest 0.2
    -bcon   3  3
    -diffc  0.0e-9
    -disp   0.002
    -punch  1
    -punch  5
    -stag        1  1.0E01    0.3        0.1
#     -stag      1  6.8e-16  0.3        0.001
#   1 stagnant layer^, ^alpha, ^theta(m), ^theta(im)
END
#RO cycling after 3.6 PV
#Assume dilution of water extracted from ground by 75% pure water
USE SOLUTION 5
MIX 0
     5       0.25
     12      0.75
```

```
SAVE SOLUTION 0
REACTION 0
   O2(g)   1.0   NaHCO3  83.8
   3.125E-5  #1 ppm O2 added  background HCO3 added
EQUILIBRIUM_PHASES 0
   Calcite 100.0   0.000
   Goethite 100.0  0.00
   FeS(ppt)  1000.0   0.00
   Se(s)   1000.0   0.00
   UO2(am) 1000.0 0.0
   Orpiment  1000.0 0.0
   FeSe2     1000.0 0.0
   Sulfur    1000.0 0.0
SAVE SOLUTION 0
END
SELECTED_OUTPUT
   #-file              breakthru.out
   -reset              false
   -solution             true
   -distance             true
   -time               true
   -pH                 true
   -pe                true
   -alkalinity           true
   -equilibrium_phases   Calcite  Goethite  FeS(ppt)  Se(s) UO2(am)  Orpiment  FeSe2 Sulfur
   -molalities           UO2+2  HCO3-  Cl-  Na+ Ca+2  HS-
                      Fe+2   SO4-2  O2 Sfo_wOUO2+

USER_PUNCH
       -head Fe2_mmol SO4_mmol HS_mmol As(V)_umol As(III)_umol U(VI)_umol Se_umol V_umol
10 PUNCH TOT("Fe(2)")*1.0E3 TOT("S(6)")*1.0E3 TOT("S(-2)")*1.0E3 TOT("As(5)")*1.0E6
TOT("As(3)")*1.0E6 TOT("U(6)")*1.0E6 TOT("Se")*1.0E6 TOT("V")*1.0E6

TRANSPORT
    -cells  5
    -shifts 1
    -lengths     5*0.2
    -timest 0.2
    -bcon   3  3
    -diffc  0.0e-9
    -disp   0.002
    -punch  1
    -punch  5
    -stag         1  1.0E01    0.3        0.1
#     -stag       1  6.8e-16  0.3        0.001
#   1 stagnant layer^, ^alpha, ^theta(m), ^theta(im)
END
#RO cycling after 3.8 PV
#Assume dilution of water extracted from ground by 75% pure water
USE SOLUTION 5
MIX 0
      5       0.25
      12      0.75
SAVE SOLUTION 0
REACTION 0
   O2(g)   1.0   NaHCO3  83.8
   3.125E-5  #1 ppm O2 added  background HCO3 added
EQUILIBRIUM_PHASES 0
   Calcite 100.0   0.000
   Goethite 100.0  0.00
   FeS(ppt)  1000.0   0.00
   Se(s)   1000.0   0.00
```

```
   UO2(am) 1000.0 0.0
   Orpiment  1000.0 0.0
   FeSe2     1000.0 0.0
   Sulfur    1000.0 0.0
SAVE SOLUTION 0
END
SELECTED_OUTPUT
   #-file              breakthru.out
   -reset              false
   -solution           true
   -distance           true
   -time               true
   -pH                 true
   -pe                 true
   -alkalinity         true
   -equilibrium_phases   Calcite  Goethite  FeS(ppt)  Se(s) UO2(am)  Orpiment  FeSe2 Sulfur
   -molalities          UO2+2  HCO3-  Cl-  Na+ Ca+2  HS-
                      Fe+2   SO4-2  O2 Sfo_wOUO2+

USER_PUNCH
      -head Fe2_mmol SO4_mmol HS_mmol As(V)_umol As(III)_umol U(VI)_umol Se_umol V_umol
10 PUNCH TOT("Fe(2)")*1.0E3 TOT("S(6)")*1.0E3 TOT("S(-2)")*1.0E3 TOT("As(5)")*1.0E6
TOT("As(3)")*1.0E6 TOT("U(6)")*1.0E6 TOT("Se")*1.0E6 TOT("V")*1.0E6

TRANSPORT
    -cells  5
    -shifts 1
    -lengths    5*0.2
    -timest 0.2
    -bcon   3  3
    -diffc  0.0e-9
    -disp   0.002
    -punch  1
    -punch  5
    -stag       1  1.0E01    0.3       0.1
#    -stag      1  6.8e-16  0.3       0.001
#   1 stagnant layer^, ^alpha, ^theta(m), ^theta(im)
END
#RO cycling after 4.0 PV
#Assume dilution of water extracted from ground by 75% pure water
USE SOLUTION 5
MIX 0
     5      0.25
     12     0.75
SAVE SOLUTION 0
REACTION 0
   O2(g)   1.0   NaHCO3  83.8
   3.125E-5  #1 ppm O2 added  background HCO3 added
EQUILIBRIUM_PHASES 0
   Calcite 100.0   0.000
   Goethite 100.0  0.00
   FeS(ppt)  1000.0   0.00
   Se(s)   1000.0   0.00
   UO2(am) 1000.0 0.0
   Orpiment  1000.0 0.0
   FeSe2     1000.0 0.0
   Sulfur    1000.0 0.0
SAVE SOLUTION 0
END
SELECTED_OUTPUT
   #-file              breakthru.out
   -reset              false
```

```
   -solution            true
   -distance            true
   -time                true
   -pH                  true
   -pe                 true
   -alkalinity          true
   -equilibrium_phases   Calcite  Goethite  FeS(ppt)  Se(s) UO2(am)  Orpiment  FeSe2 Sulfur
   -molalities          UO2+2  HCO3-  Cl-  Na+ Ca+2  HS-
                      Fe+2   SO4-2  O2 Sfo_wOUO2+

USER_PUNCH
       -head Fe2_mmol SO4_mmol HS_mmol As(V)_umol As(III)_umol U(VI)_umol Se_umol V_umol
10 PUNCH TOT("Fe(2)")*1.0E3 TOT("S(6)")*1.0E3 TOT("S(-2)")*1.0E3 TOT("As(5)")*1.0E6
TOT("As(3)")*1.0E6 TOT("U(6)")*1.0E6 TOT("Se")*1.0E6 TOT("V")*1.0E6

TRANSPORT
    -cells  5
    -shifts 1
    -lengths     5*0.2
    -timest 0.2
    -bcon   3  3
    -diffc  0.0e-9
    -disp   0.002
    -punch  1
    -punch  5
    -stag        1  1.0E01    0.3        0.1
#     -stag       1  6.8e-16  0.3        0.001
#   1 stagnant layer^, ^alpha, ^theta(m), ^theta(im)
END
#RO cycling after 4.2 PV
#Assume dilution of water extracted from ground by 75% pure water
USE SOLUTION 5
MIX 0
     5       0.25
     12      0.75
SAVE SOLUTION 0
REACTION 0
   O2(g)   1.0   NaHCO3  83.8
   3.125E-5  #1 ppm O2 added  background HCO3 added
EQUILIBRIUM_PHASES 0
   Calcite 100.0   0.000
   Goethite 100.0  0.00
   FeS(ppt)  1000.0   0.00
   Se(s)   1000.0   0.00
   UO2(am) 1000.0 0.0
   Orpiment  1000.0 0.0
   FeSe2     1000.0 0.0
   Sulfur    1000.0 0.0
SAVE SOLUTION 0
END
SELECTED_OUTPUT
   #-file              breakthru.out
   -reset              false
   -solution            true
   -distance            true
   -time                true
   -pH                  true
   -pe                 true
   -alkalinity          true
   -equilibrium_phases   Calcite  Goethite  FeS(ppt)  Se(s) UO2(am)  Orpiment  FeSe2 Sulfur
   -molalities          UO2+2  HCO3-  Cl-  Na+ Ca+2  HS-
                      Fe+2   SO4-2  O2 Sfo_wOUO2+
```

```
USER_PUNCH
      -head Fe2_mmol SO4_mmol HS_mmol As(V)_umol As(III)_umol U(VI)_umol Se_umol V_umol
10 PUNCH TOT("Fe(2)")*1.0E3 TOT("S(6)")*1.0E3 TOT("S(-2)")*1.0E3 TOT("As(5)")*1.0E6
TOT("As(3)")*1.0E6 TOT("U(6)")*1.0E6 TOT("Se")*1.0E6 TOT("V")*1.0E6

TRANSPORT
    -cells  5
    -shifts 1
    -lengths     5*0.2
    -timest 0.2
    -bcon   3  3
    -diffc  0.0e-9
    -disp   0.002
    -punch  1
    -punch  5
    -stag        1  1.0E01    0.3        0.1
#     -stag      1  6.8e-16  0.3        0.001
#   1 stagnant layer^, ^alpha, ^theta(m), ^theta(im)
END
#RO cycling after 4.4 PV
#Assume dilution of water extracted from ground by 75% pure water
USE SOLUTION 5
MIX 0
     5       0.25
     12      0.75
SAVE SOLUTION 0
REACTION 0
   O2(g)   1.0   NaHCO3  83.8
   3.125E-5  #1 ppm O2 added  background HCO3 added
EQUILIBRIUM_PHASES 0
   Calcite 100.0   0.000
   Goethite 100.0  0.00
   FeS(ppt)  1000.0   0.00
   Se(s)   1000.0   0.00
   UO2(am) 1000.0 0.0
   Orpiment  1000.0 0.0
   FeSe2     1000.0 0.0
   Sulfur    1000.0 0.0
SAVE SOLUTION 0
END
SELECTED_OUTPUT
   #-file              breakthru.out
   -reset              false
   -solution             true
   -distance             true
   -time               true
   -pH                 true
   -pe                true
   -alkalinity           true
   -equilibrium_phases   Calcite  Goethite  FeS(ppt)  Se(s) UO2(am)  Orpiment  FeSe2 Sulfur
   -molalities           UO2+2  HCO3-  Cl-  Na+ Ca+2  HS-
                      Fe+2   SO4-2  O2 Sfo_wOUO2+

USER_PUNCH
      -head Fe2_mmol SO4_mmol HS_mmol As(V)_umol As(III)_umol U(VI)_umol Se_umol V_umol
10 PUNCH TOT("Fe(2)")*1.0E3 TOT("S(6)")*1.0E3 TOT("S(-2)")*1.0E3 TOT("As(5)")*1.0E6
TOT("As(3)")*1.0E6 TOT("U(6)")*1.0E6 TOT("Se")*1.0E6 TOT("V")*1.0E6

TRANSPORT
    -cells  5
    -shifts 1
```

```
    -lengths     5*0.2
    -timest 0.2
    -bcon   3  3
    -diffc  0.0e-9
    -disp   0.002
    -punch  1
    -punch  5
    -stag        1  1.0E01    0.3       0.1
#     -stag      1  6.8e-16  0.3       0.001
#   1 stagnant layer^, ^alpha, ^theta(m), ^theta(im)
END
#RO cycling after 4.6 PV
#Assume dilution of water extracted from ground by 75% pure water
USE SOLUTION 5
MIX 0
     5       0.25
     12      0.75
SAVE SOLUTION 0
REACTION 0
   O2(g)   1.0   NaHCO3  83.8
   3.125E-5  #1 ppm O2 added  background HCO3 added
EQUILIBRIUM_PHASES 0
   Calcite 100.0   0.000
   Goethite 100.0  0.00
   FeS(ppt)  1000.0   0.00
   Se(s)   1000.0   0.00
   UO2(am) 1000.0 0.0
   Orpiment  1000.0 0.0
   FeSe2     1000.0 0.0
   Sulfur    1000.0 0.0
SAVE SOLUTION 0
END
SELECTED_OUTPUT
   #-file              breakthru.out
   -reset              false
   -solution           true
   -distance           true
   -time               true
   -pH                 true
   -pe                 true
   -alkalinity         true
   -equilibrium_phases   Calcite  Goethite  FeS(ppt)  Se(s) UO2(am)  Orpiment  FeSe2 Sulfur
   -molalities          UO2+2  HCO3-  Cl-  Na+ Ca+2  HS-
                      Fe+2   SO4-2  O2 Sfo_wOUO2+

USER_PUNCH
      -head Fe2_mmol SO4_mmol HS_mmol As(V)_umol As(III)_umol U(VI)_umol Se_umol V_umol
10 PUNCH TOT("Fe(2)")*1.0E3 TOT("S(6)")*1.0E3 TOT("S(-2)")*1.0E3 TOT("As(5)")*1.0E6
TOT("As(3)")*1.0E6 TOT("U(6)")*1.0E6 TOT("Se")*1.0E6 TOT("V")*1.0E6

TRANSPORT
    -cells  5
    -shifts 1
    -lengths     5*0.2
    -timest 0.2
    -bcon   3  3
    -diffc  0.0e-9
    -disp   0.002
    -punch  1
    -punch  5
    -stag        1  1.0E01    0.3       0.1
#     -stag      1  6.8e-16  0.3       0.001
```

```
#   1 stagnant layer^, ^alpha, ^theta(m), ^theta(im)
END
#RO cycling after 4.8 PV
#Assume dilution of water extracted from ground by 75% pure water
USE SOLUTION 5
MIX 0
     5       0.25
     12      0.75
SAVE SOLUTION 0
REACTION 0
   O2(g)   1.0   NaHCO3  83.8
   3.125E-5  #1 ppm O2 added  background HCO3 added
EQUILIBRIUM_PHASES 0
   Calcite 100.0   0.000
   Goethite 100.0  0.00
   FeS(ppt)  1000.0   0.00
   Se(s)   1000.0   0.00
   UO2(am) 1000.0 0.0
   Orpiment  1000.0 0.0
   FeSe2     1000.0 0.0
   Sulfur    1000.0 0.0
SAVE SOLUTION 0
END
SELECTED_OUTPUT
   #-file              breakthru.out
   -reset              false
   -solution           true
   -distance           true
   -time               true
   -pH                 true
   -pe                 true
   -alkalinity         true
   -equilibrium_phases   Calcite  Goethite  FeS(ppt)  Se(s) UO2(am)  Orpiment  FeSe2 Sulfur
   -molalities          UO2+2  HCO3-  Cl-  Na+ Ca+2  HS-
                      Fe+2   SO4-2  O2 Sfo_wOUO2+

USER_PUNCH
       -head Fe2_mmol SO4_mmol HS_mmol As(V)_umol As(III)_umol U(VI)_umol Se_umol V_umol
10 PUNCH TOT("Fe(2)")*1.0E3 TOT("S(6)")*1.0E3 TOT("S(-2)")*1.0E3 TOT("As(5)")*1.0E6
TOT("As(3)")*1.0E6 TOT("U(6)")*1.0E6 TOT("Se")*1.0E6 TOT("V")*1.0E6

TRANSPORT
    -cells  5
    -shifts 1
    -lengths     5*0.2
    -timest 0.2
    -bcon   3  3
    -diffc  0.0e-9
    -disp   0.002
    -punch  1
    -punch  5
    -stag        1  1.0E01    0.3        0.1
#     -stag       1  6.8e-16  0.3        0.001
#   1 stagnant layer^, ^alpha, ^theta(m), ^theta(im)
END
#RO cycling after 5.0 PV
#Assume dilution of water extracted from ground by 75% pure water
USE SOLUTION 5
MIX 0
     5       0.25
     12      0.75
SAVE SOLUTION 0
```

```
REACTION 0
   O2(g)   1.0   NaHCO3  83.8
   3.125E-5  #1 ppm O2 added  background HCO3 added
EQUILIBRIUM_PHASES 0
   Calcite 100.0   0.000
   Goethite 100.0  0.00
   FeS(ppt)  1000.0   0.00
   Se(s)   1000.0   0.00
   UO2(am) 1000.0 0.0
   Orpiment  1000.0 0.0
   FeSe2     1000.0 0.0
   Sulfur    1000.0 0.0
SAVE SOLUTION 0
END
SELECTED_OUTPUT
   #-file              breakthru.out
   -reset              false
   -solution             true
   -distance             true
   -time               true
   -pH                 true
   -pe                true
   -alkalinity           true
   -equilibrium_phases   Calcite  Goethite  FeS(ppt)  Se(s) UO2(am)  Orpiment  FeSe2 Sulfur
   -molalities           UO2+2  HCO3-  Cl-  Na+ Ca+2  HS-
                      Fe+2   SO4-2  O2 Sfo_wOUO2+

USER_PUNCH
       -head Fe2_mmol SO4_mmol HS_mmol As(V)_umol As(III)_umol U(VI)_umol Se_umol V_umol
10 PUNCH TOT("Fe(2)")*1.0E3 TOT("S(6)")*1.0E3 TOT("S(-2)")*1.0E3 TOT("As(5)")*1.0E6
TOT("As(3)")*1.0E6 TOT("U(6)")*1.0E6 TOT("Se")*1.0E6 TOT("V")*1.0E6

TRANSPORT
    -cells  5
    -shifts 1
    -lengths     5*0.2
    -timest 0.2
    -bcon   3  3
    -diffc  0.0e-9
    -disp   0.002
    -punch  1
    -punch  5
    -stag         1  1.0E01    0.3        0.1
#     -stag       1  6.8e-16  0.3        0.001
#   1 stagnant layer^, ^alpha, ^theta(m), ^theta(im)
END
SOLUTION 0  Background water conditions - oxic upgrad water, December 1983
   # NOTES:
   units   mmol/kgw
   pH         7.0
   pe         6.5
   redox    O(0)/O(-2)
   temp     25.0
   Na       4.78
   K        0.11
   Ca       0.2      Calcite
   Mg        0.082
   Cl       0.2       Charge
   S        1.04
   O(0)       1.0   O2(g) -0.7
   As      1.3E-4
   Se      1.3E-4
```

```
   V       2.75E-4
   Alkalinity 2.62
   U       0.00006
SAVE solution 0
END
SELECTED_OUTPUT
   #-file              breakthru.out
   -reset              false
   -solution           true
   -distance           true
   -time               true
   -pH                 true
   -pe                 true
   -alkalinity         true
   -equilibrium_phases   Calcite  Goethite  FeS(ppt)  Se(s) UO2(am)  Orpiment  FeSe2 Sulfur
   -molalities          UO2+2  HCO3-  Cl-  Na+ Ca+2  HS-
                      Fe+2   SO4-2  O2 Sfo_wOUO2+

USER_PUNCH
       -head Fe2_mmol SO4_mmol HS_mmol As(V)_umol As(III)_umol U(VI)_umol Se_umol V_umol
10 PUNCH TOT("Fe(2)")*1.0E3 TOT("S(6)")*1.0E3 TOT("S(-2)")*1.0E3 TOT("As(5)")*1.0E6
TOT("As(3)")*1.0E6 TOT("U(6)")*1.0E6 TOT("Se")*1.0E6 TOT("V")*1.0E6

TRANSPORT
   -cells              5
    -shifts             504
   -time_step          0.2 # seconds
   -flow_direction       forward
   -boundary_conditions   flux flux
   -lengths            5*0.2
   -dispersivities       5*0.002
   -diffusion_coefficient 0
   -stagnant           1  10  0.3  0.1
   -punch_cells         1
   -punch_cells         2
   -punch_cells         3
   -punch_cells         4
   -punch_cells         5
   -warnings           true
END
```

9 APPENDIX B: PHREEQC THERMODYNAMIC DATA FILE USED FOR THIS REPORT

The follow PHREEQC database contains thermodynamic data pertinent to this report. Thermodynamic data for many elements not considered in this report have been removed in the interest of brevity.

```
SOLUTION_MASTER_SPECIES
#
#element species       alk     gfw_formula     element_gfw
#
H       H+            -1.     H               1.008
H(0)    H2             0.0    H
H(1)    H+            -1.     0.0
E       e-            0.0     0.0             0.0
O       H2O            0.0    O               16.00
O(0)    O2             0.0    O
O(-2)   H2O            0.0    0.0
As      H3AsO4        -1.0    74.9216         74.9216
As(+3)  H3AsO3         0.0    74.9216         74.9216
As(+5)  H3AsO4        -1.0    74.9216
Ca      Ca+2           0.0    Ca              40.08
Mg      Mg+2           0.0    Mg              24.312
Na      Na+            0.0    Na              22.9898
K       K+             0.0    K               39.102
Fe      Fe+2           0.0    Fe              55.847
Fe(+2)  Fe+2           0.0    Fe
Fe(+3)  Fe+3          -2.0    Fe
Mn      Mn+2           0.0    Mn              54.938
Mn(+2)  Mn+2           0.0    Mn
Mn(+3)  Mn+3           0.0    Mn
Al      Al+3           0.0    Al              26.9815
Ba      Ba+2           0.0    Ba              137.34
Sr      Sr+2           0.0    Sr              87.62
Si      H4SiO4         0.0    SiO2            28.0843
Cl      Cl-            0.0    Cl              35.453
C       CO3-2          2.0    HCO3            12.0111
C(+4)   CO3-2          2.0    HCO3
C(-4)   CH4            0.0    CH4
Alkalinity CO3-2       1.0    Ca0.5(CO3)0.5   50.05
S       SO4-2          0.0    SO4             32.064
S(6)    SO4-2          0.0    SO4
S(-2)   HS-            1.0    S
Se      SeO4-2         0.0 78.96                78.96
Se(-2)  HSe-           0.0 78.96
Se(4)   SeO3-2         0.0    78.96
Se(6)   SeO4-2         0.0    78.96
N       NO3-           0.0    N               14.0067
N(+5)   NO3-           0.0    N
N(+3)   NO2-           0.0    N
N(0)    N2             0.0    N
N(-3)   NH4+           0.0    N
B       H3BO3          0.0    B               10.81
P       PO4-3          2.0    P               30.9738
F       F-             0.0    F               18.9984
Li      Li+            0.0    Li              6.939
Br      Br-            0.0    Br              79.904
Zn      Zn+2           0.0    Zn              65.37
Cd      Cd+2           0.0    Cd              112.4
Pb      Pb+2           0.0    Pb              207.19
```

```
Cu      Cu+2          0.0     Cu            63.546
Cu(+2)  Cu+2          0.0     Cu
Cu(+1)  Cu+1          0.0     Cu
V             VO2+    0       50.94         50.94
V(2)          V+2     0       50.94
V(3)          V+3     0       50.94
V(4)          VO+2    0       50.94
V(5)          VO2+    0       50.94
U       UO2+2                         0.0         238.0290 238.0290
#U(3)   U+3                   0.0     238.0290 238.0290
U(4)    U+4                   0.0     238.0290 238.0290
#U(5)   UO2+                          0.0         238.0290 238.0290
U(6)    UO2+2                         0.0         238.0290 238.0290
SOLUTION_SPECIES

H+ = H+
      log_k         0.000
      -gamma        9.0000    0.0000

e- = e-
      log_k         0.000

H2O = H2O
      log_k         0.000

Ca+2 = Ca+2
      log_k         0.000
      -gamma    5.0000    0.1650

Mg+2 = Mg+2
      log_k         0.000
      -gamma    5.5000    0.2000

Na+ = Na+
      log_k         0.000
      -gamma    4.0000    0.0750

K+ = K+
      log_k         0.000
      -gamma    3.5000    0.0150

Fe+2 = Fe+2
      log_k         0.000
      -gamma    6.0000    0.0000

Mn+2 = Mn+2
      log_k         0.000
      -gamma    6.0000    0.0000

Al+3 = Al+3
      log_k         0.000
      -gamma    9.0000    0.0000

H3AsO4 = H3AsO4
     log_k                  0.0

Ba+2 = Ba+2
      log_k         0.000
      -gamma    5.0000    0.0000

Sr+2 = Sr+2
      log_k         0.000
```

```
        -gamma    5.2600    0.1210

H4SiO4 = H4SiO4
        log_k           0.000

Cl- = Cl-
        log_k           0.000
        -gamma    3.5000    0.0150

CO3-2 = CO3-2
        log_k           0.000
        -gamma    5.4000    0.0000

SO4-2 = SO4-2
        log_k           0.000
        -gamma    5.0000   -0.0400

SeO4-2 = SeO4-2
      log_k                   0.0

NO3- = NO3-
        log_k           0.000
        -gamma    3.0000    0.0000

H3BO3 = H3BO3
        log_k           0.000

PO4-3 = PO4-3
        log_k           0.000
        -gamma    4.0000    0.0000

F- = F-
        log_k           0.000
        -gamma    3.5000    0.0000

Li+ = Li+
        log_k           0.000
        -gamma    6.0000    0.0000

Br- = Br-
        log_k           0.000
        -gamma    3.0000    0.0000

Zn+2 = Zn+2
        log_k           0.000
        -gamma    5.0000    0.0000

Cd+2 = Cd+2
        log_k           0.000

Pb+2 = Pb+2
        log_k           0.000

Cu+2 = Cu+2
        log_k           0.000
        -gamma    6.0000    0.0000

#UO2+2 primary master species
      UO2+2 = UO2+2
      log_k                   0.0

#UO2+ primary master species
```

```
#    UO2+ = UO2+
#    log_k                  0.0

#U+4 primary master species
     U+4 = U+4
     log_k                  0.0

#U+4 primary master species
#    U+3 = U+3
#    log_k                  0.0

H2O = OH- + H+
      log_k          -14.000
      delta_h 13.362  kcal
      -analytic      -283.971      -0.05069842  13323.0    102.24447      -1119669.0
      -gamma    3.5000    0.0000

2 H2O = O2 + 4 H+ + 4 e-
      log_k          -86.08
      delta_h 134.79 kcal

2 H+ + 2 e- = H2
      log_k          -3.15
      delta_h -1.759 kcal

CO3-2 + H+ = HCO3-
      log_k          10.329
      delta_h -3.561  kcal
      -analytic      107.8871      0.03252849  -5151.79     -38.92561       563713.9
      -gamma    5.4000    0.0000

CO3-2 + 2 H+ = CO2 + H2O
      log_k          16.681
      delta_h -5.738  kcal
      -analytic      464.1965      0.09344813  -26986.16    -165.75951      2248628.9

CO3-2 + 10 H+ + 8 e- = CH4 + 3 H2O
      log_k          41.071
      delta_h -61.039 kcal

SO4-2 + H+ = HSO4-
      log_k          1.988
      delta_h 3.85    kcal
      -analytic      -56.889       0.006473    2307.9       19.8858         0.0

HS- = S-2 + H+
      log_k          -12.918
      delta_h 12.1    kcal
      -gamma    5.0000    0.0000

SO4-2 + 9 H+ + 8 e- = HS- + 4 H2O
      log_k          33.65
      delta_h -60.140 kcal
      -gamma    3.5000    0.0000

HS- + H+ = H2S
      log_k          6.994
      delta_h -5.300  kcal
      -analytical  -11.17   0.02386  3279.0
```

```
Ca+2 + H2O = CaOH+ + H+
       log_k          -12.780

Ca+2 + CO3-2 = CaCO3
       log_k          3.224
       delta_h 3.545   kcal
       -analytic      -1228.732     -0.299440    35512.75      485.818

Ca+2 + CO3-2 + H+ = CaHCO3+
       log_k          11.435
       delta_h -0.871         kcal
       -analytic      1317.0071     0.34546894   -39916.84     -517.70761     563713.9
       -gamma    5.4000    0.0000

Ca+2 + SO4-2 = CaSO4
       log_k          2.300
       delta_h 1.650   kcal

Ca+2 + HSO4- = CaHSO4+
       log_k          1.08

Ca+2 + PO4-3 = CaPO4-
       log_k          6.459
       delta_h 3.100   kcal

Ca+2 + HPO4-2 = CaHPO4
       log_k          2.739
       delta_h 3.3 kcal

Ca+2 + H2PO4- = CaH2PO4+
       log_k          1.408
       delta_h 3.4 kcal

Ca+2 + F- = CaF+
       log_k          0.940
       delta_h 4.120   kcal

Mg+2 + H2O = MgOH+ + H+
       log_k          -11.440
       delta_h 15.952 kcal

Mg+2 + CO3-2 = MgCO3
       log_k          2.98
       delta_h 2.713   kcal
       -analytic      0.9910        0.00667

Mg+2 + H+ + CO3-2 = MgHCO3+
       log_k          11.399
       delta_h -2.771         kcal
       -analytic      48.6721       0.03252849   -2614.335     -18.00263      563713.9

Mg+2 + SO4-2 = MgSO4
       log_k          2.370
       delta_h 4.550   kcal

Mg+2 + PO4-3 = MgPO4-
       log_k          6.589
       delta_h 3.100   kcal

Mg+2 + HPO4-2 = MgHPO4
       log_k          2.87
       delta_h 3.3 kcal
```

```
Mg+2 + H2PO4- = MgH2PO4+
        log_k           1.513
        delta_h 3.4 kcal

Mg+2 + F- = MgF+
        log_k           1.820
        delta_h 3.200   kcal

Na+ + H2O = NaOH + H+
        log_k           -14.180

Na+ + CO3-2 = NaCO3-
        log_k           1.270
        delta_h 8.910   kcal

Na+ + HCO3- = NaHCO3
        log_k           -0.25

Na+ + SO4-2 = NaSO4-
        log_k           0.700
        delta_h 1.120   kcal

Na+ + HPO4-2 = NaHPO4-
        log_k           0.29

Na+ + F- = NaF
        log_k           -0.240

K+ + H2O = KOH + H+
        log_k           -14.460

K+ + SO4-2 = KSO4-
        log_k           0.850
        delta_h 2.250   kcal
        -analytical     3.106  0.0   -673.6

K+ + HPO4-2 = KHPO4-
        log_k           0.29

Fe+2 + H2O = FeOH+ + H+
        log_k           -9.500
        delta_h 13.200  kcal

Fe+2 + Cl- = FeCl+
        log_k           0.140

Fe+2 + CO3-2 = FeCO3
        log_k           4.380

Fe+2 + HCO3- = FeHCO3+
        log_k           2.0

Fe+2 + SO4-2 = FeSO4
        log_k           2.250
        delta_h 3.230   kcal

Fe+2 + HSO4- = FeHSO4+
        log_k           1.08

Fe+2 + 2HS- = Fe(HS)2
        log_k           8.95
```

```
Fe+2 + 3HS- = Fe(HS)3-
        log_k           10.987

Fe+2 + HPO4-2 = FeHPO4
        log_k           3.6

Fe+2 + H2PO4- = FeH2PO4+
        log_k           2.7

Fe+2 + F- = FeF+
        log_k           1.000

Fe+2 = Fe+3 + e-
        log_k           -13.020
        delta_h 9.680   kcal
        -gamma    9.0000    0.0000

Fe+3 + H2O = FeOH+2 + H+
        log_k           -2.19
        delta_h 10.4    kcal

Fe+3 + 2 H2O = Fe(OH)2+ + 2 H+
        log_k           -5.67
        delta_h 17.1    kcal

Fe+3 + 3 H2O = Fe(OH)3 + 3 H+
        log_k           -12.56
        delta_h 24.8    kcal

Fe+3 + 4 H2O = Fe(OH)4- + 4 H+
        log_k           -21.6
        delta_h 31.9    kcal

2 Fe+3 + 2 H2O = Fe2(OH)2+4 + 2 H+
        log_k           -2.95
        delta_h 13.5    kcal

3 Fe+3 + 4 H2O = Fe3(OH)4+5 + 4 H+
        log_k           -6.3
        delta_h 14.3    kcal

Fe+3 + Cl- = FeCl+2
        log_k           1.48
        delta_h 5.6     kcal

Fe+3 + 2 Cl- = FeCl2+
        log_k           2.13

Fe+3 + 3 Cl- = FeCl3
        log_k           1.13

Fe+3 + SO4-2 = FeSO4+
        log_k           4.04
        delta_h 3.91    kcal

Fe+3 + HSO4- = FeHSO4+2
        log_k           2.48

Fe+3 + 2 SO4-2 = Fe(SO4)2-
        log_k           5.38
        delta_h 4.60            kcal
```

```
Fe+3 + HPO4-2 = FeHPO4+
       log_k          5.43
       delta_h 5.76           kcal

Fe+3 + H2PO4- = FeH2PO4+2
       log_k          5.43

Fe+3 + F- = FeF+2
       log_k          6.2
       delta_h 2.7            kcal

Fe+3 + 2 F- = FeF2+
       log_k          10.8
       delta_h 4.8            kcal

Fe+3 + 3 F- = FeF3
       log_k          14.0
       delta_h 5.4            kcal

UO2+2  +  H2O   = UO2(OH)+    + H+
      log_K  -5.20

UO2+2  + 2H2O   = UO2(OH)2    + 2H+
      log_K -11.50

UO2+2  + 3H2O   = UO2(OH)3-   + 3H+
      log_K   -20.00

UO2+2  + 4H2O   = UO2(OH)4-2  + 4H+
      log_K   -33.00

2UO2+2 + H2O    = (UO2)2OH+3  + H+
      log_K    -2.70

2UO2+2 + 2H2O   = (UO2)2(OH)2+2  + 2H+
      log_K    -5.62

3UO2+2 + 4H2O   = (UO2)3(OH)4+2  +  4H+
      log_K    -11.90

3UO2+2  +  5H2O  =  (UO2)3(OH)5+  + 5H+
      log_K    -15.55

3UO2+2  +  7H2O  =  (UO2)3(OH)7-  + 7H+
      log_K    -31.

4UO2+2  +  7H2O  =  (UO2)4(OH)7+  + 7H+
      log_K    -21.9

UO2+2 +  CO3-2   =  UO2CO3
      log_K     9.67

UO2+2 +  2CO3-2   =  UO2(CO3)2-2
      log_K     16.94

UO2+2 +  3CO3-2   =  UO2(CO3)3-4
      log_K     21.60

3UO2+2 + 6CO3-2   =  (UO2)3(CO3)6-6
      log_K     54.
```

```
2UO2+2 + CO3-2  + 3H2O = (UO2)2CO3(OH)3- + 3H+
      log_K    -0.86

3UO2+2  + CO3-2  + 3H2O  =  (UO2)3CO3(OH)3+  + 3H+
      log_K    0.66

#11UO2+2 + 6CO3-2 + 12H2O = (UO2)11(CO3)6(OH)12-2 + 12H+
#       log_K    36.43

UO2+2  +  NO3-  = UO2NO3+
      log_K     0.3

UO2+2  + Cl-  =  UO2Cl+
      log_K     0.17

UO2+2  + 2Cl-  = UO2Cl2
      log_K     -1.1

#UO2+2 + SO4-2  =  UO2SO4
#       log_K      3.15

#UO2+2  + 2SO4-2  = UO2(SO4)-2
#       log_K      4.14

UO2+2  + F-  = UO2F+
      log_K  5.09

UO2+2  + 2F-  = UO2F2
      log_K  8.62

UO2+2  + 3F-  = UO2F3-
      log_K  10.90

UO2+2  + 4F-  = UO2F4-2
      log_K  11.70

UO2+2  + PO4-3  =  UO2PO4-
      log_K   13.23

UO2+2  + PO4-3 + H+ =  UO2HPO4
      log_K   19.59

UO2+2  + PO4-3 + 2H+ =  UO2H2PO4+
      log_K   22.82

UO2+2  + PO4-3 + 3H+ =  UO2H3PO4+2
      log_K   22.46

UO2+2  + 2PO4-3 + 4H+  = UO2(H2PO4)2
      log_K   44.04

UO2+2  +  2PO4-3  + 5H+  =  UO2(H2PO4)(H3PO4)+
      log_K   45.05

UO2+2 + 2Ca+2 + 3CO3-2 = Ca2UO2(CO3)3
      log_K  30.55

UO2+2 + Ca+2 + 3CO3-2 = CaUO2(CO3)3-2
      log_K  25.4

# U(IV)
```

```
U+4 + H2O = UOH+3 + H+
      log_K   -0.65         ! langmuir

U+4 + 4H2O = U(OH)4 + 4H+
      log_K   -12.0               ! langmuir

U+4 + Cl- = UCl+3
      log_K   1.72                ! langmuir

U+4 + SO4-2 = USO4+2
      log_K   6.58                ! langmuir

U+4 + 5CO3-2 = U(CO3)5-6
      log_K  33.9           ! langmuir

UO2+2 + 4H+ + 2e- = U+4 + 2H2O
      log_K 8.89

#H2AsO3-              478
      H3AsO3 = H2AsO3- + H+
      log_k                   -9.228
      delta_h    6.56 kcal

#As3  secondary master species   487
      H3AsO4 + 2H+ + 2e- = H3AsO3 + H2O
      log_k                   18.897
      delta_h    -30.015 kcal

#HAsO3-2             479
      H3AsO3 = HAsO3-2 + 2H+
      log_k                   -21.33
      delta_h    14.2 kcal

#AsO3-3              480
      H3AsO3 = AsO3-3 + 3H+
      log_k                   -34.744
      delta_h    20.25 kcal

#H4AsO3+             481
      H3AsO3 + H+ = H4AsO3+
      log_k                   -0.305

#H2AsO4-             482
      H3AsO4 = H2AsO4- + H+
      log_k                   -2.243
      delta_h    -1.69 kcal

#HAsO4-2             483
      H3AsO4 = HAsO4-2 + 2H+
      log_k                   -9.001
      delta_h    -0.92 kcal

#AsO4-3              484
      H3AsO4 = AsO4-3 + 3H+
      log_k                   -20.597
      delta_h    3.43 kcal

#HSe- secondary master species   549
      SeO3-2 + 7H+ + 6e- = HSe- + 3H2O
      log_k                   42.514

#H2Se                544
```

```
    HSe- + H+ = H2Se
    log_k                3.8
    delta_h    -5.3 kcal

#SeO3-2 secondary master species   548
    SeO4-2 + 2H+ + 2e- = SeO3-2 + H2O
    log_k                30.256

#H2SeO3             545
    SeO3-2 + 2H+ = H2SeO3
    log_k                11.25

#HSeO3-             546
    SeO3-2 + H+ = HSeO3-
    log_k                8.5

#HSeO4-             547
    SeO4-2 + H+ = HSeO4-
    log_k                1.66
    delta_h    4.91 kcal

VO2+ = VO2+
     log_k   0
     delta_h 0       kcal

VO2+ + e- + 2H+ = VO+2 + H2O
     log_k   16.93
     delta_h -29.32  kcal

VO2+ + 2e- + 4H+ = V+3 + 2H2O
     log_k   22.61
     delta_h -44.23  kcal

VO2+ + 3e- + 4H+ = V+2 + 2H2O
     log_k   18.38
     delta_h -35.33  kcal

V+2 + H2O = VOH+ + H+
     log_k   -5.64
     delta_h 0       kcal

V+3 + H2O = VOH+2 + H+
     log_k   -2.3
     delta_h 9.35    kcal

V+3 + 2H2O = V(OH)2+ + 2H+
     log_k   -5.83
     delta_h 0       kcal

V+3 + 3H2O = V(OH)3 + 3H+
     log_k   -11.02
     delta_h 0       kcal

V+3 + SO4-2 = VSO4+
     log_k   1.44
     delta_h 0       kcal

2V+3 + 3H2O = V2(OH)3+3 + 3H+
     log_k   -7.5
     delta_h 0       kcal

2V+3 + 2H2O = V2(OH)2+4 + 2H+
```

```
        log_k   -3.75
        delta_h 0       kcal

VO+2 + 2H2O = V(OH)3+ + H+
        log_k   -5.67
        delta_h 0       kcal

2VO+2 + 2H2O = H2V2O4+2 + 2H+
        log_k   -6.44
        delta_h 0       kcal

VO+2 + F- = VOF+
        log_k   3.34
        delta_h 1.9     kcal

VO+2 + 2F- = VOF2
        log_k   5.74
        delta_h 3.5     kcal

VO+2 + 3F- = VOF3-
        log_k   7.3
        delta_h 4.9     kcal

VO+2 + 4F- = VOF4-2
        log_k   8.11
        delta_h 6.4     kcal

VO+2 + SO4-2 = VOSO4
        log_k   2.45
        delta_h 3.72    kcal

VO+2 + Cl- = VOCl+
        log_k   0.02
        delta_h 0       kcal

VO2+ + 2H2O = H3VO4 + H+
        log_k   -3.3
        delta_h 10.63   kcal

VO2+ + 2H2O = H2VO4- + 2H+
        log_k   -7.09
        delta_h 11.33   kcal

VO2+ + 2H2O = HVO4-2 + 3H+
        log_k   -15.15
        delta_h 14.93   kcal

VO2+ + 2H2O = VO4-3 + 4H+
        log_k   -28.4
        delta_h 19.53   kcal

2VO2+ + 3H2O = V2O7-4 + 6H+
        log_k   -29.08
        delta_h 0       kcal

2VO2+ + 3H2O = HV2O7-3 + 5H+
        log_k   -16.32
        delta_h 0       kcal

2VO2+ + 3H2O = H3V2O7- + 3H+
        log_k   -3.79
        delta_h 0       kcal
```

```
3VO2+ + 3H2O = V3O9-3 + 6H+
    log_k   -15.88
    delta_h 0       kcal

4VO2+ + 4H2O = V4O12-4 + 8H+
    log_k   -20.79
    delta_h 0       kcal

10VO2+ + 8H2O = V10O28-6 + 16H+
    log_k   -17.53
    delta_h 0       kcal

10VO2+ + 8H2O = HV10O28-5 + 15H+
    log_k   -11.35
    delta_h 21.52   kcal

10VO2+ + 8H2O = H2V10O28-4 + 14H+
    log_k   -7.71
    delta_h 0       kcal

VO2+ + F- = VO2F
    log_k   3.12
    delta_h 0       kcal

VO2+ + 2F- = VO2F2-
    log_k   5.67
    delta_h 0       kcal

VO2+ + 3F- = VO2F3-2
    log_k   6.97
    delta_h 0       kcal

VO2+ + 4F- = VO2F4-3
    log_k   7.07
    delta_h 0       kcal

VO2+ + SO4-2 = VO2SO4-
    log_k   1.71
    delta_h 0       kcal

VO2+ + NO3- = VO2NO3
    log_k   -0.43
    delta_h 0       kcal

PHASES

Calcite
    CaCO3 = CO3-2 + Ca+2
    log_k           -8.480
    delta_h -2.297 kcal
    -analytic       -171.9065     -0.077993      2839.319      71.595

Aragonite
    CaCO3 = CO3-2 + Ca+2
    log_k           -8.336
    delta_h -2.589 kcal
    -analytic       -171.9773     -0.077993      2903.293      71.595

Dolomite
    CaMg(CO3)2 = Ca+2 + Mg+2 + 2 CO3-2
    log_k           -17.090
```

```
    delta_h -9.436 kcal

Siderite
    FeCO3 = Fe+2 + CO3-2
    log_k       -10.890
    delta_h -2.480 kcal

    -analytic    155.0305    0.0        -7239.594    -56.58638

Gypsum
    CaSO4:2H2O = Ca+2 + SO4-2 + 2 H2O
    log_k       -4.580
    delta_h -0.109 kcal
    -analytic    68.2401    0.0        -3221.51    -25.0627

Anhydrite
    CaSO4 = Ca+2 + SO4-2
    log_k       -4.360
    delta_h -1.710 kcal
    -analytic    197.52     0.0        -8669.8     -69.835

Hematite
    Fe2O3 + 6 H+ = 2 Fe+3 + 3 H2O
    log_k       -4.008
    delta_h -30.845 kcal

Goethite
    FeOOH + 3 H+ = Fe+3 + 2 H2O
    log_k       -1.000
    delta_h      -14.48 kcal

Fe(OH)3(a)
    Fe(OH)3 + 3 H+ = Fe+3 + 3 H2O
    log_k       4.891

Pyrite
    FeS2 + 2 H+ + 2 e- = Fe+2 + 2 HS-
    log_k       -18.479
    delta_h 11.300 kcal

FeS(ppt)
    FeS + H+ = Fe+2 + HS-
    log_k       -3.915

Mackinawite
    FeS + H+ = Fe+2 + HS-
    log_k       -4.648

Sulfur
    S + 2H+ + 2e- = H2S
    log_k       4.882
    delta_h -9.5 kcal

Vivianite
    Fe3(PO4)2:8H2O = 3 Fe+2 + 2 PO4-3 + 8 H2O
    log_k       -36.000

Pyrolusite
    MnO2 + 4 H+ + 2 e- = Mn+2 + 2 H2O
    log_k       41.380
    delta_h -65.110 kcal
```

```
Hausmannite
        Mn3O4 + 8 H+ + 2 e- = 3 Mn+2 + 4 H2O
        log_k           61.030
        delta_h -100.640 kcal

Manganite
        MnOOH + 3 H+ + e- = Mn+2 + 2 H2O
        log_k           25.340

Pyrochroite
        Mn(OH)2 + 2 H+ = Mn+2 + 2 H2O
        log_k           15.200

Halite
        NaCl = Na+ + Cl-
        log_k           1.582
        delta_h 0.918 kcal

CO2(g)
        CO2 = CO2
        log_k           -1.468
        delta_h -4.776 kcal
        -analytic       108.3865      0.01985076   -6919.53      -40.45154      669365.0

O2(g)
        O2 = O2
        log_k           -2.960
        delta_h -1.844  kcal

H2(g)
        H2 = H2
        log_k           -3.150
        delta_h -1.759  kcal

H2O(g)
        H2O = H2O
        log_k           1.51
        delta_h         -44.03   kJ
#    Stumm and Morgan, from NBS and Robie, Hemmingway, and Fischer (1978)

N2(g)
        N2 = N2
        log_k           -3.260
        delta_h -1.358  kcal

H2S(g)
        H2S = H2S
        log_k           -0.997
        delta_h -4.570  kcal

CH4(g)
        CH4 = CH4
        log_k           -2.860
        delta_h -3.373  kcal

NH3(g)
        NH3 = NH3
        log_k           1.770
        delta_h -8.170  kcal

Melanterite
        FeSO4:7H2O = 7 H2O + Fe+2 + SO4-2
```

log_k -2.209
delta_h 4.910 kcal
-analytic 1.447 -0.004153 0.0 0.0 -214949.0

Alunite
KAl3(SO4)2(OH)6 + 6 H+ = K+ + 3 Al+3 + 2 SO4-2 + 6H2O
log_k -1.400
delta_h -50.250 kcal

Jarosite-K
KFe3(SO4)2(OH)6 + 6 H+ = 3 Fe+3 + 6 H2O + K+ + 2 SO4-2
log_k -9.210
delta_h -31.280 kcal

log_k 15.33
delta_h -33.37 kcal

Uraninite
UO2 + 4H+ = U+4 + 2H2O
log_k -4.7
delta_h -18.63 kcal

UO2(am)
UO2 + 4H+ = U+4 + 2H2O
log_k 0.934
delta_h -26.23 kcal

U4O9(C)
U4O9 + 18H+ + 2e- = 4U+4 + 9H2O
log_k -3.384
delta_h -101.235 kcal

U3O8(C)
U3O8 + 16H+ + 4e- = 3U+4 + 8H2O
log_k 21.107
delta_h -116.02 kcal

USiO4(C)
USiO4 + 4H+ = U+4 + H4SiO4
log_k -7.62
delta_h -14.548 kcal

UO3(C)
UO3 + 2H+ = UO2+2 + H2O
log_k 7.719
delta_h -19.315 kcal

Gummite
UO3 + 2H+ = UO2+2 + H2O
log_k 10.403
delta_h -23.015 kcal

B_UO2(OH)2
UO2(OH)2 + 2H+ = UO2+2 + 2H2O
log_k 5.544
delta_h -13.73 kcal

Schoepite
UO2(OH)2:H2O + 2H+ = UO2+2 + 3H2O
log_k 5.404
delta_h -12.045 kcal

```
Rutherfordine
    UO2CO3 = UO2+2 + CO3-2
    log_k   -14.439
    delta_h -1.44   kcal
    -analytical 4.54      -0.03318    -2716.0

VMetal
    V = V+3 + 3e-
    log_k   42.35
    delta_h -62.9   kcal

VO
    VO + 2H+ = V+3 + H2O + e-
    log_k   13.08
    delta_h -28.02  kcal

VCl2
    VCl2 = V+3 + 2Cl- + e-
    log_k   17.97
    delta_h -35.8   kcal

V2O3
    VO1.5 + 3H+ = V+3 + 1.5H2O
    log_k   4.9
    delta_h -19.72  kcal

V(OH)3
    V(OH)3 + 3H+ = V+3 + 3H2O
    log_k   7.65
    delta_h -0      kcal

VCl3
    VCl3 = V+3 + 3Cl-
    log_k   21.73
    delta_h -43.96  kcal

VOCl
    VOCl + 2H+ = V+3 + Cl- + H2O
    log_k   9.41
    delta_h -26.17  kcal

V2O4
    VO2 + 2H+ = VO+2 + H2O
    log_k   4.27
    delta_h -14.07  kcal

VO(OH)2
    VO(OH)2 + 2H+ = VO+2 + 2H2O
    log_k   5.85
    delta_h -0      kcal

VF4
    VF4 + H2O = VO+2 + 4F- + 2H+
    log_k   14.93
    delta_h -47.59  kcal

VOSO4(C)
    VOSO4 = VO+2 + SO4-2
    log_k   3.57
    delta_h -20.72  kcal

VOCl2
```

```
    VOCl2 = VO+2 + 2Cl-
    log_k   12.79
    delta_h -28.2   kcal

V2O5
    VO2.5 + H+ = VO2+ + 0.5H2O
    log_k   -0.72
    delta_h -4.16   kcal

Tyuyamunite
    Ca0.5UO2VO4 + 4H+ = 0.5Ca+2 + UO2+2 + VO2+ + 2H2O
    log_k   2.04
    delta_h -18.3   kcal

Ca_Vanadate
    Ca0.5VO3 + 2H+ = 0.5Ca+2 + VO2+ + H2O
    log_k   2.83
    delta_h -10.13  kcal

Ca3(VO4)2
    Ca1.5VO4 + 4H+ = 1.5Ca+2 + VO2+ + 2H2O
    log_k   19.48
    delta_h -35.07  kcal

Ca2V2O7
    CaVO3.5 + 3H+ = Ca+2 + VO2+ + 1.5H2O
    log_k   8.75
    delta_h -19.06  kcal

Fe_Vanadate
    Fe0.5VO3 + 2H+ = 0.5Fe+2 + VO2+ + H2O
    log_k   -1.86
    delta_h -7.37   kcal

Mg_Vanadate
    Mg0.5VO3 + 2H+ = 0.5Mg+2 + VO2+ + H2O
    log_k   5.64
    delta_h -16.33  kcal

Mg2V2O7
    MgVO3.5 + 3H+ = Mg+2 + VO2+ + 1.5H2O
    log_k   13.18
    delta_h -30.5   kcal

Mn_Vanadate
    Mn0.5VO3 + 2H+ = 0.5Mn+2 + VO2+ + H2O
    log_k   2.45
    delta_h -11.05  kcal

NH4VO3
    NH4VO3 + 2H+ = NH4+ + VO2+ + H2O
    log_k   2.69
    delta_h -3.77   kcal

Na_Vanadate
    NaVO3 + 2H+ = Na+ + VO2+ + H2O
    log_k   3.71
    delta_h -7.01   kcal

Na3VO4
    Na3VO4 + 4H+ = 3Na+ + VO2+ + 2H2O
    log_k   36.94
```

```
        delta_h -44.42  kcal

Na4V2O7
        Na2VO3.5 + 3H+ = 2Na+ + VO2+ + 1.5H2O
        log_k   18.7
        delta_h -24.03  kcal

Pb3(VO4)2
        Pb1.5VO4 + 4H+ = 1.5Pb+2 + VO2+ + 2H2O
        log_k   3.07
        delta_h -8.68   kcal

Pb2V2O7
        PbVO3.5 + 3H+ = Pb+2 + VO2+ + 1.5H2O
        log_k   -0.95
        delta_h -3.22   kcal

Carnotite
        KUO2VO4 + 4H+ = K+ + UO2+2 + VO2+ + 2H2O
        log_k   0.23
        delta_h -8.7    kcal

VO2Cl
        VO2Cl = VO2+ + Cl-
        log_k   2.81
        delta_h -9.65   kcal

V3O5
        V3O5 + 4H+ = 3VO+2 + 2H2O + 2e-
        log_k   1.87
        delta_h -23.53  kcal

V4O7
        V4O7 + 6H+ = 4VO+2 + 3H2O + 2e-
        log_k   7.14
        delta_h -39.15  kcal

V6O13
        V6O13 + 2H+ = 6VO2+ + H2O + 4e-
        log_k   -60.86
        delta_h 64.89   kcal

Se(s)               550
     Se + H+ + 2e- = HSe-
     log_k                  -17.322

#SemetalSe4         551
#    Se + 3H2O = SeO3-2 + 6H+ + 4e-
#    log_k                  -59.836

FeSe2               552
     FeSe2 + 2H+ + 2e- = Fe+2 + 2HSe-
     log_k                  -18.580

SeO2                553
     SeO2 + H2O = SeO3-2 + 2H+
     log_k                  -8.380

CaSeO3              554
     CaSeO3 = Ca+2 + SeO3-2
     log_k                  -5.6
```

```
BaSeO3              555
     BaSeO3 = Ba+2 + SeO3-2
     log_k                -6.390

Fe2(SeO3)3          556
     Fe2(SeO3)3 = 2Fe+3 + 3SeO3-2
     log_k                -35.430

Orpiment            500
     As2S3 + 6H2O = 2H3AsO3 + 3HS- + 3H+
     log_k                -60.971
     delta_h    82.890 kcal

Realgar             501
     AsS + 3H2O = H3AsO3 + HS- + 2H+ + e-
     log_k                -19.747
     delta_h    30.545 kcal

EXCHANGE_MASTER_SPECIES
      X       X-
EXCHANGE_SPECIES
      X- = X-
      log_k          0.0

      Na+ + X- = NaX
      log_k   0.0
      -gamma  4.0     0.075

      K+ + X- = KX
      log_k   0.7
      -gamma  3.5     0.015
      delta_h  -4.3   # Jardine & Sparks, 1984

      Li+ + X- = LiX
      log_k   -0.08
      -gamma  6.0     0.0
      delta_h  1.4    # Merriam & Thomas, 1956

      NH4+ + X- = NH4X
      log_k   0.6
      -gamma  2.5     0.0
      delta_h  -2.4   # Laudelout et al., 1968

      Ca+2 + 2X- = CaX2
      log_k   0.8
      -gamma  5.0     0.165
      delta_h  7.2    # Van Bladel & Gheyl, 1980

      Mg+2 + 2X- = MgX2
      log_k   0.6
      -gamma  5.5     0.2
      delta_h  7.4    # Laudelout et al., 1968

      Sr+2 + 2X- = SrX2
      log_k   0.91
      -gamma  5.26    0.121
      delta_h  5.5    # Laudelout et al., 1968

      Ba+2 + 2X- = BaX2
      log_k   0.91
      -gamma  5.0     0.0
      delta_h  4.5    # Laudelout et al., 1968
```

```
        Mn+2 + 2X- = MnX2
        log_k   0.52
        -gamma  6.0     0.0

        Fe+2 + 2X- = FeX2
        log_k   0.44
        -gamma  6.0     0.0

        Cu+2 + 2X- = CuX2
        log_k   0.6
        -gamma  6.0     0.0

        Zn+2 + 2X- = ZnX2
        log_k   0.8
        -gamma  5.0     0.0

        Cd+2 + 2X- = CdX2
        log_k   0.8

        Pb+2 + 2X- = PbX2
        log_k   1.05

        Al+3 + 3X- = AlX3
        log_k   0.41
        -gamma  9.0     0.0

        AlOH+2 + 2X- = AlOHX2
        log_k   0.89
        -gamma  0.0     0.0

SURFACE_MASTER_SPECIES
        Hfo_s  Hfo_sOH
        Hfo_w  Hfo_wOH
        Sfo_w  Sfo_wOH
        Sfo_s  Sfo_sOH
        Sfo_z  Sfo_zOH

SURFACE_SPECIES

    Sfo_wOH = Sfo_wOH
        log_k  0.0

    Sfo_wOH  + UO2+2 + H2O  =  Sfo_wOUO2OH  +  2H+
      Log_K   –3.487

    Sfo_wOH + H3AsO4 = Sfo_wAsO4H-  +  H+  +  H2O
        Log_K  3.697

    Sfo_wOH + H3AsO3 = Sfo_wAsO3H2 +  H2O
        Log_K  5.397

    Sfo_wOH + SeO3-2  +  H+   =  Sfo_wSeO3-  +  H2O
        Log_K  12.745

#   Sfo_wOH + VO4-3  +  2H+   = Sfo_wVO4H-  +  H2O
#        Log_K  29.18

# 9/19/96
#       Added analytical expression for H2S, NH3, KSO4.
#       Added species CaHSO4+.
#       Added delta H for Goethite
```